

***DISPERSION INDUCED ADVECTION
OF AN ISOTOPE RATIO***

BY

***MARK R. WOLFF
JOHN L. WILSON***

***HYDROLOGY REPORT NO. 89-5
NEW MEXICO TECH HYDROLOGY REPORT SERIES
HYDROLOGY PROGRAM
SOCORRO, NEW MEXICO 87801***

DECEMBER 1989

***THIS REPORT WAS ALSO SUBMITTED BY MARK R. WOLFF AS AN INDEPENDENT
STUDY IN PARTIAL FULFILLMENT OF THE REQUIREMENTS OF THE M.S. DEGREE
IN HYDROLOGY***

INDEPENDENT STUDY

**DISPERSION INDUCED ADVECTION
OF AN ISOTOPE RATIO**

by

Mark R. Wolff

**Submitted in Partial Fullfillment of Requirements
for Master of Science in Hydrology
New Mexico Institute of Mining and Technology
Department of Geoscience
Socorro, New Mexico 87801**

December 1989

ACKNOWLEDGEMENTS

THE FOLLOWING INDIVIDUALS CONTRIBUTED TO THIS RESEARCH:

***DR. JOHN L. WILSON, DR. FRED M. PHILLIPS, AND PAPADOPULOS & ASSOCIATES,
INC.***

X

Acknowledgements: I would like to thank Fred Phillips for the questions that were the inspiration for this study, John Wilson for his guidance and patience, and S.S. Papadopulos & Associates, Inc. for their support.

DISPERSION INDUCED ADVECTION
OF AN ISOTOPE RATIO

List of Figures.....	i
List of Tables	vii
Abstract.....	viii
Introduction.....	1
Groundwater Transport.....	4
A. Introduction.	4
B. Development of the Advective-Dispersive Equation.....	7
Dispersion Induced Advection.....	11
A. Development of the Dispersion Induced Advection Equation.....	11
B. Common Isotope Concentration Gradients.....	15
C. Importance to Applications.....	17
Graphical Examination of Dispersion Induced Advection.....	19
A. One Dimensional Finite Element Transport Model.....	19
B. Graphical Superposition.....	22
1. Diffusion.....	22
2. Pulse Input.....	23

3.	Source/Sink Boundary Condition.....	25
4.	Radioactive Decay.....	26
5.	Step Input.....	26
C.	Discussion.....	28
Dispersion Induced Advection Model.....		29
A.	Constant Common Isotope Concentration Gradient.....	30
B.	Constant Dispersion Induced Advection Term.....	31
Conclusions.....		32
References.....		36
Figures.....		39
Tables.....		92
Appendices.....		96

LIST OF FIGURES

Figure 1	Tracer dispersion	39
Figure 2	Solute transport mass balance.	40
Figure 3	Isotopic concentration trends	41
Figure 4	An example of isotopic concentrations as individual components and as a ratio for the assumed case (a constant reference species concentration)	42
Figure 5	An example of isotopic concentrations as individual components and as a ratio for a positive reference species concentration gradient (BCG).	43
Figure 6	Comparison of ratio isotopic concentrations for an assumed case and a positive BCG case.	44
Figure 7	Direct comparison of an assumed case and a BCG case difficult at large times or large distances from source	45
Figure 8	Direct comparison of an assumed case and a BCG case facilitated by normalizing each curve by its maximum value.	46

Figure 9	Chapeau shape and weighting functions47
Figure 10	Comparison of analytical and numerical solutions to the one-dimensional, semi-infinite, advective-dispersive case48
Figure 11	Gaussian distribution of a pulse input of tracer in a system controlled by diffusion only49
Figure 12	Comparison of a diffusion only case for the assumed isotopic case and for four BCG cases50
Figure 13	Linear positive background (reference species) concentration gradient (BCG)51
Figure 14	Comparison of numerical solutions to the assumed case and a positive BCG case for a pulse input52
Figure 15	Comparison of numerical solutions to the assumed case and a negative BCG case for a pulse input53
Figure 16	Comparison of normalized numerical solutions to the assumed case and a positive BCG case for a pulse input54
Figure 17	Comparison of normalized numerical solutions to the assumed case and a negative BCG case for a pulse input55
Figure 18	Analytical solution for advective-dispersive transport of a tracer pulse in the presence of a source56

Figure 19	Analytical solution to the dilution effect of a source on a constant reference species concentration.	57
Figure 20	Change in advective velocity with distance due to a source or sink.	58
Figure 21	Analytical solution for advective-dispersive transport of a pulse input, in terms of an isotopic ratio, with the effect of a source on both the tracer and reference species taken into account.	59
Figure 22	Comparison of numerical solutions from Figure 18 and Figure 21	60
Figure 23	Comparison of normalized numerical solutions from Figure 18 and Figure 21	61
Figure 24	Analytical solution for advective-dispersive transport of a tracer pulse in the presence of a sink.	62
Figure 25	Analytical solution to the dilution effect of a sink on a constant reference species concentration.	63
Figure 26	Analytical solution for advective-dispersive transport of a pulse input, in terms of an isotopic ratio, with the effect of a sink on both the tracer and reference species taken into account.	64
Figure 27	Comparison of numerical solutions from Figure 24 and Figure 26	65
Figure 28	Comparison of normalized numerical solutions from Figure 24 and Figure 26	66

Figure 29	Comparison of the numerical solutions to advective-dispersive transport of a tracer pulse with and without radioactive decay67
Figure 30	Comparison of the numerical solutions to advective-dispersive transport of a tracer pulse with and without radioactive decay in the presence of a source68
Figure 31	Comparison of the numerical solutions to advective-dispersive transport of a tracer pulse with and without radioactive decay in the presence of a sink.69
Figure 32	Comparison of the numerical solutions to advective-dispersive transport of a tracer pulse, in terms of a isotopic ratio, with and without radioactive decay in the presence of a source70
Figure 33	Comparison of the numerical solutions to advective-dispersive transport of a tracer pulse, in terms of a isotopic ratio, with and without radioactive decay in the presence of a sink.71
Figure 34	Numerical solution to advective-dispersive transport of a steady tracer input72
Figure 35	Linear positive background (reference species) concentration gradient (BCG).73
Figure 36	Comparison of numerical solutions to advective-dispersive transport of a steady tracer input for the assumed and positive linear BCG case.74
Figure 37	Linear negative background (reference species) concentration gradient (BCG).75

Figure 38	Comparison of numerical solutions to advective-dispersive transport of a steady tracer input for the assumed and negative linear BCG case76
Figure 39	Comparison of numerical solutions to advective-dispersive transport of a steady tracer input with and without a source.77
Figure 40	Comparison of numerical solutions to advective-dispersive transport of a steady tracer input with and without a sink78
Figure 41	Comparison of numerical solutions to advective-dispersive transport of a steady tracer input with and without radioactive decay79
Figure 42	Comparison of numerical solutions to advective-dispersive transport of a steady tracer input for the positive linear BCG case with and without radioactive decay80
Figure 43	Comparison of numerical solutions to advective-dispersive transport of a steady tracer input for the negative linear BCG case with and without radioactive decay81
Figure 44	Comparison of normalized numerical solutions from Figure 4382

Figure 45	Comparison of numerical solutions to advective-dispersive transport of a steady tracer input for the positive linear BCG case with and without a source.83
Figure 46	Comparison of numerical solutions to advective-dispersive transport of a steady tracer input for the positive linear BCG case with and without a sink84
Figure 47	Comparison of DIA model with graphical superposition for constant DIA correction.85
Figure 48	Comparison of DIA model with graphical superposition for constant DIA correction.86
Figure 49	Comparison of DIA model with graphical superposition for constant DIA correction.87
Figure 50	Comparison of DIA model with graphical superposition for constant DIA correction.88
Figure 51	Comparison of DIA model with graphical superposition for constant DIA correction.89
Figure 52	Comparison of DIA model with graphical superposition for constant DIA correction.90

Figure 53 Comparison of DIA model with graphical superposition for constant DIA
correction.91

ABSTRACT

In hydrologic investigations, knowledge of the groundwater age can be valuable in better understanding the hydrologic system and its properties. Isotopic dating is a commonly used method of determining groundwater age. In using isotopic dating it is frequently assumed that the common isotope, of the isotopic ratio, remains constant in concentration over the domain of the area under investigation. What effect does constant spatial variability of the concentration of the common isotope have upon the isotopic ratio and inferences that might be drawn from that ratio?

An equation to describe one-dimensional groundwater transport of an isotope in terms of a ratio between rare and common isotopes of an element is developed in this paper. This description of the transport process differs from others in that an additional term to account for the effects of spatial variation in the common isotope concentration upon the effective advective velocity of the system, termed dispersion induced advection, is introduced. The effects upon isotopic transport of a dispersion induced advection term sufficiently large to change the effective advective velocity by more than 10 percent are examined using analytical and numerical techniques. Analytical results indicate that when significant dispersion induced advection is present, the spatial distribution of an isotopic ratio is effected. Numerical results indicate the difficulty in the selection of the appropriate realistic boundary and initial conditions to simulate the effects of dispersion induced advection.

The implications of these findings suggest that prior to the modeling of isotopic transport in terms of a ratio, careful examination of all isotopic data for a spatial common isotope concentration gradient is required. In the presence of such a concentration gradient, both components of the isotopic ratio should be modeled separately.

INTRODUCTION

In hydrologic investigations, knowing the age of groundwater can be valuable in better understanding the hydrologic system and its properties. A study of the spatial distribution of ground-water ages can provide information on flow paths, flow velocity, residence time, hydraulic conductivity distribution and anisotropy, and sources of water including the spatial and temporal distribution of recharge events. Davis and Bentley (1982) define groundwater age as the length of time the water has been isolated from the atmosphere. Not reflected in this definition is the fact that groundwater flows following a complex, tortuous path. The mixing effects of dispersion are always present and vary with the scale of the system, and therefore no two water molecules in a given sample will be exactly the same age. Thus, the concept of a precise groundwater age is somewhat obscure. Nevertheless, the idea of an "average" groundwater age for a sample is still a very useful one (Bentley et al, 1986).

Determining groundwater ages may be accomplished by numerous methods. The review by Davis and Bentley (1982) summarizes available techniques. The two most common methods of dating groundwater are based upon the use of Darcy's Law and the continuity equation, and the use of isotopic data.

Hydrodynamic calculation of travel times to estimate groundwater age using Darcy's Law and the continuity equation, is the oldest, most widely used method. This approach requires assignment of the estimated spatially variable parameters of recharge and discharge rates, hydraulic conductivity, cross-sectional area, hydraulic gradient, and effective porosity. The additional problem of historic temporal variability in the hydraulic gradient and rates of recharge and discharge must also be addressed. Inability to define all critical hydrogeologic parameters always leaves large uncertainties in the estimation of groundwater ages by purely hydrodynamic methods. As pointed out by Davis and Bentley (1982), and

others (eg, Freeze, 1975; Gelhar and Axness, 1983), even apparently homogeneous aquifers have exhibited permeabilities varying through at least two orders of magnitude. This range of permeabilities will give rise to the phenomenon of macrodispersion (Gelhar,1986; Gelhar and Axness, 1983), which can yield water of mixed ages in any given zone of an aquifer. Use of the hydrodynamic method for dating groundwater is perhaps best reserved for quick calculations and as an easy means of checking dates obtained by more direct methods.

Isotopic tracers have been used in determining flow rates, the mixing of groundwaters, and related hydrologic parameters within aquifers since the early 1950's. The tracers employed may be isotopes produced naturally, as a by-product of man's activities, or artificially. Isotopes may be classed either as radioactive (non-stable) and stable. A large number of radionuclides are produced continuously in the upper atmosphere by interactions between gases and cosmic radiation. An underlying assumption in the use of these isotopes is that the cosmic radiation flux and resultant production of radioactive isotopes has been constant with time (Davis and Bentley, 1982). The radioactive isotopes most frequently of hydrologic interest are presented by Davis and Bentley (1982, Table 1). Tritium (^3H), ^{14}C and, more recently, ^{36}Cl , are most commonly used. Frequently used stable isotopes in hydrologic investigations are Deuterium (^2H), ^{13}C , ^{18}O , and ^{34}S (F. Phillips. pers. comm. 12/2/86). It is well documented that atmospheric testing of nuclear weapons from 1952 to 1963 in the South Pacific produced an artificially large number of radionuclides, such as ^3H , ^{14}C , ^{36}Cl . Atmospherically produced isotopes enter the groundwater cycle in the form of precipitation recharge, with those produced by weapons testing forming a pulse input above background, or natural, levels. Stable isotopes may enter the groundwater cycle as recharge (i.e. ^2H , ^{18}O), or from dissolution of aquifer matrix or organic material (eg, ^{13}C).

In order to minimize complications, isotopes for hydrologic use should have the following idealized properties; 1) widespread and abundant, 2) high solubility, 3) simple hydrogeochemistry, 4)

conservative, or non-reactive, with respect to the aquifer matrix, 5) the relative mass difference between the common and the rare isotope should be large, and 6) the relative abundance of the isotope should be modified by some naturally occurring process (Toran, 1982; Bentley et al, 1986). Artificial tracer isotopes are man-made and introduced into the hydrologic cycle at chosen locations, in calculated concentrations, to study the specific facets of the hydrologic system. Halvey and Nir (1960) and many others have examined the chemical and physical considerations necessary for choosing an artificial tracer.

Isotopic data is most often examined in terms of a ratio between the rare isotope and the common, or reference, isotope. Stable isotope ratios are expressed in delta units (δ), or per mille (parts per thousand or ‰) differences relative to a standard ratio:

$$\delta \text{‰} = [(R - R_{\text{standard}}) / R_{\text{standard}}] \times 1000 \quad (1)$$

where R and R_{standard} are the respective isotope ratios of the sample and the standard. For the environmental isotopes of ^2H and ^{18}O the reference ion concentrations may be considered constant, as they (^1H and ^{16}O) compose the solute, water. The reference ion concentration for other stable isotopes may vary with physical and chemical controls. For example, a change in pH or temperature within the aquifer may alter the carbonate species balance, thereby modifying the ^{12}C concentration and the related $^{13}\text{C}/^{12}\text{C}$ ratio.

The law of radioactive decay describes the rate at which the activity of all radioactive substances decrease with time (Freeze and Cherry, 1979). This is expressed as

$$A = A_0 2^{-(t/T)} \quad (2)$$

where A_0 is the level of radioactivity at some initial time, A is the level at some later time, t , and T is the half-life of the isotope. Rearranging equation (2) to estimate the groundwater age yields

$$t = - \left[\frac{T}{\ln(2)} \right] \left[\ln \frac{A}{A_0} \right] \quad (3)$$

where t is the decay age, A is the activity (disintegrations per unit time per unit mass of sample), and A_0 is the specific activity. The activities, A and A_0 , may also be expressed as a concentration ratio of radioactive isotope relative to the reference isotope, or as percent modern $[(A/A_0) \times 100\%]$ with A_0 equal to the modern input activity or ratio. As with ^2H and ^{18}O , it is unlikely the reference isotope concentration for ^3H (^1H) will vary. For the other radioactive isotopes, such as ^{14}C and ^{36}Cl , physical and chemical controls may once again vary the reference ion concentration.

This study examines the effects of a concentration gradient in the common (reference) isotope on isotopic ratios, and inferences that might be carelessly drawn from them. Specifically, what effect does a common isotope concentration gradient have upon the magnitude and apparent travel distance of an isotope ratio? A mathematical model is developed in this paper to describe the transport of isotopic tracers in terms of a ratio between the rare (stable and non-stable) and the common isotopes. The concentration of the common isotope is allowed to vary in space along the direction of flow. Mechanisms that may result in common isotope concentration gradients are reviewed. The results of numerical and analytical solutions for a variety of situations are given. The effects of a background concentration gradient upon the spatial distribution of an isotopic ratio are shown. Finally, limitations and applicability of examining isotopic transport in terms of a ratio are discussed.

GROUNDWATER TRANSPORT

Introduction

Examination of the groundwater flow system in terms of its ability to transport solutes is of increasing interest in hydrologic investigations. The solutes may be comprised of natural isotopes, artificial tracers, or contaminants. The following discussion of solute transport is based upon the

extensive work of Bear (1972, 1979) and a review of Freeze and Cherry (1979). Solutes are transported by the bulk motion of flowing groundwater in a process known as advection. Conservative solutes move at a rate equal to the seepage velocity, v , of the water. If advection, or piston flow, was the only process by which solutes were transported, a step input of solute would be observed upon arrival at any point downstream as the same step front. However, the solute tends to spread out from the path it would be expected to follow (Figure 1).

Dispersion is responsible for the spreading phenomenon, causing dilution of the solute. Adopting the Darcian approach, or looking at fluid velocities macroscopically, ignores the microscopic scale of mechanical mixing during fluid flow and molecular diffusion of solute particles. The flow velocity varies within a pore, from pore to pore, and in direction between pores. The component of dispersion caused solely by motion of the fluid is known as mechanical dispersion. Mechanical dispersion is expressed as the product of the dispersivity, α (a characteristic property of the porous media), and the seepage velocity, v . Molecular diffusion is the process by which solute constituents move under their kinetic activity in the direction of their decreasing concentration gradient. This process is described by Fick's First Law. In order to account for the effect of the matrix on diffusion, the coefficient of molecular diffusion, D^* (a reduced fraction of the solute diffusion coefficient), is calculated. Thus, in one dimension, the coefficient of hydrodynamic dispersion, D , is expressed as

$$D_l = \alpha_l v + D^* \tag{4}$$

where l is a curvilinear coordinate direction taken along the flowline. The result of dispersion is that some of the water and solute molecules move faster than the seepage velocity and some slower. The solute tends to spread out in the direction of flow and become more dilute (Figure 1). The phenomenon of dispersion on the macroscopic scale is produced by microscopic processes on the pore scale.

There are additional processes that can also cause tracer behavior to deviate from the idealized piston flow model. Stratification or heterogeneities on the macroscopic scale may cause additional dispersion, by introducing heterogeneities in the velocity field (de Marsily, 1986, Gelhar, 1986 and Gelhar and Axness, 1982). As with mechanical dispersion, these variations in the velocity will cause the solute to mix and spread, and are referred to as macrodispersion. Other mechanisms occur in aquifers comprised of fractures and blocks of porous media. Solute transport is in the fracture network, but steep concentration gradients between the fractures and the porous media matrix can cause solute to first diffuse into the blocks and, in the case of a passing tracer pulse, later diffuse back into the fracture. Solute transport may be retarded and spread out by this process, often referred to as "matrix diffusion."

Radioactive decay of the solute can cause a decrease in concentration, depending upon the particular half-life of the tracer and the residence time within the aquifer. Dilution or concentration of the solute may occur with recharge, a leakage of water through aquitards. The effects of water evaporation, condensation, and chemistry may also modify solute concentration and transport, particularly in the unsaturated zone and with environmental isotopes such as ^{36}Cl .

There are many mechanisms that may be responsible for the mixing and spreading of a solute in a porous medium. The focus of this study is upon the transport of an isotopic solute in terms of a ratio between its rare and common isotopes. An equation for the transport of a solute in a saturated matrix is developed. As the process of dispersion is always present on all scales (microscopic and macroscopic), it must be accounted for in any transport model. Some commonly used isotopes decay radioactively and the effects of such decay upon isotopic concentration and transport is addressed specifically. Matrix diffusion, and concentration/dilution of the tracer due to water loss/gain is included in the transport equation as a source/sink term.

Development of the Advective-Dispersive Equation

Derivation of the advective-dispersive equation is based upon a statement of the law of conservation of mass. The derivation here follows those of Ogata (1970), Bear (1972,1979), and Freeze and Cherry (1979). The equation is developed in terms of Cartesian (x,y,z) coordinates for simplicity. Forms of the equation in terms of other coordinate systems may be obtained by either known transformations, or from the aforementioned authors and others.

A simplified one dimensional model is adopted in order to examine the issues of isotope transport more easily. It is assumed Darcy's Law applies. The Darcy assumption implies that an average linear velocity (i.e. seepage velocity) may be used to describe the flow rate of all particles, which carry the dissolved substance by advection. Inherent in this assumption is the neglect of microscopic fluid velocity variations. If advection were the only mechanism active in transport of the non-reactive solutes, they would move with the fluid as a plug. However, the variation of fluid velocities within each pore, from one pore to another, and due to heterogeneities of larger scale, requires the introduction of the additional mechanism of dispersion. Inclusion of dispersion as a transport mechanism is necessary in order to describe the process of mass transport on macroscopic scales, using macroscopic parameters, and still account for microscopic mixing effects. In addition, it is assumed that the porous medium of the model is homogeneous and isotropic, that the medium is saturated, and that the flow is steady-state. The illustrated concepts are easily extended to other situations.

The mathematical statement of conservation of mass is established by considering solute flux into and out of a small elemental volume in the porous media (Figure 2). In three-dimensional Cartesian space the specific discharge, q , has components (q_x, q_y, q_z) and the seepage velocity, $v = q/n_e$, has components (v_x, v_y, v_z) , where n_e is the effective porosity. The advective transport rate is equal to the seepage velocity, v . Defining the solute concentration, C , as the mass of solute per unit volume of solution, it follows that

the mass of solute per unit volume of media is $n_e C$. The two modes of solute transport in the x direction have been described as advection and dispersion. For uniform flow in the x-direction these may be expressed mathematically as

$$\text{transport by advection} = \bar{v}_x n_e C dA \quad (5)$$

$$\text{transport by dispersion} = n_e D_x \left(\frac{\partial C}{\partial x} \right) dA \quad (6)$$

where D_x is the dispersion coefficient in the x direction and dA is the elemental cross-sectional area of the element. The dispersion coefficient D_x is related to the dispersivity, α_x , and the diffusion coefficient, D^* by (4)

$$D_x = \alpha_x \bar{v}_x + D^* \quad (7)$$

If F_x represents the total amount of mass per unit cross-sectional area transported in the x direction per unit time, then

$$F_x = \bar{v}_x n_e C - n_e D_x \left(\frac{\partial C}{\partial x} \right) \quad (8)$$

Contaminant disperses towards the zone of lower fluid concentration as indicated by the negative sign before the second term. Expressions in the y and z directions are similarly written, for uniform flow in the x-direction ($\bar{v}_y = \bar{v}_z = 0$):

$$F_y = - n_e D_y \left(\frac{\partial C}{\partial y} \right) \quad (9)$$

$$F_z = - n_e D_z \left(\frac{\partial C}{\partial z} \right) \quad (10)$$

From Figure 2, the total amount of solute entering the cubic element is

$$F_x dy dz + F_y dx dz + F_z dx dy \quad (11)$$

The total amount leaving the cubic element is

$$\left(F_x + \frac{\partial F_x}{\partial x} dx \right) dy dz + \left(F_y + \frac{\partial F_y}{\partial y} dy \right) dx dz + \left(F_z + \frac{\partial F_z}{\partial z} dz \right) dx dy \quad (12)$$

where the partial terms indicate the spatial change of the solute mass in the specified direction. Accordingly, the difference in the amount of solute entering and leaving the cubic element is

$$\left(\frac{\partial F_x}{\partial x} + \frac{\partial F_y}{\partial y} + \frac{\partial F_z}{\partial z} \right) dx dy dz \quad (13)$$

Assuming the solute to be non-reactive, the difference between the flux entering and leaving the element must be equal to the amount of solute accumulated within the element. The rate of mass change is represented by

$$- n_e \left(\frac{\partial C}{\partial t} \right) dx dy dz \quad (14)$$

Equating the difference of inflow and outflow (13) to the amount of solute accumulated within the element (14) leads to the expression

$$\frac{\partial F_x}{\partial x} + \frac{\partial F_y}{\partial y} + \frac{\partial F_z}{\partial z} = - n_e \frac{\partial C}{\partial t} \quad (15)$$

Substituting the expressions for F_x , F_y , and F_z into (15) and cancellation of n_e from both sides yields

$$\left[\frac{\partial}{\partial x} \left(D_x \frac{\partial C}{\partial x} \right) + \frac{\partial}{\partial y} \left(D_y \frac{\partial C}{\partial y} \right) + \frac{\partial}{\partial z} \left(D_z \frac{\partial C}{\partial z} \right) \right] - \left[\frac{\partial}{\partial x} (\bar{v}_x C) \right] = \frac{\partial C}{\partial t} \quad (16)$$

For a homogeneous medium in which the velocity, v , is steady and uniform, dispersion coefficients D_x , D_y , and D_z do not vary in space. Equation (16) becomes

$$\left[D_x \frac{\partial^2 C}{\partial x^2} + D_y \frac{\partial^2 C}{\partial y^2} + D_z \frac{\partial^2 C}{\partial z^2} \right] - \left[\bar{v}_x \frac{\partial C}{\partial x} \right] = \frac{\partial C}{\partial t} \quad (17)$$

In one dimension,

$$D_x \frac{\partial^2 C}{\partial x^2} - v_x \frac{\partial C}{\partial x} = \frac{\partial C}{\partial t} \quad (18)$$

As required, additional terms to describe the mass balance effects of a source-sink or radioactive

decay of the tracer may be added to the advective-dispersive equation (18). The change in concentration of a tracer along its flowpath due to a source-sink of strength q' (assuming density, ρ , is constant) may be expressed in one-dimension as

$$\frac{\partial C}{\partial t} = \frac{C'}{n_e} \frac{\partial q_x}{\partial x} - \frac{C}{n_e} \frac{\partial q_x}{\partial x} \quad (19)$$

where C' is the injection-withdrawal concentration (usually zero or equal to C) and $q_x = \bar{v}_x n_e$ is the specific discharge. If the tracer employed undergoes radioactive decay as it is being transported through the porous medium, the change in tracer concentration is expressed as

$$\frac{\partial C}{\partial t} = -\lambda C \quad (20)$$

where λ is the decay constant of the tracer (equal to the inverse of the tracer's half life).

The advective-dispersive equation for a tracer with radioactive decay and with a source-sink may be expressed (in one dimension) as

$$D \frac{\partial^2 C}{\partial x^2} - v \frac{\partial C}{\partial x} - \frac{C}{n_e} \frac{dq_x}{dx} + \frac{C'}{n_e} \frac{dq_x}{dx} - \lambda C = \frac{\partial C}{\partial t} \quad (21)$$

where C' represents source-sink injection or withdrawal concentrations ($C' = C$ for a withdrawal). For the remainder of this paper it is assumed the one dimensional form of the advective-dispersive equation (21)

adequately describes the considered solute transport, and q_x is assumed to be constant in time, but not space. Consequently the "x" subscripts will be dropped from the dispersion coefficient, the seepage, or advective, velocity, v , and the specific discharge, q . To further simplify the notation, it is assumed that the effective porosity is equal to the porosity of the medium ($n = n_e$). Equation (21) may be written as

$$D \frac{\partial^2 C}{\partial x^2} - v \frac{\partial C}{\partial x} - \frac{C}{n} \frac{dq}{dx} + \frac{C'}{n} \frac{dq}{dx} - \lambda C = \frac{\partial C}{\partial t} \quad (22)$$

DISPERSION INDUCED ADVECTION

Development of the Dispersion Induced Advection Equation

Isotopic dating of groundwater requires the measurement of the ratio between the abundance of rare and common isotopic species of an element. As stated earlier, an underlying assumption in the use of isotopes for dating is that the production and rate of introduction into the hydrologic system of radioactive isotopes has been constant with time (Davis and Bentley, 1982), and that only a naturally occurring process (i.e. radioactive decay) modify the concentration of the rare isotope (Toran, 1982; Bentley et al, 1986).

Although the common species concentration may vary due to physical and chemical controls, it is often assumed to be a constant. The variation in the isotopic ratio is then simplified to a function of time, the rare isotope characteristics, and the hydrologic system in which it is transported. In the previous section, an equation describing the transport of an isotope in a one-dimensional, homogenous system was developed. If the common isotope concentration is assumed to be constant, then transport of a isotopic ratio may also be described using the same equation (22). In order to investigate the degree to which spatial variation of the common isotope concentration effects isotopic ratio transport modeling, a more general form of the isotopic ratio transport equation is developed in terms of the two isotopic components.

Given one-dimensional steady, saturated flow with a constant effective porosity, n , and assuming p is constant; the advective-dispersive equation (22) for the tracer (or rare species), C , may be written as

$$D \frac{\partial^2 C}{\partial x^2} - v \frac{\partial C}{\partial x} - \frac{C}{n} \frac{dq}{dx} + \frac{C'}{n} \frac{dq}{dx} - \lambda C = \frac{\partial C}{\partial t} \quad (23)$$

where λ is the tracer isotope decay constant. The advective-dispersive equation (22) for the stable

reference (or common) species, S, may be written as

$$D \frac{\partial^2 S}{\partial x^2} - v \frac{\partial S}{\partial x} - \frac{S}{n} \frac{dq}{dx} + \frac{S'}{n} \frac{dq}{dx} = \frac{\partial S}{\partial t} \quad (24)$$

C' and S' represent injection-withdrawal concentrations, and are usually equal to zero, or C or S respectively. The tracer/reference species ratio, C/S, transport equation may be obtained by two methods. The first is to divide the equation for the tracer concentration, C, (23) by the reference concentration, S, and carry out the necessary derivative calculations. The second method is to sum the transport equations for the tracer (23) and the reference species (24), and again perform the required derivative calculations. The following derivation of the ratio equation uses the summation method.

The addition of the tracer and reference species transport equations (23,24) yields

$$D \frac{\partial^2 (C + S)}{\partial x^2} - v \frac{\partial (C + S)}{\partial x} - \frac{(C + S)}{n} \frac{dq}{dx} + \frac{(C' + S')}{n} \frac{dq}{dx} - \lambda C - \frac{\partial (C + S)}{\partial t} = 0 \quad (25)$$

Given that

$$C + S = S \left(\frac{C}{S} + 1 \right) \quad (26)$$

then

$$\frac{\partial}{\partial x} \left[S \left(\frac{C}{S} + 1 \right) \right] = \left(\frac{C}{S} + 1 \right) \frac{\partial S}{\partial x} + S \frac{\partial \left(\frac{C}{S} \right)}{\partial x} \quad (27)$$

$$\frac{\partial}{\partial t} \left[S \left(\frac{C}{S} + 1 \right) \right] = \left(\frac{C}{S} + 1 \right) \frac{\partial S}{\partial t} + S \frac{\partial \left(\frac{C}{S} \right)}{\partial t} \quad (28)$$

and

$$\frac{\partial^2}{\partial x^2} \left[S \left(\frac{C}{S} + 1 \right) \right] = \left(\frac{C}{S} + 1 \right) \frac{\partial^2 S}{\partial x^2} + 2 \frac{\partial S}{\partial x} \frac{\partial \left(\frac{C}{S} \right)}{\partial x} + S \frac{\partial^2 \left(\frac{C}{S} \right)}{\partial x^2} \quad (29)$$

Equations (27,28, and 29) may be substituted into equation (25) to yield

$$S \left[D \frac{\partial^2 \left(\frac{C}{S} \right)}{\partial x^2} - v \frac{\partial \left(\frac{C}{S} \right)}{\partial x} - \lambda \frac{C}{S} - \frac{\partial \left(\frac{C}{S} \right)}{\partial x} \right] + \frac{S'}{n} \left(\frac{C'}{S'} + 1 \right) \frac{dq}{dx} + \left(\frac{C}{S} + 1 \right) \left[D \frac{\partial^2 S}{\partial x^2} - v \frac{\partial S}{\partial x} - \frac{S}{n} \frac{dq}{dx} - \frac{\partial S}{\partial x} \right] + 2D \frac{\partial S}{\partial x} \frac{\partial \left(\frac{C}{S} \right)}{\partial x} = 0 \quad (30)$$

But the term

$$D \frac{\partial^2 S}{\partial x^2} - v \frac{\partial S}{\partial x} - \frac{S}{n} \frac{dq}{dx} - \frac{\partial S}{\partial x} = - \frac{S'}{n} \frac{\partial q}{\partial x} \quad (31)$$

from (30) is equal to the reference species transport equation (24). Substituting the result of (31) into (30) and dividing (30) by S yields

$$D \frac{\partial^2 R}{\partial x^2} - v \frac{\partial R}{\partial x} - \lambda R - \frac{\partial R}{\partial t} + \frac{S'}{S n} \left(\frac{C'}{S'} + 1 \right) \frac{dq}{dx} - \frac{S'}{S n} \left(\frac{C}{S} + 1 \right) \frac{dq}{dx} + \frac{2D}{S} \frac{\partial S}{\partial x} \frac{\partial R}{\partial x} = 0 \quad (32)$$

where C/S is equal to R, or the "ratio". Simplifying (32) leads to

$$D \frac{\partial^2 R}{\partial x^2} - v \frac{\partial R}{\partial x} - \lambda R - \frac{\partial R}{\partial t} + \frac{2D}{S} \frac{\partial S}{\partial x} \frac{\partial R}{\partial x} + \frac{S'}{S n} \left(\frac{C'}{S'} - R \right) \frac{dq}{dx} = 0 \quad (33)$$

Rearranging (33), assuming the source-sink term is independent

$$D \frac{\partial^2 R}{\partial x^2} - \left(v - \frac{2D}{S} \frac{\partial S}{\partial x} \right) \frac{\partial R}{\partial x} - \lambda R + \frac{S'}{S n} \left(\frac{C'}{S'} - R \right) \frac{dq}{dx} = \frac{\partial R}{\partial t} \quad (34)$$

From (34) the effective velocity, V_{eff} , of the isotope ratio is

$$v_{\text{eff}} = v - \frac{2D}{S} \frac{\partial S}{\partial x} \quad (35)$$

Thus, the advective term of the ratio transport equation (34) is influenced by dispersion and the concentration gradient of the reference isotope. This new term will be referred to as dispersion induced advection (DIA). Please note that this phenomenon is purely conceptual - it refers only to the isotope ratio. The actual physical advection of either the rare or common isotopes is quite normal. The relative effect of the new apparent velocity can be seen by examining the ratio:

$$\left| \frac{v_{\text{eff}} - v}{v} \right| = \tau = \left| \frac{1}{v} \frac{2D}{S} \frac{\partial S}{\partial x} \right| \quad (36)$$

The effective velocity will differ significantly from the average linear velocity whenever the term, τ , is a significant proportion of 1. For cases where mechanical, or macro, dispersion is the dominant component of hydrodynamic dispersion (i.e. $\alpha V \gg D^*$), dispersion may be approximated by

$$D \cong \alpha v \quad (37)$$

For this case, the criteria for when the velocity correction term (36) is significant becomes

$$\tau = \left| \frac{2\alpha}{S} \frac{\partial S}{\partial x} \right| \gg 0 \quad (38)$$

If x equals the distance over which the reference species concentration, S , varies by an order of magnitude, then the corrective term is important if

$$\tau = \left| \frac{2\alpha}{S} \frac{dS}{dx} \right| = \left| 2\alpha \frac{d(\ln S)}{dx} \right| = \left| (2\alpha) 2.3 \frac{d(\log S)}{dx} \right| \quad (39)$$

But $d(\log S) = 1$ if $dx = \Delta x$, and the corrective term (39) becomes

$$\tau = \left| \frac{2\alpha}{S} \frac{dS}{dx} \right| = \left| \frac{(2\alpha)(2.3)}{\Delta x} \right| > \beta \quad (40)$$

where β is any significant part of 1 (say 0.1 or greater). If as an example $\beta = 0.1$, then

$$\frac{\alpha}{\Delta x} > \frac{\beta}{4.6} = \frac{1}{46} \quad \text{or} \quad \Delta x < 46\alpha \quad (41)$$

That is, an isotopic ratio, uncorrected for a reference species concentration gradient of one order of magnitude over a distance of 46 dispersivity lengths, may have an effective velocity which will deviate from the true velocity by 10%.

Difficulty arises in determination of the dispersivity of a porous medium. The problem of scale dependent dispersivities is reviewed by de Marsily (1986), and Graham and McLaughlin (1989), who conclude that probably only after large times or large distances traveled by the tracer is the classical dispersion equation valid. The distance may be up to 10 to 100 times the "correlation length" of the medium heterogeneities, or for horizontal flow in the field, up to hundreds or thousands of meters in typical sediments. Thus, examination of isotopic transport requires knowledge of the reference species concentration over an even greater distance for a model in terms of an isotopic ratio to consider dispersion-induced advection.

In this section an equation for isotopic ratio transport was developed, and the effect of a reference species concentration gradient has upon effective velocity was examined. The difficulty in determining the dispersivity and related distance over which the reference species concentration varies was noted. Natural controls upon the concentration variance of an isotopic reference species is examined in the following section.

Common Isotope Concentration Gradients

Concentrations of isotope tracers in groundwater are usually expressed in delta units, δ (if stable), or as percent modern (if radioactive). Both are relative to a standard reference sample representative of modern, pre-nuclear fallout, atmospheric input tracer content. This tracer content is not the true concentration of the tracer in solution, but rather the tracer concentration in the elemental sample removed

from the groundwater, with the tracer measured relative to a known elemental mass. If the concentration of the reference species varies, then the ratio of the isotopes is not a naturally conserved. When mass transport models are used in the analysis of isotope data, it is theoretically necessary to base the analysis on the actual concentration of each isotope in solution (Sudicky and Frind, 1981).

Variations in the reference species concentration may exist due to a variety of physical and chemical controls. In examining the Milk River Aquifer (Alberta, Canada) studies by Schwartz and Muehlenbachs (1979), and Phillips et al (1986) discuss three possible mechanisms for reference species concentration variation.

- 1) Climatic change. Increases in the evaporation of precipitation due to a sustained climatic warming could cause higher reference ion (species) concentrations in meteoric recharge water. Conversely, sustained climatic cooling could have the effect of reducing evaporation and reference ion concentrations in recharge. Examination of paleoclimatic indicators should be included in consideration of this mechanism.

- 2) Dispersive processes. Concentration gradients of a reference species down the hydraulic gradient may be due to a flushing of more saline, perhaps connate, water from the aquifer due to meteoric recharge. An examination of the hydraulic conductivity and gradient should indicate whether the aquifer has been swept of waters differing in composition from the recharge. Simple mixing mass balance models between meteoric and connate water, or seawater, should also be checked to see if observed conditions may be reproduced. Instead of simple flushing by meteoric water, fluids with the appropriate reference species concentration may be introduced by leakage into the aquifer and displace, dilute or concentrate aquifer water. Simple mixing mass balance models should be checked, as should the presence of necessary

hydraulic gradients. Spatial/temporal differences in evapotranspiration rates in the vadose zone may also effect reference species concentrations.

3) Ion filtration. Ion filtration can increase both the ionic concentration and the isotopic weight of a solution (Hanshaw and Coplen, 1973; Coplen and Hanshaw, 1973). Isotope fractionation can be caused by membrane effects of groundwater passing through silt and clay beds (Davis and Bentley, 1982). The degree of isotope fractionation is proportional to the extent of aquifer water filtration through the membranes (Phillips et al, 1986). Careful examination of the hydrogeologic setting is necessary to determine the extent of filtration, if any.

Two other possible mechanisms for reference species concentration variations have been suggested.

4) Fluid inclusion diffusion. The diffusion of a reference species from fluid inclusions within crystalline rocks could be significant in altering species concentrations within an aquifer (Davis and Bentley, 1982).

5) Matrix solution. Possible dissolution or precipitation of minerals and aquifer matrix materials associated with the reference species may change the groundwater composition along the direction of flow within an aquifer (Phillips et al, 1986).

The mechanisms given above are site specific, and individually or collectively may not apply to a given site. Careful case by case evaluation is necessary (Davis and Bentley, 1982).

Importance to Applications

Dispersion induced advection can have a noticeable effect on groundwater age and related

calculations whenever the corrective term for effective velocity (36) is significant. Application of the dispersion induced advection to groundwater investigations requires the recognition of reference species concentration gradients. As previously noted, even apparently homogeneous aquifers can have a wide variation in properties depending upon the scale of the investigation. Reference concentration gradients may exist due to physical and chemical controls. Thus, a thorough study and sampling of the aquifer and surrounding units is requisite to help determine hydraulic gradients, concentration gradients and their mechanisms, and geologic controls on the system.

Graphic presentation of gathered isotopic data is useful in the recognition of concentration gradients and the underlying driving forces. Approximate groundwater ages may be calculated from isotopic ratios at sampling points, plotted on an aerial map, and compared with hydrodynamic ages. A discrepancy may indicate a reference species concentration gradient.

Trends in isotopic concentration can also be examined by plotting the isotopic ratio against the rare isotope concentration. For a case with only radioactive decay operating, simple trends are expected. An example is given for ^{36}Cl is given in Figure 3. The composition progresses along a line between the initial composition and the origin if the only active process is aging by decay (Phillips et al., 1986). The presence of other controls on the isotope concentration may be easily deduced. The progressive addition of "dead" chlorine will decrease the $^{36}\text{Cl}/\text{Cl}$ ratio, but the ^{36}Cl concentration will remain constant and the samples fall on a vertical line. Evaporation or ion filtration will increase the ^{36}Cl concentration, but the ratio will remain constant and the samples fall on a horizontal line (Bentley et al., 1986, Phillips et al., 1986). The older samples in the example do not fall on a simple decay line, and many extend horizontally away from the origin. Phillips et al. (1986) conclude that another process along with simple decay influenced the composition of the older samples. In general, discrepancies between data collected and the hydrogeologic model warrant reevaluation of the hydrodynamic model, the conceptual model, or further

investigation of the hydrologic system.

GRAPHICAL EXAMINATION OF DISPERSION INDUCED ADVECTION

One Dimensional Finite Element Transport Model

The superposition of a tracer isotope mass transport solution upon a reference species concentration gradient demonstrates the effects of dispersion-induced advection. Tracer mass transport distribution curves for a pulse input may be generated using the one-dimensional analytic solutions to the convective-dispersive equation, such as those published by van Genuchten and Alves (1982). When tracer curves with a pulse input, no radioactive decay, and no sources or sinks are superimposed upon a reference species concentration without a gradient (the commonly assumed case, Figure 4), the symmetry of the ratio curves does not change with respect to their x axis centroids. Only the relative concentration magnitude may vary uniformly over the model. Given $\partial S/\partial x = 0$, the dispersion-induced advection term (34) goes to zero, and the ratio transport equation reduces to the standard one dimensional advective-dispersive equation (21). Superimposing tracer curves upon a reference species concentration with a significant gradient (41) yields ratio transport curves altered with respect to their original form (Figure 5). The individual ratio curves are spatially distributed in terms of the effective velocity (35), not in terms of the average linear velocity. Symmetry about the x axis centroid no longer exists. Instead, the curves are skewed about their former centroids. The ratio curves now have a steeper slope in the down gradient (reference species) direction and a more shallow slope in the up gradient direction. The shape and sign of the reference species concentration gradient control the degree of ratio curve modification (Figure 6). The hydrologic parameters selected for the analytic and finite element transport solutions for all cases examined in this study may be found in Table 2.

The ratio concentration magnitude decreases as the reference ion concentration increases. Thus,

for ratio transport curves at large times (i.e. low isotope concentrations) or where the background concentration is high, comparison of the original trace isotope curves and the ratio curves is difficult (Figure 7). Normalizing both the trace isotope and ratio curves by the maximum concentration for each curve produces a family of curves that are readily comparable (Figure 8). The effects of dispersion-induced advection are first examined graphically by the superposition of trace isotope curves upon reference isotope concentrations with gradients varying in shape and sign.

Solutions to the one-dimensional advective-dispersive equation (22) for isotopic tracer mass transport are accomplished numerically with a finite element model. The one-dimensional model assumes that: the media is homogeneous, isotropic, and completely saturated; the flow is steady state; any isotope or reference ion entering the system downstream completely mixes over the cross-sectional area; and the model is aligned with the principal flow axis. The Galerkin approach to the method of weighted residuals solution technique is naturally suited to finite element applications (Huyakorn and Pinder, 1983) and was employed in the model. Relying upon the assumption that the integral mass balance over the entire solution region is equal to the summation of the integrals performed over the element subregions, the method of weighted residuals approximates the solution over the element subregion and minimizes the residual, or difference between the actual and approximate solutions, through the use of elemental weighting functions. The Galerkin approach sets the elemental weighting functions and elemental shape functions equal. For a more detailed explanation of the Galerkin approach see Wang and Anderson (1982) and Huyakorn and Pinder (1983).

The arbitrary domain chosen to solve the advective-dispersive equation (22) is 100cm in length and discretized into 100 linear finite elements, each 1 cm in length. Chapeau shape and weighting functions are applied to each element (Figure 9). The average linear velocity is 2 cm/sec and the dispersion coefficient is equal to 5 cm²/sec. Huyakorn and Pinder (1983) suggest that for the solution of advection-dominated problems the element size, Δl , should be such that $\Delta l \leq 10D/v$ and that the time step

size Δt be selected such that the local Courant number, defined as $C_r = v\Delta t/\Delta l$, is less than or equal to 1. With these criteria in mind, a time step of 0.25 seconds is chosen so that both conditions are satisfied, (i.e. $\Delta l = 1\text{cm} \leq 10(5\text{cm}^2/\text{sec})/2\text{cm}/\text{sec} = 25\text{cm}$ and $\Delta t = 0.25\text{sec} \leq \Delta l/v = 1\text{cm}/2\text{cm}/\text{sec} = 0.5\text{ sec}$). Use of the unconditionally stable Crank-Nicholson time stepping technique (Huyakorn and Pinder, 1983) is employed in the model.

Wang and Anderson (1982) note that all numerical solutions of the advective-dispersive equation include numerical errors to some degree. In advection-dominated cases, numerical overshoot and undershoot may be observed in the Galerkin finite element solution near the concentration front. Pinder and Grey (1977) offer one theoretical explanation of this behavior. Theoretical investigation and experience of other workers (Price et al, 1966, Huyakorn and Pinder, 1983, and others) suggest that numerical oscillations can be greatly reduced in Galerkin finite element solutions by using linear shape functions, if the local Peclet number does not exceed 2. The local Peclet number is defined as $P_e = v\Delta l/D$ and for this model, $P_e = (2\text{cm}/\text{sec})(1\text{cm}/5\text{cm}^2/\text{sec}) = 0.4$. The criteria is met.

The boundary and initial conditions for a step trace isotope input are given as

$$\begin{aligned} C(0, t) &= C_0 & t \leq t_0 \\ C(0, t) &= 0 & t > t_0 \end{aligned} \tag{42}$$

$$C(100, t) = 0 \quad \text{for all } t \tag{43}$$

The left boundary condition is a Dirichlet condition for a pulse input of duration t_0 . The right boundary condition is an approximation of the infinite boundary condition $C(\infty, t) = 0$. As suggested by Wang and Anderson (1982), the finite element solution is limited to times less than the time necessary for the solute front to travel two-thirds of the model length, i.e. 66cm of the 100cm model. The initial condition is

$$C(x, 0) = 0 \quad \text{for all } x \tag{44}$$

Terms for radioactive decay of the tracer and a mass-lumped source/sink are included in the model. A

complete listing of the model code is given in Appendix A.

The finite element model was validated by comparison of results with those of van Genuchten and Alves' (1982) analytic solution to the one-dimensional, semi-infinite advective-dispersive case. Examination of Figure 10 reveals a very slight disparity between the two solutions only near the left boundary for early time. The agreement between the two solutions at all other times and locations is excellent.

Graphical Superposition

Effects of a reference species concentration gradient upon the spatial distribution of isotopic ratios are examined first by the superposition of an isotope tracer distribution upon a reference species gradient. The Galerkin finite element model for the one-dimensional advective-dispersive transport described in the previous section was used to generate the trace isotope distribution curves. Reference species concentration gradients are chosen using the criteria that the concentration change by one order of magnitude in a distance not to exceed 46 dispersivity lengths (41). The term "positive gradient" refers to an increasing reference isotope concentration from left to right in the model. Conversely, a "negative gradient" refers to a decreasing reference isotope concentration from left to right. A summary of all model constraints is given in Table 2. As noted earlier, superposition of the trace isotope curve upon the reference species produces a ratio distribution curve that is reduced in concentration magnitude. To facilitate comparison, the curves are normalized by multiplying each by the reciprocal of their respective maximums.

Diffusion

In the absence of an advective velocity, a pulse input of tracer exhibits a Gaussian distribution of concentration in space with respect to time (Figure 11). The decrease in concentration and corresponding increase in the spread of the curve is governed by Fick's First Law. Given the Gaussian spatial

concentration distribution, a curve at any point in time may be normalized by its standard deviation and maximum concentration. Thus, the effect of a reference species concentration gradient on a pulse input, acted upon by diffusion only, at any point in time is derived from superimposing a Gauss normal curve upon the background gradient.

Examined are four cases, the background concentration gradient varied by one order of magnitude over two and four standard deviations about the x-axis of the Gaussian tracer curve, with both positive and negative gradients (Figure 12). The ratio transport equation (34) reduces to

$$D \frac{\partial^2 R}{\partial x^2} + \frac{2D}{S} \frac{\partial S}{\partial x} = \frac{\partial R}{\partial t} \quad (45)$$

for the diffusion only case ($v, \lambda, q = 0$). Since $D = \alpha v + D^*$ (7) and $v = 0$, then $D = D^*$ and (45) becomes

$$D^* \frac{\partial^2 R}{\partial x^2} + \frac{2D^*}{S} \frac{\partial S}{\partial x} = \frac{\partial R}{\partial t} \quad (46)$$

In the positive (reference isotope concentration) gradient direction the concentration front of the ratio becomes steeper and retarded from the original tracer position. As S gets large, the term

$$\frac{2D^*}{S} \frac{\partial S}{\partial x} \quad (47)$$

becomes negligible, and the separation distance between the two curves diminishes. In the negative gradient direction the correction term (47) increases the separation distance and decreases the slope of the ratio front. As the strength of the gradient becomes larger, the separation distance between the two curves grows.

Pulse Input

A one-second tracer pulse input is modeled using the one-dimensional Galerkin finite element model previously described. It is assumed that the tracer is ideal (i.e. non-reactive with the media), no

sources or sinks are present, and no radioactive decay of the tracer takes place. As before, the model is assumed to have a constant advective velocity of 2 cm/sec, ~~no sources or sinks, no radioactive decay, and an ideal tracer~~. The isotope tracer pulse duration is 1 second and the advective front curves are given at 2, 10, 20, and 30 seconds. A complete set of model parameters is given in Table 2. The reference species concentration gradient varies by one order of magnitude over 50 cm, equivalent to 20 dispersivity lengths. Superposition of the tracer curves upon the positive background concentration gradient (Figure 13) results in ratio tracer curves increasingly diminished in strength as the distance traveled becomes greater (Figure 14). ^{IN THE UPPER RIGHT HAND CORNER OF FIGURE 14 IS A PICTOGRAPH OF} The negative gradient case (Figure 15) results in maximum reduction of ratio concentration near the ^{THE INITIAL CONDITION AND BOUNDARY CONDITIONS USED IN THIS SIMULATION.} origin and diminishing effects towards the right boundary.

~~SIMILAR PICTOGRAPHS ARE INCLUDED IN ALL ISOTOPE FIGURES CONCERNING ISOTOPE RATIOS.~~ ^{FOLLOWING}

Examination of the normalized curves for the positive gradient case reveal the retardation and skewing of the ratio pulse with respect to the original tracer pulse (Figure 16). Note that the curve separation grows towards a maximum rapidly and then stabilizes. This behavior is explained by re-examination of the effective velocity term (35). The effective velocity was given as

$$v_{\text{eff}} = v - \frac{2D}{S} \left(\frac{\partial S}{\partial x} \right) \tag{48}$$

For the case when dS/dx is a constant, that is

$$S = S_0 + bx \tag{49}$$

the effective velocity (49) may be rewritten as

$$v_{\text{eff}} = v - \frac{2D}{S_0 + bx} \frac{d(S_0 + bx)}{dx} \tag{50}$$

or

$$v_{\text{eff}} = v - \frac{2Db}{S_0 + bx} \tag{51}$$

As x gets large,

$$\frac{2Db}{S_0 + bx} \cong \frac{2D}{x} \quad \text{or} \quad v_{\text{eff}} = v \tag{52}$$

and the ratio advects at the same rate as the isotope.

The same is true for the negative gradient case (Figure 17). Positions of the tracer and isotope curves are almost identical near the left boundary, and the ratio curve advances more rapidly than the isotope curve towards the right boundary. Given that

$$S = S_o - bx \quad (53)$$

(52) becomes

$$-\frac{2Db}{S_o - bx} \equiv -\frac{2D}{x} \quad (54)$$

or simplifying

$$v_{\text{eff}} \equiv v \quad (55)$$

At great distances dispersion effects make the correction insignificant in either case.

Source/Sink Boundary Condition

A selective source/sink case is examined by the addition of a prescribed leakage along the length of the model. Applied in the source/sink term of the Galerkin finite element model, only water, no solute, is allowed to enter or exit the system. The strength of the flux, $q' = 4.5E-3$ cm/s was chosen with consideration of the mass balance in the sink case.

The finite element model is run with the source/sink to produce consistent tracer curves and a reference species background curve. Uniform influx of water has the effect of diluting both the tracer and reference concentrations, and advancing the tracer pulse (Figures 18,19) by increasing the advective velocity of the system (Figure 20). Further advanced are the ratio curves (Figure 21) by the decreasing reference concentration towards the right boundary. Comparison of the source/sink ratio curves with the isotope curves from the simple model above (Figures 22,23) emphasize the effects of both the source/sink

and the background concentration gradient. The ratio curves have progressed further and are larger in magnitude. The converse holds true for the uniform sink case (Figures 24,25). Decreasing advective velocity and increasing concentrations towards the right boundary retard and reduce the ratio curves relative to the isotope only case (Figures 26,27,28). Failure to recognize either phenomenon could produce anomalous results in the interpretation of isotope ratio data. Again, all the hydrologic parameters used are given in Table 2.

Radioactive Decay

The model is run for radioactive decay of the tracer, with and without the source/sink term, for the positive and negative gradient cases examined earlier. Decay of the tracer has the effect of more rapidly reducing the ratio curves as the right-hand boundary is approached (Figure 29). The source/sink term will respectively accelerate or decelerate the transport time of the isotope through the model, and thereby diminish or accentuate the effect of radioactive decay of the tracer (Figures 30,31). Additionally, the associated effect of the source/sink upon the reference species will enhance the effects upon the tracer (Figures 32,33). Normalization of the curves negates the radioactive decay and the ratio curves are the same as those previously described for the linear background concentration gradient.

Step Input

Step tracer input is examined using the developed finite element model. Only the tracer input time changed from the pulse input parameters. Travel times were limited to a maximum of 30 seconds to stay within the semi-infinite approximation. The boundary conditions were given as

$$\begin{aligned}
 C(0, t) &= C_0 & t > 0 \\
 C(100, t) &= 0 & t > 0
 \end{aligned} \tag{56}$$

and the initial condition remained as

$$C(x, 0) = 0 \quad \text{for all } x \quad (57)$$

As above, the effect of a linear background concentration gradient or a source/sink boundary, both with and without radioactive decay of the tracer, on the concentration and spatial distribution of the isotopic ratio curves are examined.

Step tracer input concentration curves (Figure 34) are superimposed upon a linear reference species concentration gradient (Table 2). A positive background concentration gradient has no effect at the left boundary and significant influence away from the left boundary (Figure 35). Superposition results in isotopic ratio curves that are greatly retarded and diminished from the original tracer curves (Figure 36). As all curves with a positive reference species gradient have a common relative concentration of 1 at the left boundary, normalization of both families of curves by their respective maximum relative concentrations would produce identical results. A negative background concentration gradient with increasing x effects the left boundary and the entire modeled length (Figure 37). Examination of the normalized curves reveals that the isotope ratio curves are spatially advanced and have redistributed concentrations relative to the tracer curves (Figure 38). Perhaps most significant is the shape of the ratio curves, as any one curve does not appear to reflect the constant tracer input.

Transport curves for both the isotopic tracer and the background reference concentration are modeled using a step tracer input with addition of the source/sink boundary condition given previously. As observed in the pulse input source/sink case, a water source advances the isotopic ratio advective front (Figure 39) and a water sink retards the front (Figure 40) with respect to the no source/sink tracer front. At large distances, the displacement is approximately halfway between the analytical curve at the same time and the analytical curve at the next time (in this case, 20 and 30 seconds) for the sink case (Figure 40). The common left boundary condition of the relative concentration as one eliminates normalizing the curves.

Radioactive decay of the isotopic tracer is the final case run to examine the effects of a reference species gradient on the isotopic ratio distribution. Decay of the tracer reduces the tracer concentration and further spreads the ratio advective front relative to the no decay case (Figure 41). Addition of a reference species gradient affects the advective front further. Similar to the no decay case, a positive linear gradient retards the front (Figure 42) and a negative linear gradient advances it (Figures 43,44). A source/sink boundary condition affects the advective front to a lesser degree (Figures 45,46).

Discussion

Superposition of finite element model solutions to the one dimensional transport of an isotopic tracer upon a reference species concentration gradient demonstrates the principal of dispersion induced advection. A positive concentration gradient of the reference species in the direction of isotopic transport retards the travel distance of the isotopic ratio front. The front becomes steeper. A negative reference species concentration gradient has opposite effects. The travel distance of the isotopic ratio front increases and the front becomes shallower. Effects of additional terms such as a source/sink or radioactive decay may be strengthened or weakened depending upon the DIA term and direction of the reference species concentration gradient.

Dispersion induced advection does effect the observed magnitude and distribution of an isotopic ratio transported in a groundwater system. The extent to which the isotopic ratio is effected is a function of physical and chemical input and controls of each system. In the following section the one dimensional, finite element model is modified in an attempt to directly model the dispersion induced advection equation (34) derived earlier.

DISPERSION INDUCED ADVECTION MODEL

Dispersion induced advection is modeled directly by modifying the one dimensional Galerkin finite element advective-dispersive model developed above (Appendix A) in order to directly simulate isotope ratios. The only correction need is for the influence of a non-zero reference species concentration gradient on the effective advective velocity term (35). Then the ratio model, with the dispersion induced advection equation (34), can be represented by the same computer code as the advective-dispersive equation (23). Formulation of the advective element matrix is altered to include the reference isotope gradient correction term (35). Model input parameters remain unchanged unless otherwise noted. Modification of the boundary conditions were required to include a ratio concentration input. The boundary conditions for a pulse input are given as

$$\begin{aligned}
 R(0, t) &= R_0 & 0 < t \leq t_0 \\
 &= 0 & t > t_0, t < 0 \\
 R(100, t) &= 0 & \text{for all } t
 \end{aligned} \tag{58}$$

Given an initial isotope tracer concentration condition

$$C(x, 0) = 0 \tag{59}$$

and a reference concentration condition

$$S(x, t) = f(x) \quad \text{for all } t \tag{60}$$

the initial condition was given as

$$R(x, 0) = 0. \tag{61}$$

The reference species concentration gradient condition is imposed temporally and spatially upon the model in the advective velocity correction term (35). For a non-zero initial trace isotope condition over the length of the model, the ratio initial tracer condition would also be non-zero. This condition can not be physically "held" by the boundary conditions, either in the mathematical formulation of the model or by a

step input of a reference species along the boundary, if the reference species concentration varies in space. Holding the background condition violates Le Chatlier's Principle of Equilibrium and the processes of dispersion and diffusion acting on both the tracer and reference species. A stepped input along the upper or lower boundary of the model for the reference species would require the input of concentration only, no mass, so as not to affect the mass balance. This boundary condition is not representative of actual field conditions. The use of a more complicated chemical model to allow diffusion of the reference species across the an upper or lower model boundary is not considered in this study.

With the inclusion of the advective velocity correction term, two cases are considered for the finite element model: pulse tracer input with a constant reference species gradient, $dS/dx = G_1$; and pulse tracer input with a constant advective velocity correction term, $1/S * dS/dx = G_2$. As before, the model is assumed to have a constant advective velocity of 2 cm/sec, no sources or sinks, no radioactive decay, and an ideal tracer. The isotope tracer pulse duration is 1 second and the advective front curves are given at 2, 10, 20, and 30 seconds. A complete set of model parameters is given in Table 2.

Constant Common Isotope Concentration Gradient

Mathematical description of the initial and boundary conditions required to allow a flow model to accurately represent advective - dispersive processes and maintain a constant reference species gradient is difficult. Attempted convolutions of the input boundary condition deviate widely from physical reality and still do not bring the numerical solution into agreement with the analytical. Two conclusions may be drawn from the results; 1) the description of the appropriate initial and boundary conditions requires study at much greater length, and may still remain unsolvable, 2) when an isotopic ratio is encountered and the possibility of a linear reference species concentration gradient is discerned, it is best to examine both components of the ratio individually

Constant Advective Correction Term

A reference species concentration is chosen to vary along the length of the model such that

$$\frac{1}{S} \frac{dS}{dx} = G, \text{ a constant} \quad (62)$$

Rearranging the terms of (62)

$$\frac{1}{S} dS = G dx \quad (63)$$

Integrating both sides yields

$$\ln(S) = Gx \quad (64)$$

or

$$S = e^{Gx} \quad (65)$$

Substitution of (65) into the advective velocity correction term (35) yields

$$v - \frac{2D}{S} \frac{dS}{dx} = v - \frac{2D}{e^{Gx}} \frac{d(e^{Gx})}{dx} \quad (66)$$

$$= v - \frac{2DGe^{Gx}}{e^{Gx}} \quad (67)$$

$$= v - 2DG \quad (68)$$

Using the values of the model parameters in (68), it is found that $G > v/2D$ in order for the correction term to exceed advective velocity.

The numerical model is examined versus the analytical model for three values of the constant advective correction term, G . The reference species concentration is allowed to vary by 1 and 2 orders of magnitude through the selection of the constant, G , as 0.023 and 0.046 respectively. In addition, a value of $G = 0.03$ is selected to approximate a reference species concentration change similar to that of the positive linear gradient case. The input boundary conditions are again a 1 second pulse input and a step input.

The disparity between the ratio concentrations for the numerical and analytical solutions increases with the greater variation in the reference species concentration across the model for the pulse input (Figures 47,48,49). Normalization of the solutions to both models for all three values of the constant demonstrates the agreement in spatial distribution (Figure 50). The constant input solutions for the two models agree neither in concentration nor spatially, with an increasing difference in distribution with increasing values of the constant G. It is apparent from the results above that agreement between the two solutions to the constant advective velocity correction term is approached only as the correction term approaches zero.

CONCLUSIONS

Groundwater age determination is a valuable tool in understanding a hydrologic system and its properties. The methods most commonly used are hydrodynamic and isotopic dating. Hydrodynamic dating requires estimation of hydrogeologic parameters that may vary spatially, temporally, or both. In systems involving long travel times, large distances, or complex geology, the hydrodynamic approach is limited in usefulness by the requisite assumption of uniformity in space and time.

Isotopic tracers have been used since the 1950's to determine flow rates, mixing of groundwaters, and related hydrogeologic parameters. Introduced into the hydrologic cycle naturally, as a by-product of man's activities, or artificially, isotopes used as tracers may be either stable or radioactive. Ideal properties for isotopes to be used as tracers have been summarized briefly in this paper, and at greater length by Bentley et al. (1985) and Toran (1982).

All chemical elements possess two or more isotopes. Isotopic data is most often examined in terms of a mass ratio between the rare isotope and reference, or common, isotope in a sample. The isotope ratio is "dated" by comparison with a reference standard, if both isotopes are stable, or with an assumed initial input ratio, if the tracer is radioactive. The measurement of isotopes in terms of a ratio frequently leads to the modeling of isotopic mass transport in terms of a ratio.

Sudicky and Frind (1981) have noted that if the reference species concentration varies, the tracer content in any mass transport model must be in terms of a solution concentration. Isotopic ratios are measured as the mass of the rare isotope relative to a given mass of the common isotope. If the concentration of the common isotope varies within a hydrologic system, then the volume of water required to contain a given mass varies as well. No longer does the ratio, or concentration of the rare isotope, vary solely due to natural processes. For the stable isotopes of ^{18}O and ^2H and the radioactive isotope ^3H , the reference species concentrations are unlikely to vary as they (^{16}O and ^1H respectively) comprise the solute, water. For other commonly used isotopes such as ^{13}C , ^3H and ^{36}Cl , the concentration of the reference species may change within an aquifer due to physical and chemical controls.

Examination of the effects of a concentration gradient in the common (reference) isotope upon isotopic ratios and inferences that might be drawn from them were examined in this paper through the development of a mass transport equation in terms of both the rare and common isotope. Derivation of the isotope ratio transport equation led to an additional advective term due to the reference species gradient. This term was labeled dispersion induced advection. Dispersion induced advection was observed to have the effect of altering the effective velocity for the ratio.

Further examination of dispersion induced advection was achieved by two means. First, analytical and finite element solutions to the transport of the rare isotope were graphically superposed upon a

reference species gradient. Second, a one dimensional finite element transport model for the ratio was developed to include dispersion induced advection.

Graphical superposition of an numerical solution to rare isotope transport upon a common isotope concentration gradient clearly indicates that dispersion induced advection can significantly alter the position and magnitude of an isotopic ratio. The centroid of the isotopic ratio pulse along the flow line shifts relative to the original rare isotope pulse. The magnitude of the isotopic ratio with a common isotope concentration gradient is reduced relative to an isotope ratio without a common isotope concentration gradient. In the case of a step input, the position and magnitude of an isotopic ratio with a common isotope concentration gradient is altered in relation to a zero gradient common isotope concentration isotopic ratio.

The direct model of isotope ratios, with DIA, did not work. Difficulty was encountered in maintaining the initial condition for the case of a constant reference species gradient in the finite element model. Holding a reference species gradient constant in time and space, while introducing a pulse of the rare species that will move and disperse, would either violate Le Chatlier's Principle of Equilibrium or disrupt the mass balance within the model. Differences between the actual rate of flux and that given by the dispersion induced advection ratio equation into the left hand side of the model led to modification of the left hand boundary condition by multiplication of the input ratio by the ratio of the two fluxes. The ratio model and graphical superposition still did not agree.

A second reference species gradient was chosen for the isotope ratio numerical model such that the dispersion induced advection correction term was a constant. Numerical and analytical solutions were compared for both the pulse and constant input boundary conditions. The degree by which the ratio and superposition solutions disagreed was directly correlated to the magnitude of the correction constant. This

observation serves to support Sudicky and Frind's (1981) conclusion that if even small variations in the reference species concentration exist, the two components of the isotope in question should be examined individually.

Variations in reference species concentrations do occur in hydrologic systems. Difficulties encountered in modeling dispersion induced advection in a simplified one dimensional setting serve to point out problems that may be encountered in modeling ratio mass transport when the reference species concentration varies. Description of the reference species concentration gradient and the boundary conditions are complicated and may no longer be well grounded in physical reality. The addition of a second or third dimension, and heterogeneities only serve to further complicate the task. In summary, if differences in the reference species exist within the hydrologic system studied, the isotope concentrations should be expressed as solution concentrations and their transport modeled individually.

REFERENCES

- Bear, J. 1972. *Dynamics of Fluids in Porous Media*. American Elsevier, New York.
- Bear, J. 1979. *Hydraulics of Groundwater*. McGraw-Hill, New York.
- Bentley, H.W., F.M. Phillips, S.N. Davis, M.A. Habermehl, P.L. Airey, G.E. Calf, D. Elmore, H.E. Gove, and T. Torgersen. 1986. Chlorine 36 Dating of Very Old Groundwater, 1, The Great Artesian Basin, Australia. *Water Resources Res.*, 22, no 13, pp 1991-2001.
- Coplen, T.B. and B.B. Hanshaw. 1973. Ultrafiltration by a Compacted Clay Membrane: I. Oxygen and Hydrogen Isotope Fractionation. *Geochim. Cosmochim. Acta*, 37, pp 2295-2310.
- Davis, S.N. and H.W. Bentley. 1982. Dating Ground Water. A Short Review. ACS Symposium Series No. 176. *Nuclear and Chemical Dating Techniques: Interpreting the Environmental Record*, ed. L.A. Currie. American Chemical Society, pp 188-222.
- Freeze, R.A. 1975. A Stochastic-Conceptual Analysis of One-dimensional Groundwater Flow in Nonuniform Homogeneous Media. *Water Resources Res.*, 11, no 5, pp 725-741.
- Freeze, R.A. and J.A. Cherry. 1979. *Groundwater*. Prentice-Hall, Englewood Cliffs, N.J.
- Gelhar, L.W. 1986. Stochastic Subsurface Hydrology From Theory to Applications. *Water Resources Res.*, 22, no 8, supplement, pp 135s-145s.

Gelhar, L.W. and C.L. Axness. 1983. Three-Dimensional Stochastic Analysis of Macrodispersion in Aquifers. *Water Resources Res.*, 19, no 1, pp 161-180.

Graham, W. and D. McLaughlin. 1989. Stochastic Analysis of Nonstationary Subsurface Solute Transport, 1, Unconditional Moments. *Water Resources Res.*, 25, no 2, pp 215-232.

Halvey, E. and A. Nir. 1960. Use of Radio-Isotopes in Studies of Groundwater Flow. *Water Planning for Israel Ltd.*, Tel-Aviv.

Hanshaw, B.B. and T.B. Coplen. 1973. Ultrafiltration by Compacted Clay Membrane: II. Sodium Ion Exclusion at Various Ionic Strengths. *Geochim. Cosmochim. Acta*, 37, pp 2311-2327.

Huyakorn, P.S. and G.F. Pinder. 1983. *Computational Methods in Subsurface Flow*. Academic Press, Orlando.

Ogata, A. 1970. Theory of Dispersion in a Granular Medium. *U.S. Geol. Surv. Prof. Paper 411-I*. 34p.

Phillips, F.M., H.W. Bentley, S.N. Davis, D. Elmore, and G.B. Swanick. 1986. Chlorine 36 Dating of Very Old Groundwater, 2, Milk River Aquifer, Alberta. *Water Resources Res.*, 22, no 13, pp 2003-2016.

Pinder, G.F. and W.G. Gray. 1977. *Finite Element Simulation in Surface and Subsurface Hydrology*. Academic Press, Orlando.

Price, H.S., R.S. Varga, and J.E. Warren. 1966. Application of Oscillation Matrices to Diffusion-Convection Equations. *J. Math Phys.*, 45, pp 301 - 311.

Schwartz, F.W. and K. Muchlenbachs. 1979. Isotope and Ion Geochemistry of Groundwaters in the Milk River Aquifer, Alberta. *Water Resources Res.*, 15, no 2, pp 259-268.

Sudicky, E.A. and E.O. Frind. 1981 Carbon 14 Dating of Groundwater in Confined Aquifers: Implications of Aquitard Diffusion. *Water Resources Res.*, 17, no 4, pp 1060-1064.

Toran, L. 1982. Isotopes in Ground-Water Investigations. *Groundwater*, 20, no 6, pp 740-745.

van Genuchten, M.T. and W.J. Alves. 1982. Analytical Solutions of the One-Dimensional Convective-Dispersive Solute Transport Equation. U.S. Department of Agriculture, Technical Bulletin No. 1661.

Wang, H.F. and M.P. Anderson. 1982. Introduction to Groundwater Modeling. Finite Difference and Finite Element Methods. Freeman, San Francisco.

```

C
C *****
C
C ONE DIMENSIONAL CONVECTIVE-DISPERSIVE EQUATION
C
C SEMI-INFINITE PROFILE
C
C NO PRODUCTION OR DECAY
C LINEAR ADSORPTION (R)
C CONSTANT INITIAL CONCENTRATION (CI)
C INPUT CONCENTRATION = CO (T.LE.TO)
C = 0 (T.GT.TO)
C *****
C *****
C
C DIMENSION TITLE(20)
C DOUBLE PRECISION A,B,C,CM,CM2,CP,D,E,EXF,Q,T
C CHARACTER*20 PDF
C OPEN(97,FILE='A1IN.DAT')
C* OPEN(98,FILE='A1OUT.DAT')
C WRITE(*,*) 'OUTPUT PLOT DATA FILE?'
C READ(*,'(A)') PDF
C OPEN(99,FILE=PDF,STATUS = 'NEW')
C
C **READ NUMBER OF CURVES TO BE CALCULATED**
C READ(97,1000) NC
C DO 4 K=1,NC
C READ(97,1001) TITLE
C* WRITE(98,1002) TITLE
C
C **READ AND WRITE INPUT PARAMETERS**
C READ(97,1003) V,D,R,TO,CI,CO
C READ(97,1003) XI,DX,XM,TI,DT,TM
C WRITE(*,1004) V,D,R,TO,CI,CO
C WRITE(*,*) 'INPUT 4 TIMES FOR WHICH CURVES ARE TO BE PLOTTED'
C READ(*,*) T1,T2,T3,T4
C WRITE(*,50) T1,T2,T3,T4
50 FORMAT('TIMES = ',4F5.2)
C
C *****
C D=D/R
C V=V/R
C IF(DX.EQ.0.0) DX=1.0
C IF(DT.EQ.0.0) DT=1.0
C IMAX=(XM+DX-XI)/DX
C JMAX=(TM+DT-TI)/DT
C E=0.0
C DO 4 J=1,JMAX
C** IF(IMAX.GE.J) WRITE(98,1005)
C TIME=TI+(J-1)*DT
C DO 4 I=1,IMAX
C WRITE(*,100) TIME,X

```

```

100      FORMAT(' + TIME = ',F5.2,' X = ',F6.2)
        X=X1+(1-1)*DX
        VVO=0.0
        IF(X.EQ.0.0) GO TO 1
        VVO=V*R*TIME/X
1        DO 2 M=1,2
          A1=0.0
          A2=0.0
          T=TIME+(1-M)*TO
          IF(T.LE.0.0) GO TO 2
          CM=(X-V*T)/DSQRT(4.0*D*T)
          CP=(X+V*T)/DSQRT(4.0*D*T)
          Q=V*X/D
          A1=0.5*(EXF(E,CM)+EXF(Q,CP))
          CM2 = -CM*CM
          A2=0.5*EXF(E,CM)+V*DSQRT(.3183099*T/D)*EXF(CM2,E)
1-0.5*(1.0+Q+V*V*T/D)*EXF(Q,CP)
          IF(M.EQ.2) GO TO 3
          CONC1=C1+(C0-C1)*A1
          CONC2=C1+(C0-C1)*A2
2        CONTINUE
3        CONC1=CONC1-C0*A1
        CONC2=CONC2-C0*A2
C*      WRITE(98,1006) X,TIME,VVO,CONC1,CONC2
        IF (TIME.EQ.T1) THEN
          WRITE(99,*) X,CONC1
        ELSEIF (TIME.EQ.T2) THEN
          WRITE(99,*) X,CONC1
        ELSEIF (TIME.EQ.T3) THEN
          WRITE(99,*) X,CONC1
        ELSEIF (TIME.EQ.T4) THEN
          WRITE(99,*) X,CONC1
        ENDIF
4        CONTINUE
C
C      *****
1000     FORMAT(15)
1001     FORMAT(20A4)
C1002    FORMAT(1H1,10X,82(1H*)/11X,1H*,80X,1H*/11X,1H*,
C        19X,'ONE-DIMENSIONAL CONVECTIVE-DISPERSIVE EQUATION',
C        225X,1H*/11X,1H*,80X,1H*/11X,1H*,9X,'SEMI-INFINITE
C        3PROFILE',50X,1H*/11X,1H*,9X,'NO PRODUCTION AND DELAY'
C        4,48X,1H*/11X,1H*,9X,'LINEAR ADSORPTION (R)',50X,1H*/
C        511X,1H*,9PX,'CONSTANT INITIAL CONCENTRATION (C1)',36X,
C        61H*/11X,1H*,9X,'INPUT CONCENTRATION = C0 (T.LE.TO)',
C        737X,1H*/11X,1H*,29X,'= 0 (T.GT.TO)',37X,1H*/11X,1H*,
C        880X,1H*/11X,1H*,20A4,1H*,80X,1H*/11X,82(1H*))
1003     FORMAT(8F10.0)
1004     FORMAT(//11X,' INPUT PARAMETERS'/11X,16(1H=)//11X,
1'V =',F12.4,15X,'D =',F12.4/11X,'R =',F12.4,15X,
2'TO =',F11.4/11X,'C1 =',F11.4,15X,'C0 =',F11.4)
1005     FORMAT(///11X,'DISTANCE',11X,'TIME',7X,'PORE
1 VOLUME',12X,'CONCENTRATION'/14X,'(X)',13X,'(T)',
211X,'(VVO)',6X,'FIRST TYPE BC',4X,'THIRD TYPE BC')
1006     FORMAT(4X,3(5X,F10.4),3X,F12.4,5X,F12.4)

```

```

C
C      *****
C*     CLOSE(UNIT=97)
      CLOSE(UNIT=98)
      CLOSE(UNIT=99)
      STOP
      END

      DOUBLE PRECISION FUNCTION EXF(A,B)
C
C     PURPOSE: TO CALCULATE EXP(A) ERFC(B)
C

      DOUBLE PRECISION A,B,C

      EXF=0.0
      IF((DABS(A).GT.170.0).AND.(B.GT.0.0)) RETURN
      IF(B.NE.0.0) GO TO 1
      EXF=DEXP(A)
      RETURN
1     C=A-B*B
      IF((DABS(C).GT.170.0).AND.(B.GT.0.0)) RETURN
      IF(C.LT.-170.0) GO TO 4
      X=DABS(B)
      IF(X.GT.3.0) GO TO 2
      T=1.0/(1.0+.3275911*X)
      Y=T*(.2548296-T*(.2844967-T*(1.421414-T*(1.453152-1.061405*T))))
      GO TO 3
2     Y=.5641896/(X+0.5/(X+1.5/(X+2.0/(X+2.5/(X+1.0))))))
3     EXF=Y*DEXP(C)
4     IF(B.LT.0.0) EXF=2.0*EXP(A)-EXF
      RETURN
      END

```

```

C-----
C GALERKIN (WEIGHTED-AVERAGE) FINITE-ELEMENT PROGRAM TO SOLVE
C 1-D CONVECTIVE-DISPERSION EQUATION WITH 1ST TYPE B.C.
C WRITTEN BY MARK WOLFF
C
C COMPUTES A/D EQ WITH SOURCE/SINK TERM
C-----
C
C Input Variables:
C
C NE = NO. ELEMENTS
C NNE = NO. NODES/ELEMENT
C TL = TOTAL LENGTH OF MODEL
C DL = LONGITUDINAL DISPERSION COEFFICIENT
C V = VELOCITY
C DELT = TIME INCREMENT
C T1 = TIME AFTER WHICH SOURCE IS SHUT DOWN
C T1 = FIRST PRINTOUT TIME
C T2 = SECOND PRINTOUT TIME
C T3 = THIRD PRINTOUT TIME
C FINTIM = TOTAL SIMULATION TIME
C E = WEIGHTING FACTOR
C 0.0 - EXPLICIT
C 0.5 - CRANK-NICHLSON
C 1.0 - IMPLICIT
C
C Other Program Variables:
C
C EL = ELEMENT LENGTH
C NN = NO. NODES
C CCO = NUMERICAL C/Co
C CCOA = ANALYTICAL C/Co
C PV = PORE VOLUMES
C
C-----
C* IMPLICIT REAL (L)
C* DIMENSION A(450),B(450),C(450),RHS(450),CCO(450),EPSI(450),
C* * CCOA(450),CCON(450),Z(450),W(450),
C* * A211(450),A212(450),A221(450),A222(450)
C* IMPLICIT REAL (ALAMBD,EL,TL)
C* CHARACTER PF*20
C
C Create input, output, and plot files
C
C OPEN (31,FILE='DIAIN.DAT')
C* OPEN (30,FILE='DIAOUT.DAT')
C* WRITE(*,*) 'OUTPUT PLOT FILE?'
C* READ(*,'(A1)') PF
C* OPEN (32,FILE='MRW.DAT')
C* OPEN (99,FILE='VELO.DAT')
C
C Read In data
C

```



```

READ (31,*) NE,NNE,TL,DL,V,DELT,T1,T1,T2,T3,FINTIM,E
READ (31,*) EPS,PORE,THETA,ALAMBD
WRITE(*,*) 'LAMBDA = ',ALAMBD
EL=TL/FLOAT(NE)
NN=NE*(NNE-1)+1
C
C*      WRITE(NWRITE,1003) NN,NE,NNE,EL,TL,DL,V,DELT,FINTIM,E
C*1003  FORMAT(' NO. NODES=',I2,3X,'NO. ELEMENTS=',I2,3X,
C*      * 'NODES/ELEMENT=',I2,/' ELEMENT LENGTH=',F6.4,3X
C*      * 'TOTAL LENGTH=',F8.2,3X,' DISPERSION=',F8.6/
C*      * ' VELOCITY=',F8.6,3X,'DT=',F8.2,3X,'FINTIM=',
C*      * F10.2,3X,'E=',F6.2/)
C
C  SET INITIAL CONDITIONS
C
      CCO(1) = 1.0
      DO 10 I = 2,NN
10      CCO(I) = 0.0
C
C  Form element matrices A1, A2, B
C
      DELC = 0.0
      A111 = (DL/EL) * 1.0
      A112 = -(DL/EL) * 1.0
      A121 = -(DL/EL) * 1.0
      A122 = (DL/EL) * 1.0
      DO 600 I = 1,NN
C*      DELC = -((EPS/(V*PORE))/(1.0+((EPS*(I-1))/(V*PORE))))
C*      EPS1(I) = -((V*PORE)/(I-1))*EXP(-1.0)
      VT = V + (EPS*(EL*(I-1)))/PORE
      WRITE(*,*) 'VELOCITY(CM/S) = ',VT,' AT X = ',I-1
      WRITE(99,*) I,VT
      A211(I) = -((VT/2)-(DL*DELC)) * 1.0
      A212(I) = ((VT/2)-(DL*DELC)) * 1.0
      A221(I) = -((VT/2)-(DL*DELC)) * 1.0
      A222(I) = ((VT/2)-(DL*DELC)) * 1.0
600    CONTINUE
      B11 = (EL/DELT) / 3.0
      B12 = (EL/DELT) / 6.0
      B21 = (EL/DELT) / 6.0
      B22 = (EL/DELT) / 3.0
C
C  Form A, B & C diagonals of global matrix
C
      DO 20 I=2,NN
      A(I) = E*(A121+A221(I))+B21
20    CONTINUE
      B(1) = E*(A111+A211(1))+B11
      B1 = B(1)
      B(NN) = E*(A122+A222(NN))+B22
      DO 30 I=2,NN-1
      B(I) = E*(A111+A122+A211(I)+A222(I))+B11+B22
30    CONTINUE

```

```

        DO 40 I=1,NN-1
          C(I) = E*(A112+A212(I))+B12
40      CONTINUE
C
C Begin time loop
C CALCULATE W TERMS FOR D.I.A. CASE
C W = (EPSILON/ne)*(C-Co)*THETA
C
1      CO = 0.0
        DO 500 II=1,NN
          W(II)=(EPS/PORE)*(CCO(II)-CO)*THETA + CCO(II)*ALAMBD
500    CONTINUE

        T=T+DELT
        WRITE(*,*) 'TIME = ',T
        IF(T.GT.T1)THEN
          CCO(1)=0.0
        ENDIF
C
C Form right-hand-side matrix
C
        RHS(1)=(E-1)*(A111*CCO(1)+A112*CCO(2))
        *      +(E-1)*(A211(1)*CCO(1)+A212(1)*CCO(2))
        *      +(B11*CCO(1)+B12*CCO(2))-W(1)/2.0
        DO 50 I=2,NN-1
          RHS(I)=(E-1)*(A121*CCO(I-1)+(A111+A122)*CCO(I)+A112*CCO(I+1))
        *      +(E-1)*(A221(I-1)*CCO(I-1)+(A211(I)+A222(I))*CCO(I)
        *      +A212(I)*CCO(I+1))+(B21*CCO(I-1)+(B11+B22)*CCO(I)
        *      +B12*CCO(I+1))-W(I)
50      CONTINUE
          RHS(NN)=(E-1)*(A121*CCO(NN-1)+A122*CCO(NN))
        *      +(E-1)*(A221(I)*CCO(NN-1)+A222(I)*CCO(NN))
        *      +(B21*CCO(NN-1)+B22*CCO(NN))-W(NN)/2.0
C
C Incorporate boundary condition of C/Co(1)=1.0
C
        IF(T.LE.T1)THEN
          RHS(1)=1.0*1E+15*B1
          B(1)=B1*1E+15
        ENDIF
C
C Call subroutine Tridag to solve for C/Co at next time step
C
        CALL TRIDAG (1,NN,A,B,C,RHS,CCO)
C
        IF (T.EQ.T1)THEN
          GOTO 100
        ELSEIF (T.EQ.T2)THEN
          GOTO 100
        ELSEIF (T.EQ.T3)THEN
          GOTO 100
C**      IF (T.EQ.FINTIM)THEN
        ELSEIF (T.EQ.FINTIM)THEN
          GOTO 100

```

```

        ENDIF
        GOTO 1

C
C   Compute Analytical Solution
C
C*100   X=2.*SQRT(DL*T)
C*      DO 70 I=1,NN
C*          Z(I)=FLOAT(I-1)*EL
C*          S1=ERFC((Z(I)-V*T)/X)
C*          S2=ERFC((Z(I)+V*T)/X)
C*          CCOA(I)=0.5*(S1+EXP(V*Z(I)/DL)*S2)
C*70    CONTINUE
100     CONTINUE

C
C   Print out results
C
C*      PV=V*T/TL
C*      WRITE(30,1000) PV
C*1000  FORMAT(/' PORE VOLUMES=',F6.3/)
C*      WRITE(30,1005)
C*1005  FORMAT('  I',3X,'      Z      ',3X,'      CCO(I)  ',3X,
C*      *      CCOA(I)  '/')
C*      DO 60 I=1,NN
C*          WRITE(30,1002) I,Z(I),CCO(I),CCOA(I)
C*1002  FORMAT(' ',12,3X,D12.4,3X,E12.6,3X,E12.6)
C*60    CONTINUE
C
C   Write data for plotting
C
        DO 75 I=1,NN
95      WRITE(32,1010) Z(I),CCO(I)
C*      DO 80 I=1,NN
C* 80    WRITE(32,1010) Z(I),CCOA(I)
1010   FORMAT(2F20.10)
C
        IF (T.EQ.FINTIM) STOP
        GOTO 1
        END

-----
C
C   SUBROUTINE TRIDAG (IF,L,A,B,C,D,V)
C
C   DIMENSION A(450),B(450),C(450),D(450),V(450),BETA(450),GAMMA(450)
C
C   BETA(IF)=B(IF)
C   GAMMA(IF)=D(IF)/BETA(IF)
C   IFP1=IF+1
C   DO 2001 I=IFP1,L
2001   BETA(I)=B(I)-A(I)*C(I-1)/BETA(I-1)
       GAMMA(I)=(D(I)-A(I)*GAMMA(I-1))/BETA(I)
C
C   V(L)=GAMMA(L)
C   LAST=L-IF
C   DO 2002 K=1,LAST

```

```
      I=L-K
2002  V(I)=GAMMA(I)-C(I)*V(I+1)/BETA(I)
      RETURN
      END
```

```

C-----
C GALERKIN (WEIGHTED-AVERAGE) FINITE-ELEMENT PROGRAM TO SOLVE
C 1-D CONVECTIVE-DISPERSION EQUATION WITH 1ST TYPE B.C.
C WRITTEN BY MARK WOLFF
C
C COMPUTES A/D EQ WITH SOURCE/SINK TERM
C-----
C
C Input Variables:
C
C NE = NO. ELEMENTS
C NNE = NO. NODES/ELEMENT
C LT = TOTAL LENGTH OF MODEL
C DL = LONGITUDINAL DISPERSION COEFFICIENT
C V = VELOCITY
C DELT = TIME INCREMENT
C T1 = TIME AFTER WHICH SOURCE IS SHUT DOWN
C T1 = FIRST PRINTOUT TIME
C T2 = SECOND PRINTOUT TIME
C T3 = THIRD PRINTOUT TIME
C FINTIM = TOTAL SIMULATION TIME
C E = WEIGHTING FACTOR
C 0.0 - EXPLICIT
C 0.5 - CRANK-NICHLSON
C 1.0 - IMPLICIT
C
C Other Program Variables:
C
C LE = ELEMENT LENGTH
C NN = NO. NODES
C RRO = NUMERICAL C/Co
C RROA = ANALYTICAL C/Co
C PV = PORE VOLUMES
C
C EPS = SOURCE/SINK RATE
C PORE = EFFECTIVE POROSITY
C THETA = WEIGHTING FACTOR
C LAMBDA = DECAY CONSTANT
C SLOPE = SLOPE OF BCG
C SO = Y AXIS INTERCEPT OF BCG
C S = BACKGROUND CONCENTRATION
C SP = SOURCE/SINK INPUT CONCENTRATION OF BACKGROUND SPECIES
C RROP = SOURCE/SINK INPUT RATIO
C
C-----
C IMPLICIT REAL (L)
C DIMENSION A(450),B(450),C(450),RHS(450),RRO(450),EPSI(450),
C * RROA(450),RRON(450),Z(450),W(450),S(450),
C * A211(450),A212(450),A221(450),A222(450)
C CHARACTER PF*20
C
C Create input, output, and plot files
C
C OPEN (31,FILE='DIAIN.DAT')
C* OPEN (30,FILE='DIAOUT.DAT')

```

```

WRITE(*,*) 'OUTPUT PLOT FILE?'
C* READ(*, '(A1)') PF
OPEN (32, FILE='EXP.DAT')
OPEN (99, FILE='VELO.DAT')
C
C Read In data
C
READ (31,*) NE,NNE,LT,DL,V,DELT,T1,T2,T3,FINTIM,E
READ (31,*) EPS,PORE,THETA,LAMBDA,SLOPE,SO,SP
LE=LT/FLOAT(NE)
NN=NE*(NNE-1)+1
C
C* WRITE(NWRITE,1003) NN,NE,NNE,LE,LT,DL,V,DELT,FINTIM,E
C*1003 FORMAT(' NO. NODES=',I2,3X,'NO. ELEMENTS=',I2,3X,
C* * 'NODES/ELEMENT=',I2,/' ELEMENT LENGTH=',F6.4,3X
C* * 'TOTAL LENGTH=',F8.2,3X,' DISPERSION=',F8.6/
C* * ' VELOCITY=',F8.6,3X,'DT=',F8.2,3X,'FINTIM=',
C* * F10.2,3X,'E=',F6.2/)
C
C SET INITIAL CONDITIONS
C
RRO(1) = 1.0/SO
S(1) = SO
DO 10 I = 2,NN
  S(I) = SO + SLOPE*(I-1)
  RRO(I) = RRO(I)/S(I)
WRITE(*,*) 'S(I) = ',I,S(I)
10 CONTINUE
C
C Form element matrices A1, A2, B
C
A111 = (DL/LE) * 1.0
A112 = -(DL/LE) * 1.0
A121 = -(DL/LE) * 1.0
A122 = (DL/LE) * 1.0
DO 600 I = 1,NN
  VT = V + (EPS*(LE*(I-1)))/PORE
  WRITE(99,*) I,VT
  A211(I) = -((VT/2)-(DL*(SLOPE/(SLOPE*(I-1)+SO)))) * 1.0
  A212(I) = ((VT/2)-(DL*(SLOPE/(SLOPE*I+SO)))) * 1.0
  A221(I) = -((VT/2)-(DL*(SLOPE/(SLOPE*(I-1)+SO)))) * 1.0
  A222(I) = ((VT/2)-(DL*(SLOPE/(SLOPE*I+SO)))) * 1.0
600 CONTINUE
B11 = (LE/DELT) / 3.0
B12 = (LE/DELT) / 6.0
B21 = (LE/DELT) / 6.0
B22 = (LE/DELT) / 3.0
C
C Form A, B & C diagonals of global matrix
C
DO 20 I=2,NN
  A(I) = E*(A121+A221(I))+B21

```

```

20     CONTINUE
      B(1) = E*(A111+A211(1))+B11
      B1 = B(1)
      B(NN) = E*(A122+A222(NN))+B22
      DO 30 I=2,NN-1
        B(I) = E*(A111+A122+A211(I)+A222(I))+B11+B22
30     CONTINUE
      DO 40 I=1,NN-1
        C(I) = E*(A112+A212(I))+B12
40     CONTINUE
C
C   Begin time loop
C   CALCULATE W TERMS FOR D.I.A. CASE
C   W = (EPSILON/ne)*(C-Co)*THETA
C
1     CO = 0.0
      DO 500 I1=1,NN
        W(I1)=(RRO(I1))*(SP/(S(I1)))*THETA+RRO(I1)*LAMBDA
500    CONTINUE

      T=T+DELT
      WRITE(*,*) 'TIME = ',T
      IF(T.GT.T1)THEN
        RRO(1)=0.0
      ENDIF
C
C   Form right-hand-side matrix
C
      RHS(1)=(E-1)*(A111*RRO(1)+A112*RRO(2))
      *      +(E-1)*(A211(1)*RRO(1)+A212(1)*RRO(2))
      *      +(B11*RRO(1)+B12*RRO(2))-W(1)/2.0
      DO 50 I=2,NN-1
        RHS(I)=(E-1)*(A121*RRO(I-1)+(A111+A122)*RRO(I)+A112*RRO(I+1))
        *      +(E-1)*(A221(I-1)*RRO(I-1)+(A211(I)+A222(I))*RRO(I)
        *      +A212(I)*RRO(I+1))+(B21*RRO(I-1)+(B11+B22)*RRO(I)
        *      +B12*RRO(I+1))-W(I)
50     CONTINUE
      RHS(NN)=(E-1)*(A121*RRO(NN-1)+A122*RRO(NN))
      *      +(E-1)*(A221(I)*RRO(NN-1)+A222(I)*RRO(NN))
      *      +(B21*RRO(NN-1)+B22*RRO(NN))-W(NN)/2.0
C
C   Incorporate boundary condition of C/Co(1)=1.0
C
      IF(T.LE.T1)THEN
        RHS(1)=1.0*1E+15*B1
        B(1)=(B1*1E+15)*S0
      ENDIF
C
C   Call subroutine Tridag to solve for C/Co at next time step
C
      CALL TRIDAG (1,NN,A,B,C,RHS,RRO)
C
      IF (T.EQ.T1)THEN

```

```

        GOTO 100
    ELSEIF (T.EQ.T2) THEN
        GOTO 100
    ELSEIF (T.EQ.T3) THEN
        GOTO 100
C**    IF (T.EQ.FINTIM) THEN
    ELSEIF (T.EQ.FINTIM) THEN
        GOTO 100
    ENDIF
    GOTO 1
100    CONTINUE

```

```

C
C Print out results
C

```

```

C*    PV=V*T/LT
C*    WRITE(30,1000) PV
C*1000 FORMAT(/' PORE VOLUMES=',F6.3/)
C*    WRITE(30,1005)
C*1005 FORMAT('  I',3X,'      Z      ',3X,'      RRO(I)  ',3X,
C*    * '      RROA(I)  '/')
C*    DO 60 I=1,NN
C*        WRITE(30,1002) I,Z(I),RRO(I),RROA(I)
C*1002    FORMAT(' ',12,3X,D12.4,3X,E12.6,3X,E12.6)
C*60    CONTINUE
C

```

```

C Write data for plotting
C

```

```

    DO 75 I=1,NN
    75    WRITE(32,1010) Z(I),RRO(I)
C*    DO 80 I=1,NN
C* 80    WRITE(32,1010) Z(I),RROA(I)
    1010    FORMAT(2F20.10)
C

```

```

    IF (T.EQ.FINTIM) STOP
    GOTO 1
    END

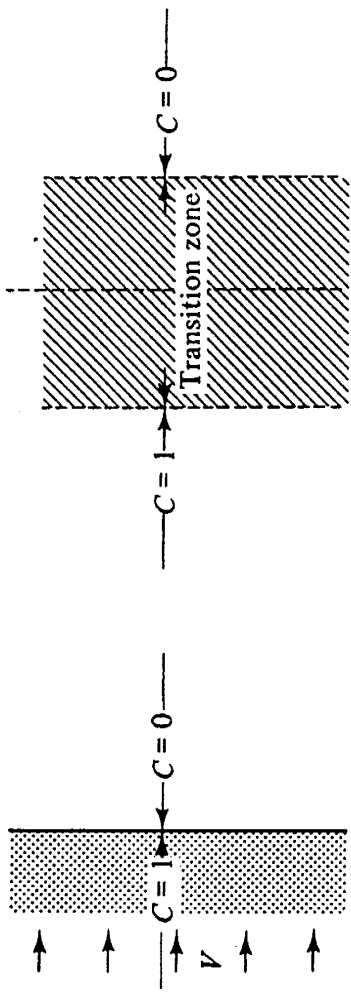
```

```

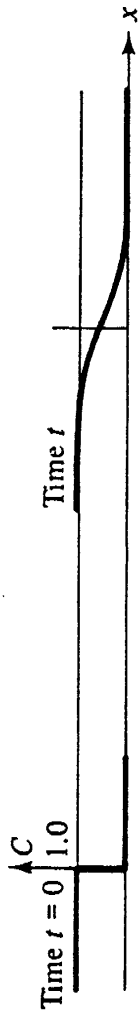
C
C    SUBROUTINE TRIDAG (IF,L,A,B,C,D,V)
C
C    DIMENSION A(450),B(450),C(450),D(450),V(450),BETA(450),GAMMA(450)
C
C    BETA(IF)=B(IF)
C    GAMMA(IF)=D(IF)/BETA(IF)
C    IFP1=IF+1
C    DO 2001 I=IFP1,L
C        BETA(I)=B(I)-A(I)*C(I-1)/BETA(I-1)
2001    GAMMA(I)=(D(I)-A(I)*GAMMA(I-1))/BETA(I)
C
C    V(L)=GAMMA(L)
C    LAST=L-IF
C    DO 2002 K=1, LAST
C        I=L-K
2002    V(I)=GAMMA(I)-C(I)*V(I+1)/BETA(I)

```

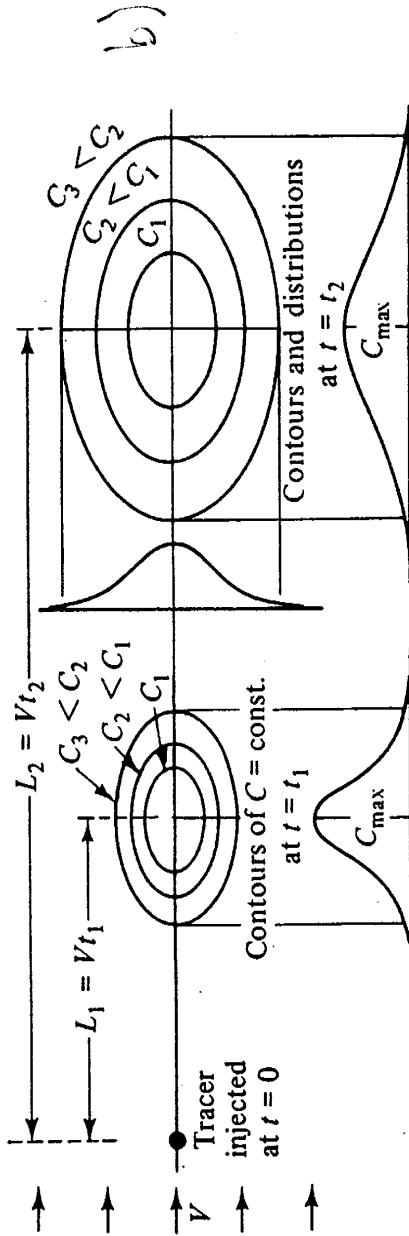

RETURN
END



c)



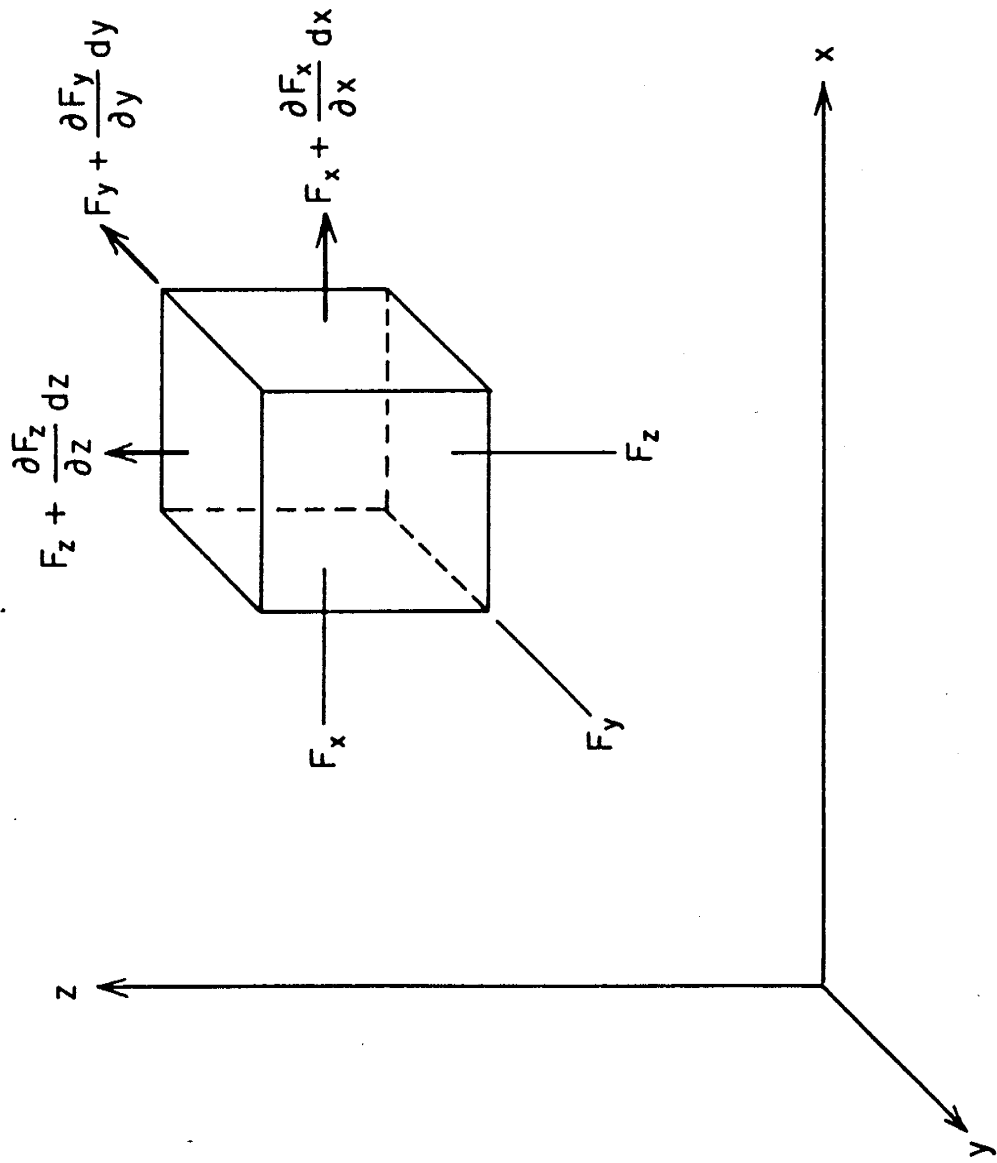
~~Legend~~



FROM YEAR 1972

TRACER DISPERSION
(MAY CHANGE)

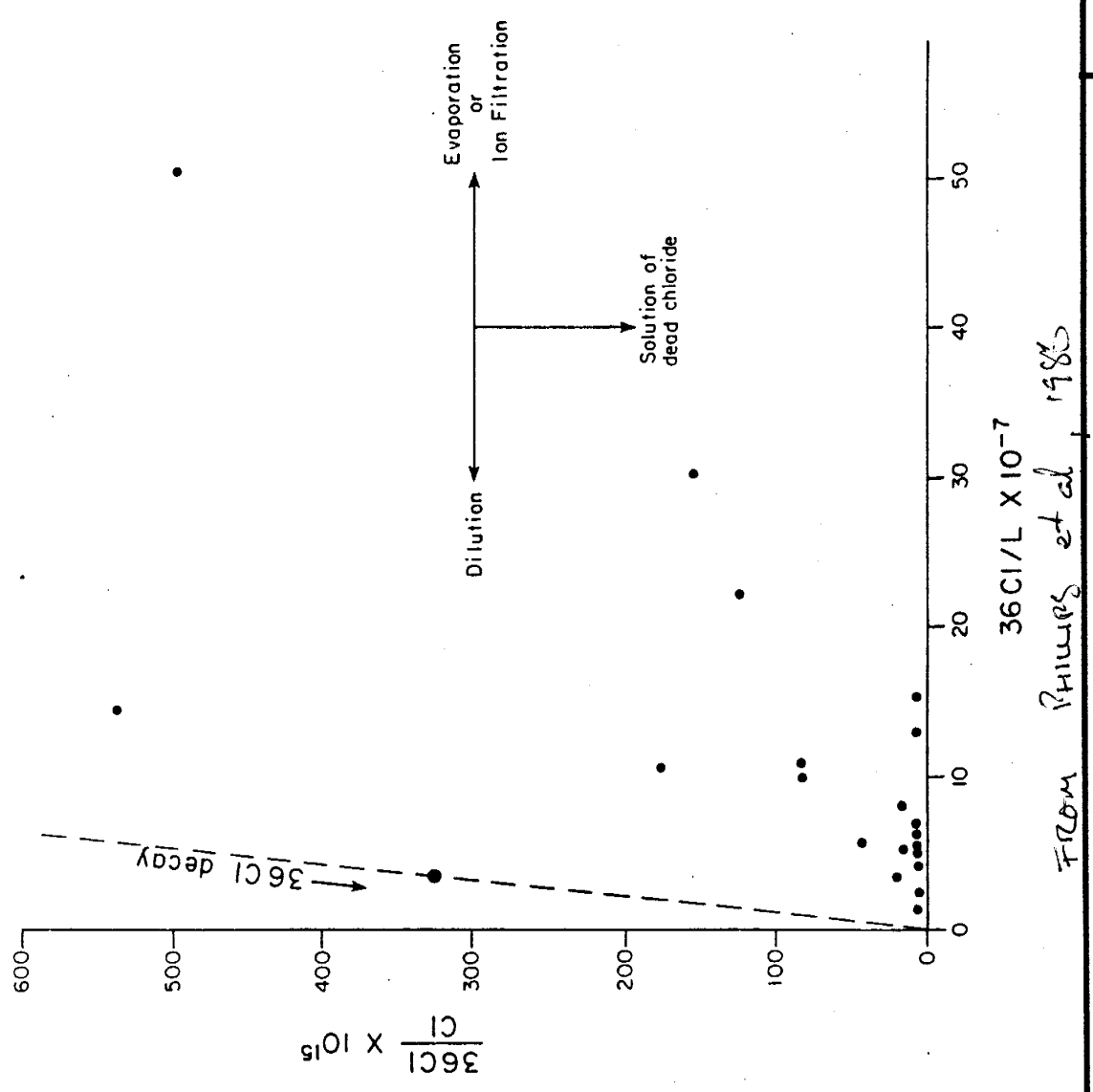
Figure 1



FROM ~~STREETS~~ FREEE; CHERRY 1979

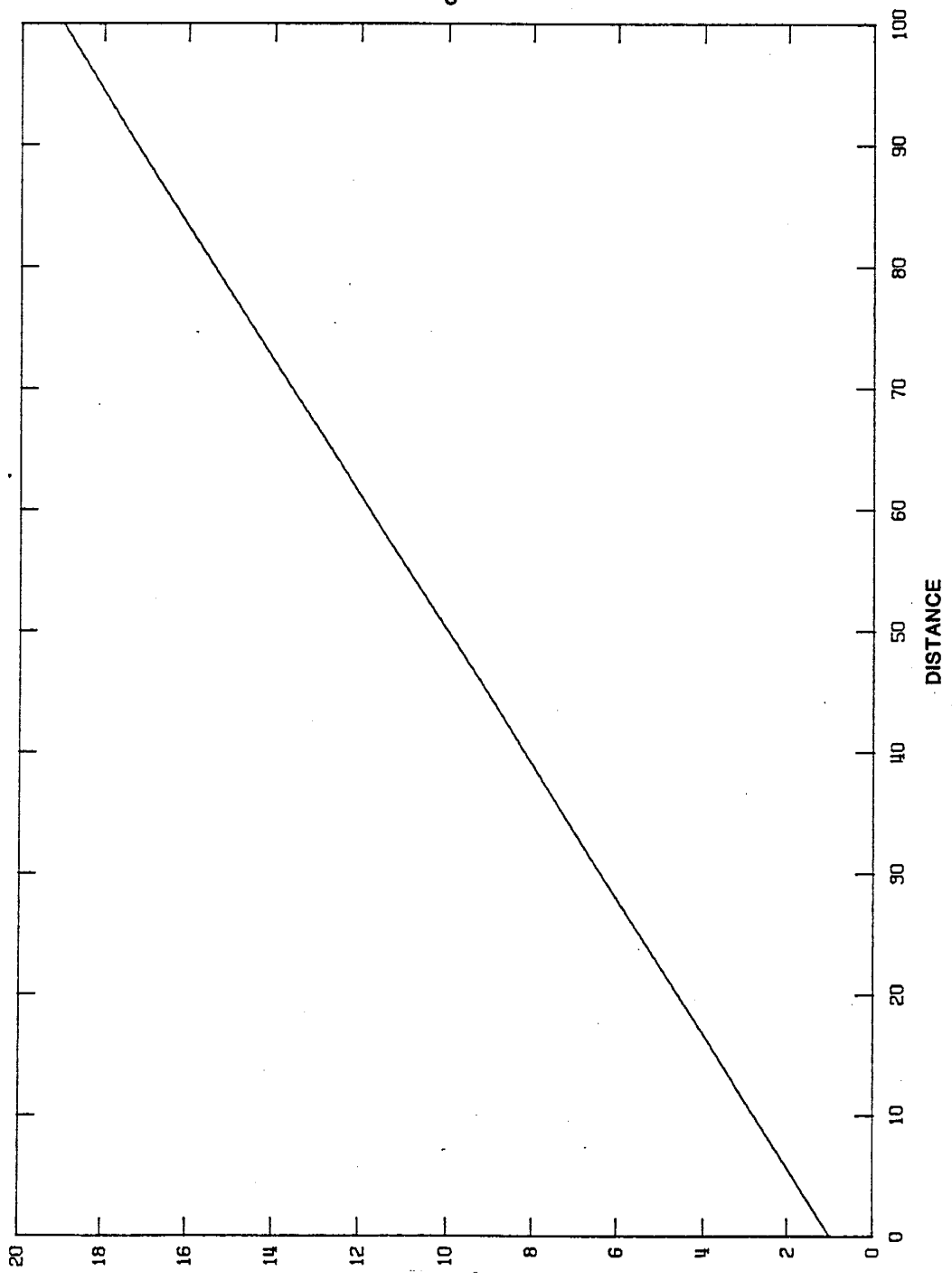
Solute transport mass balance

Figure 2



Isotopic concentration trends

Figure 3

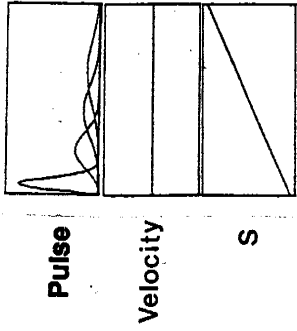
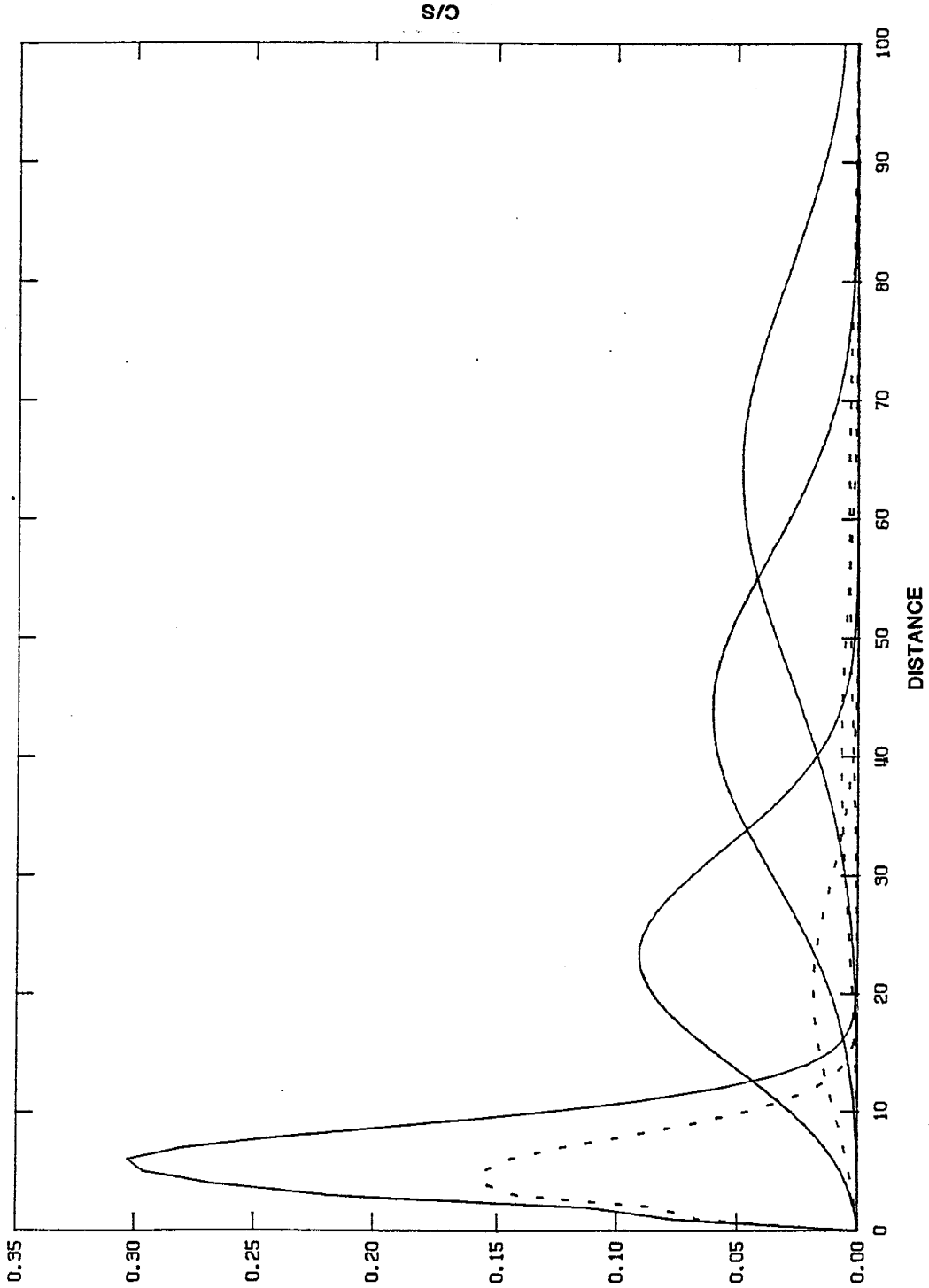


Legend

— Common
(or Reference) Isotope

Linear positive background (reference species) concentration gradient (BCG)

Figure 13

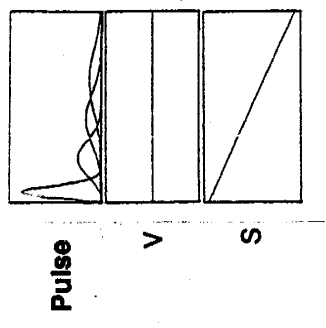
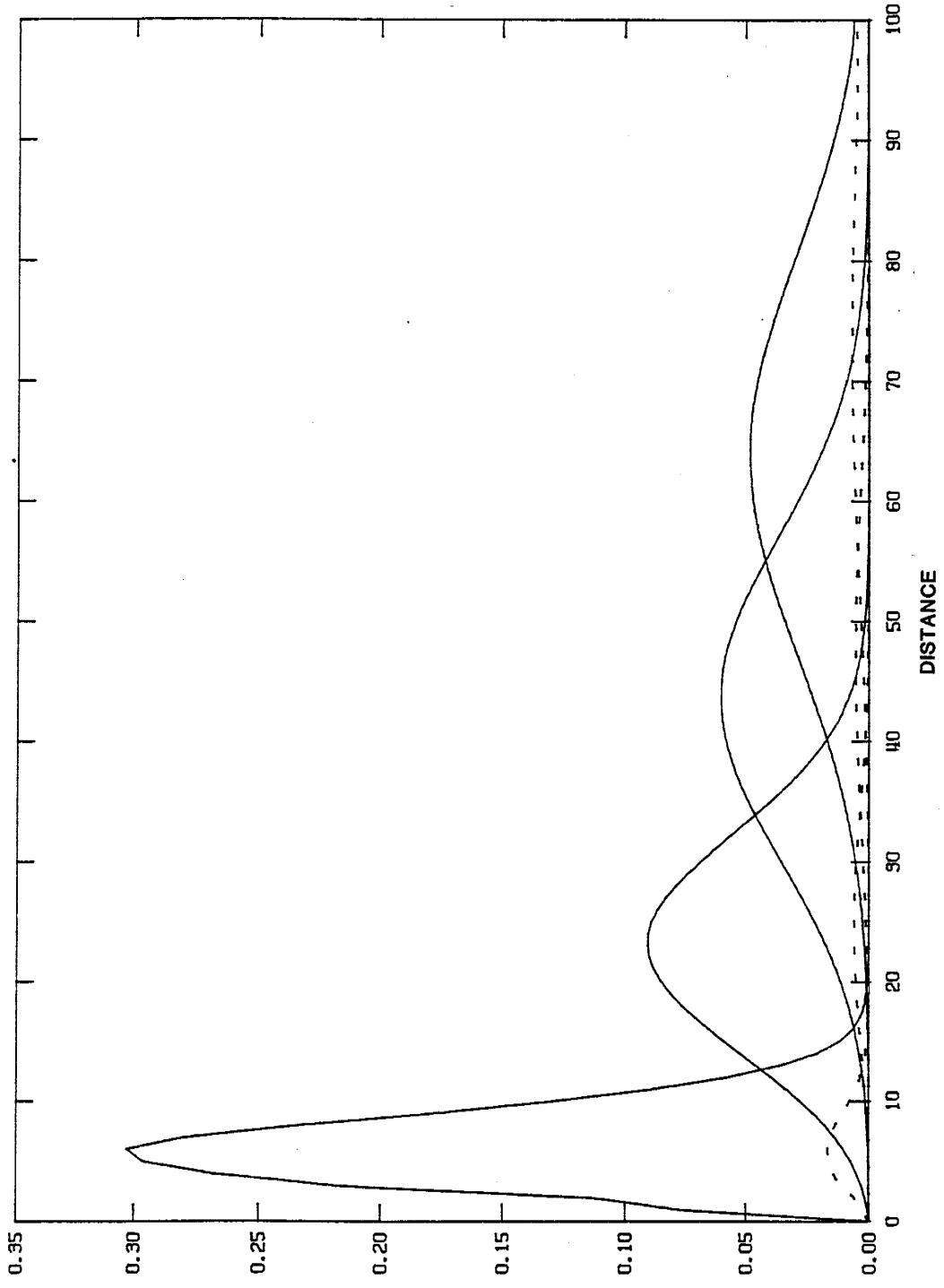


Legend

- NCG (No Concentration Gradient) Case
- - - BCG (Background Concentration Gradient) Case

Comparison of numerical solutions to the assumed case and a positive BCG case for a pulse input

Figure 14



S/C

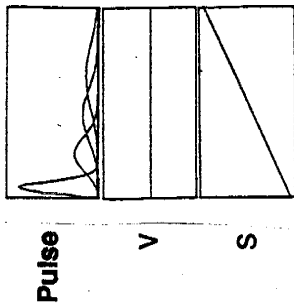
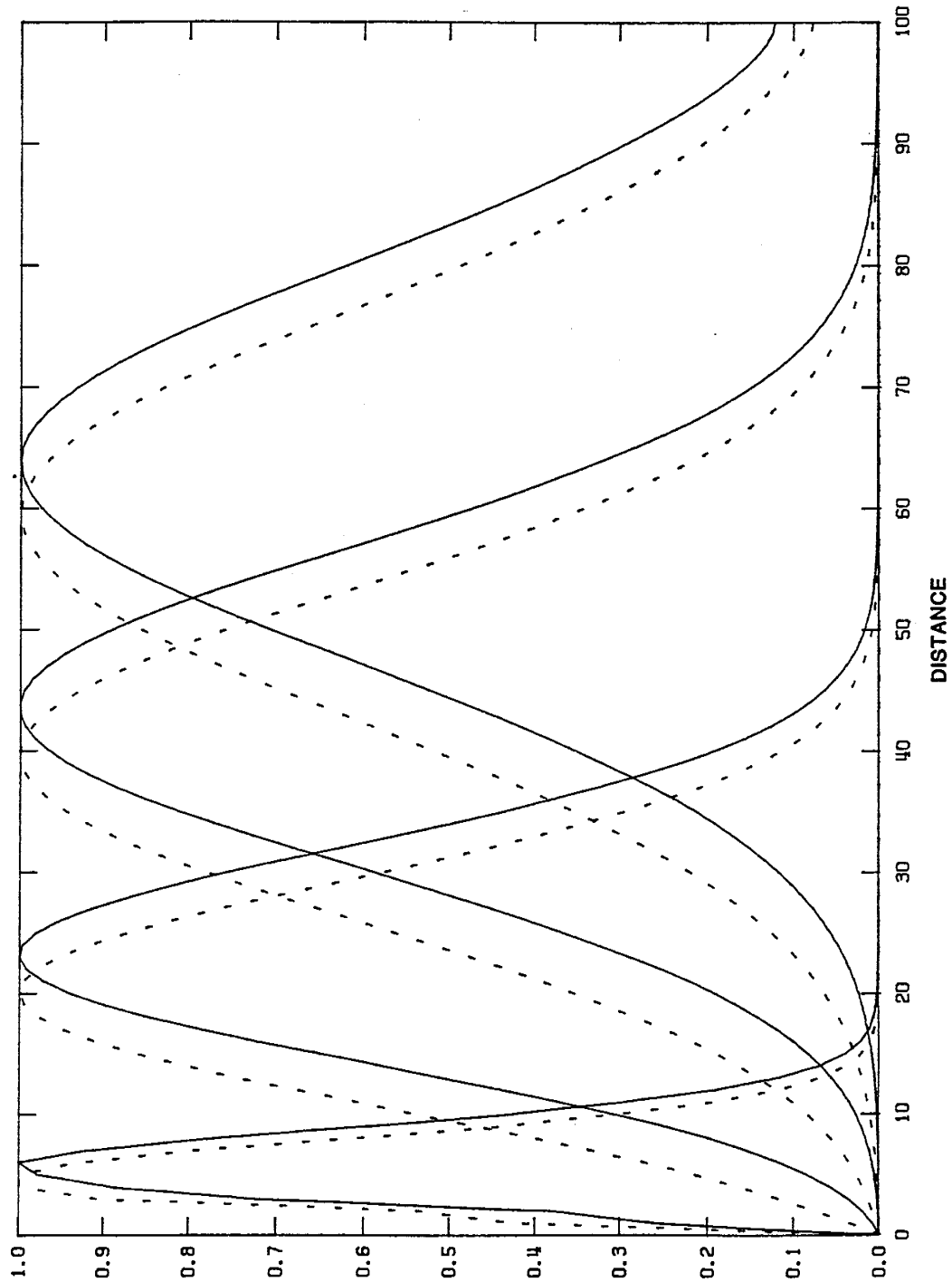
Legend

—— NCG Case

- - - BCG Case

Comparison of numerical solutions to the assumed case and a negative BCG case for a pulse input

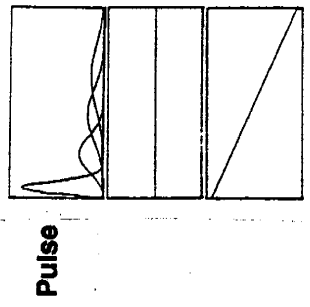
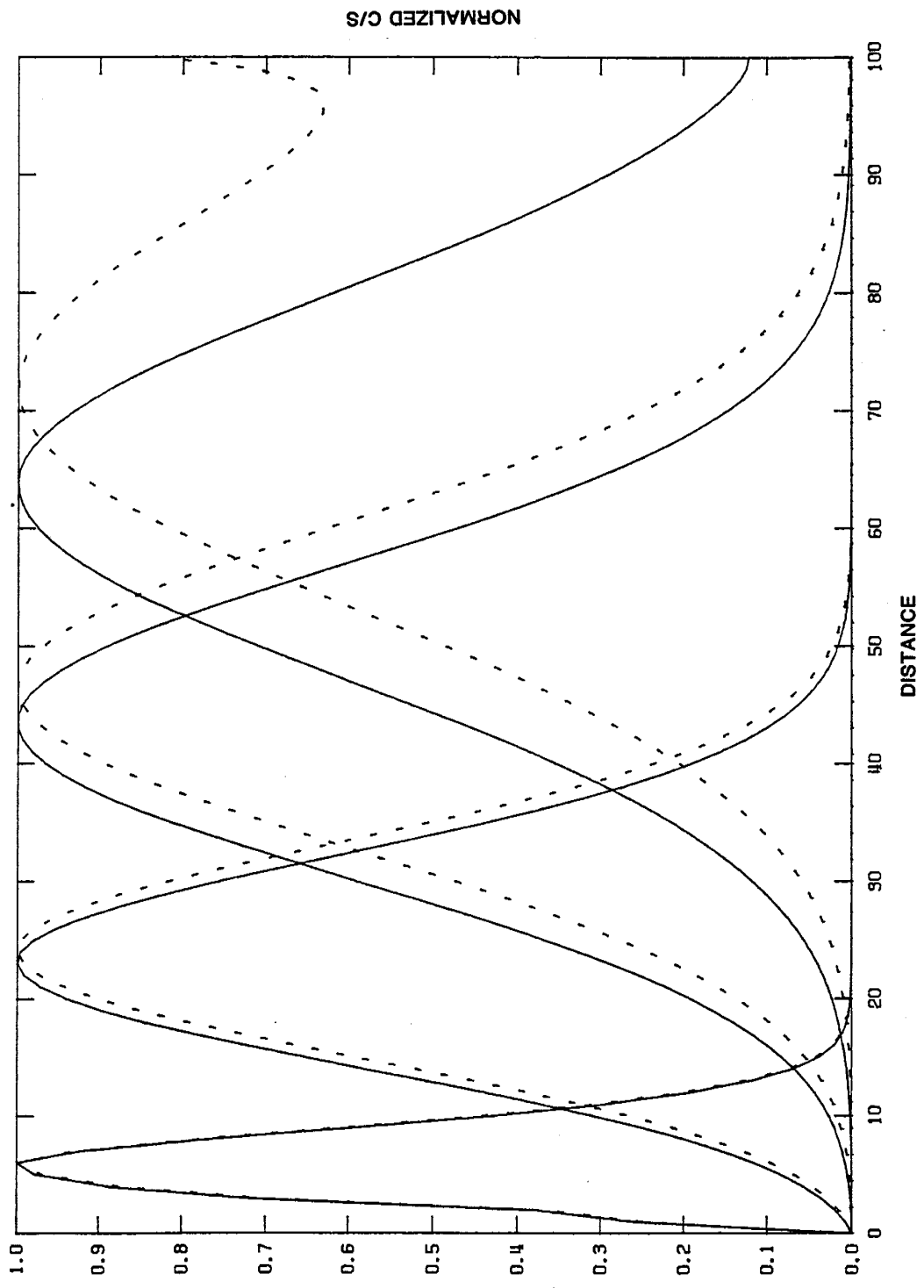
Figure 15



Legend
 — NCG Case
 - - BCG Case

Comparison of normalized numerical solutions to the assumed case and a positive BCG case for a pulse input

Figure 16



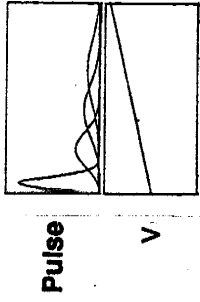
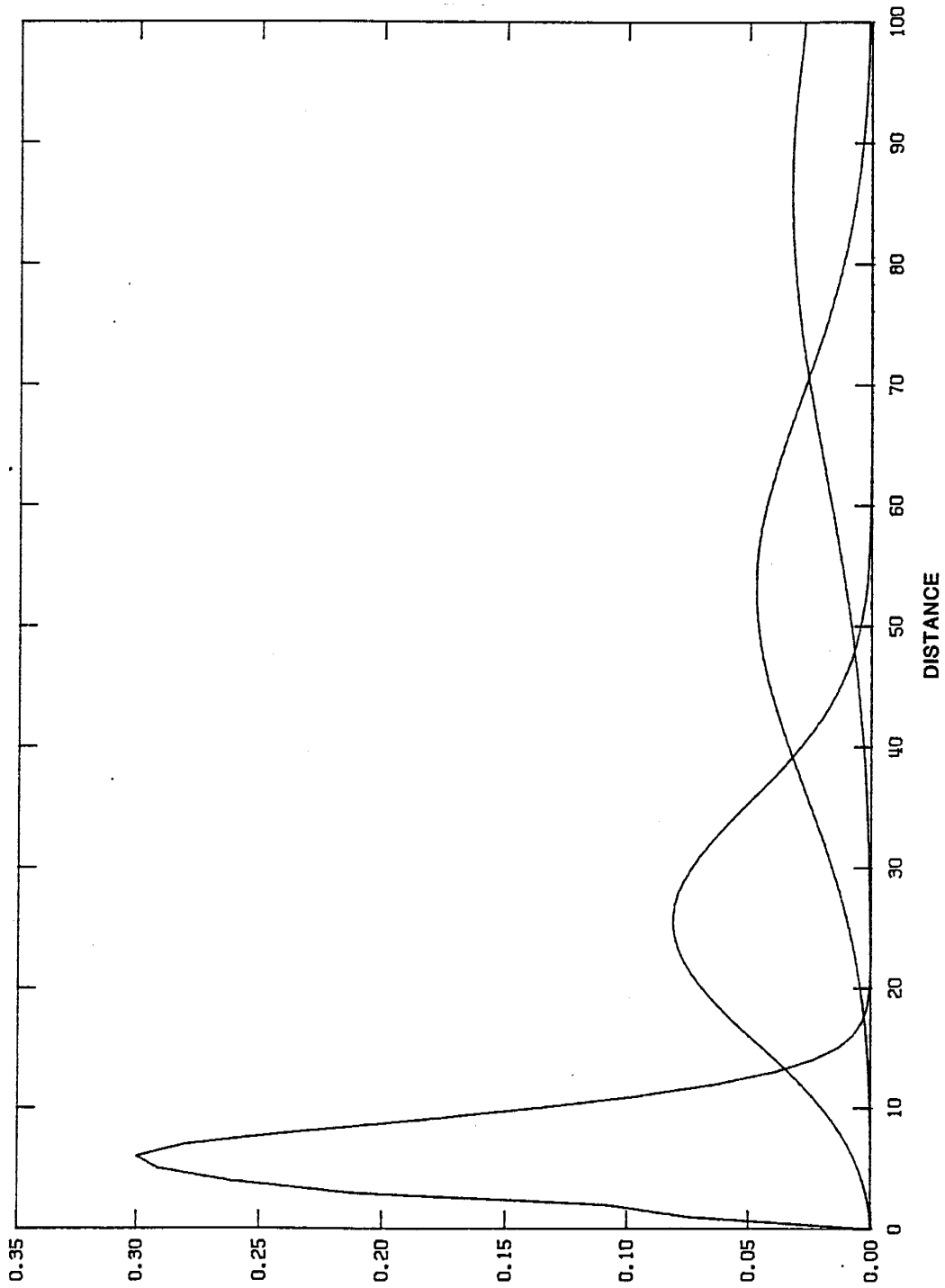
Legend

— NCG Case

- - - BCG Case

Comparison of normalized numerical solutions to the assumed case and a negative BCG case for a pulse input

Figure 17



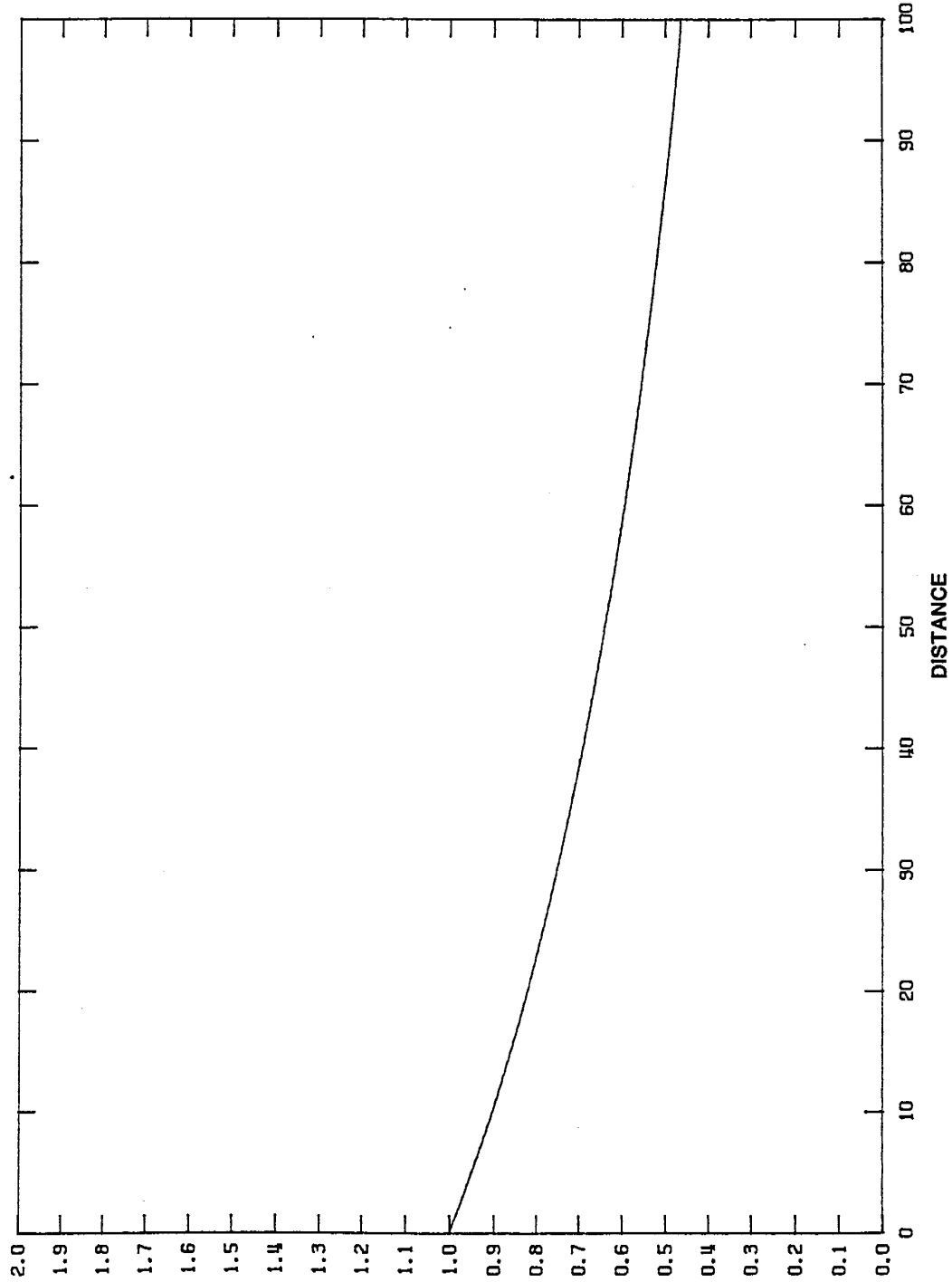
C/S

Legend

— Trace Isotope

Analytical solution for advective-dispersive transport of a tracer pulse in the presence of a source

Figure 18

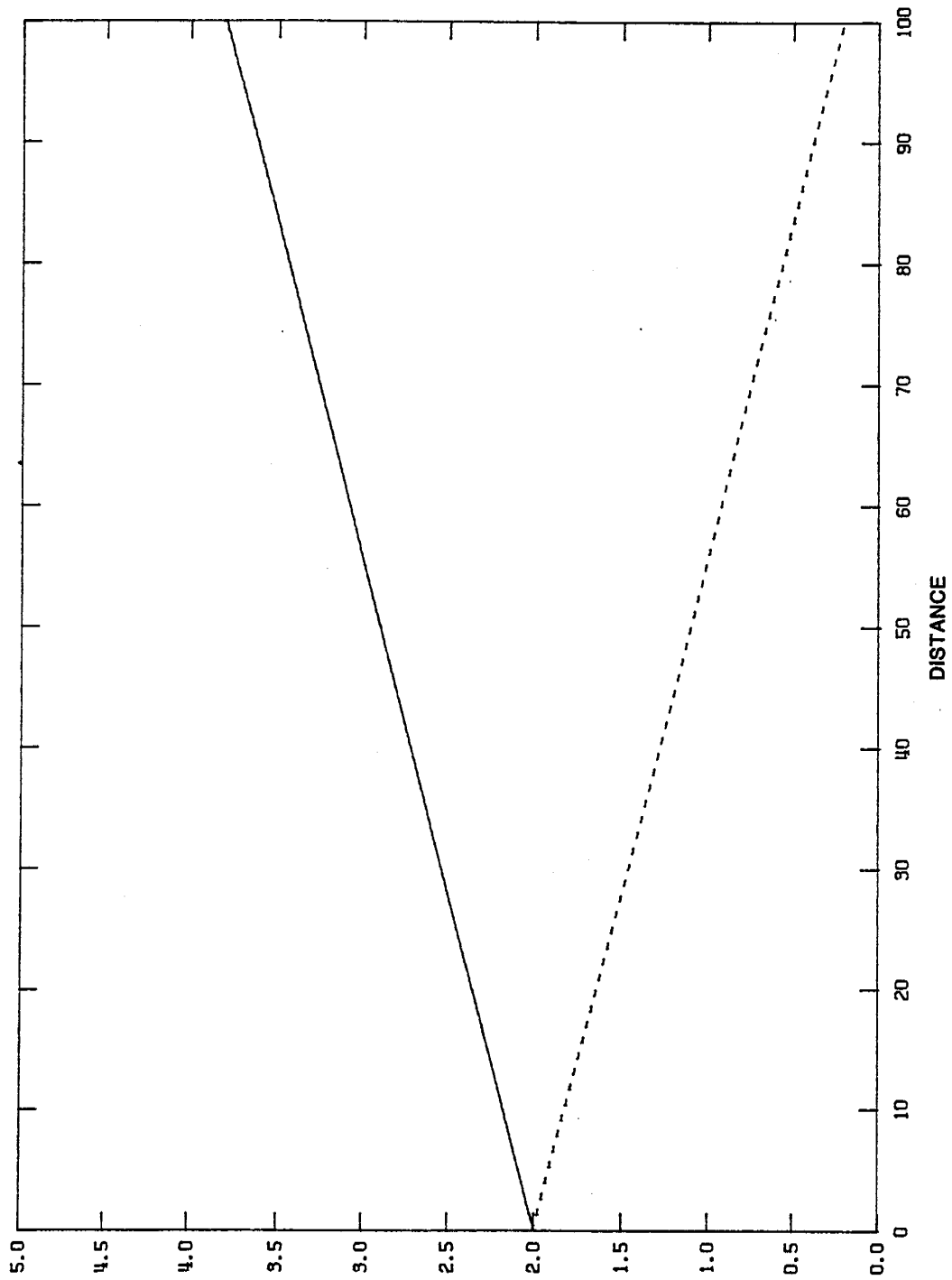


Legend

— Common Isotope

Analytical solution to the dilution effect of a source on a constant reference species concentration

Figure 19



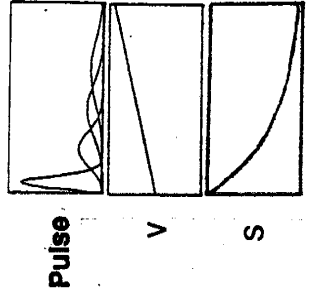
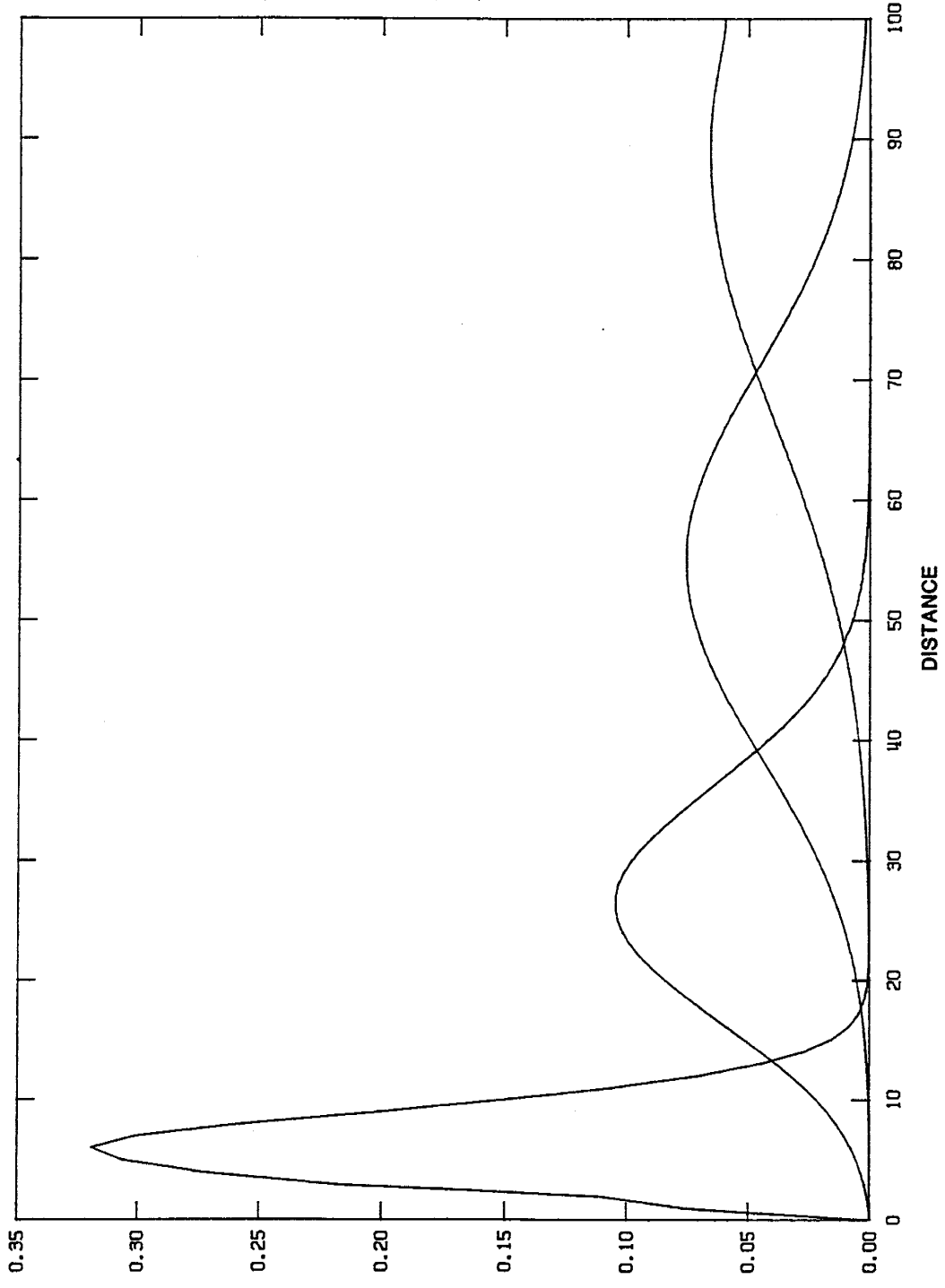
Legend

— Advective Velocity with a Source

- - Advective Velocity with a Sink

Figure 20

Change in advective velocity with distance due to a source or sink



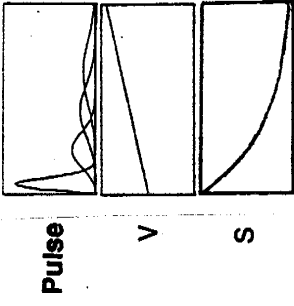
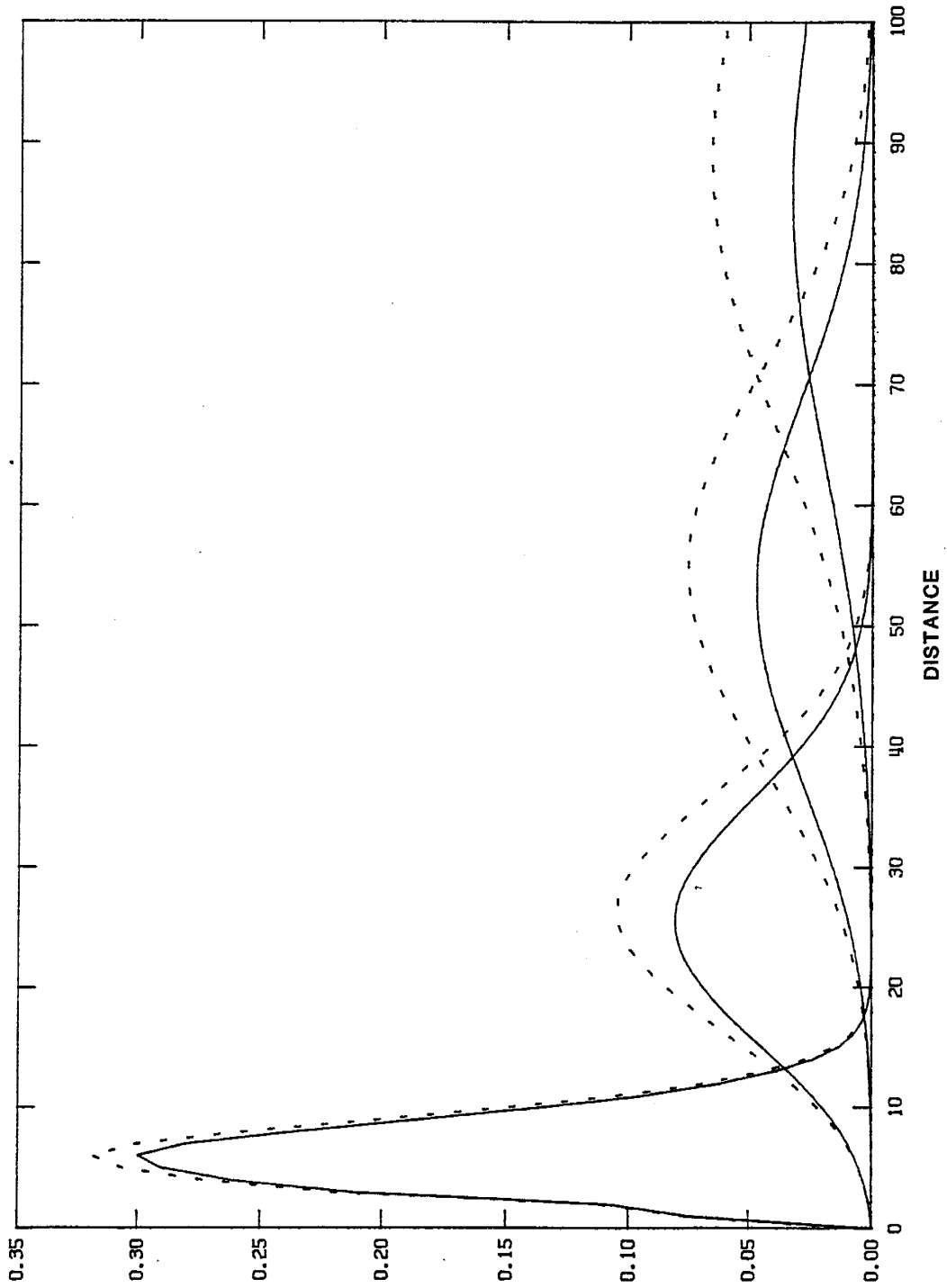
C/S

Legend

—— BCG Case

Analytical solution for advective-dispersive transport of a pulse input, in terms of an isotopic ratio, with the effect of a source on both the tracer and reference species taken into account

Figure 21



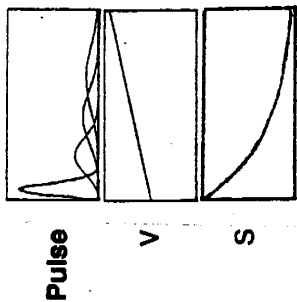
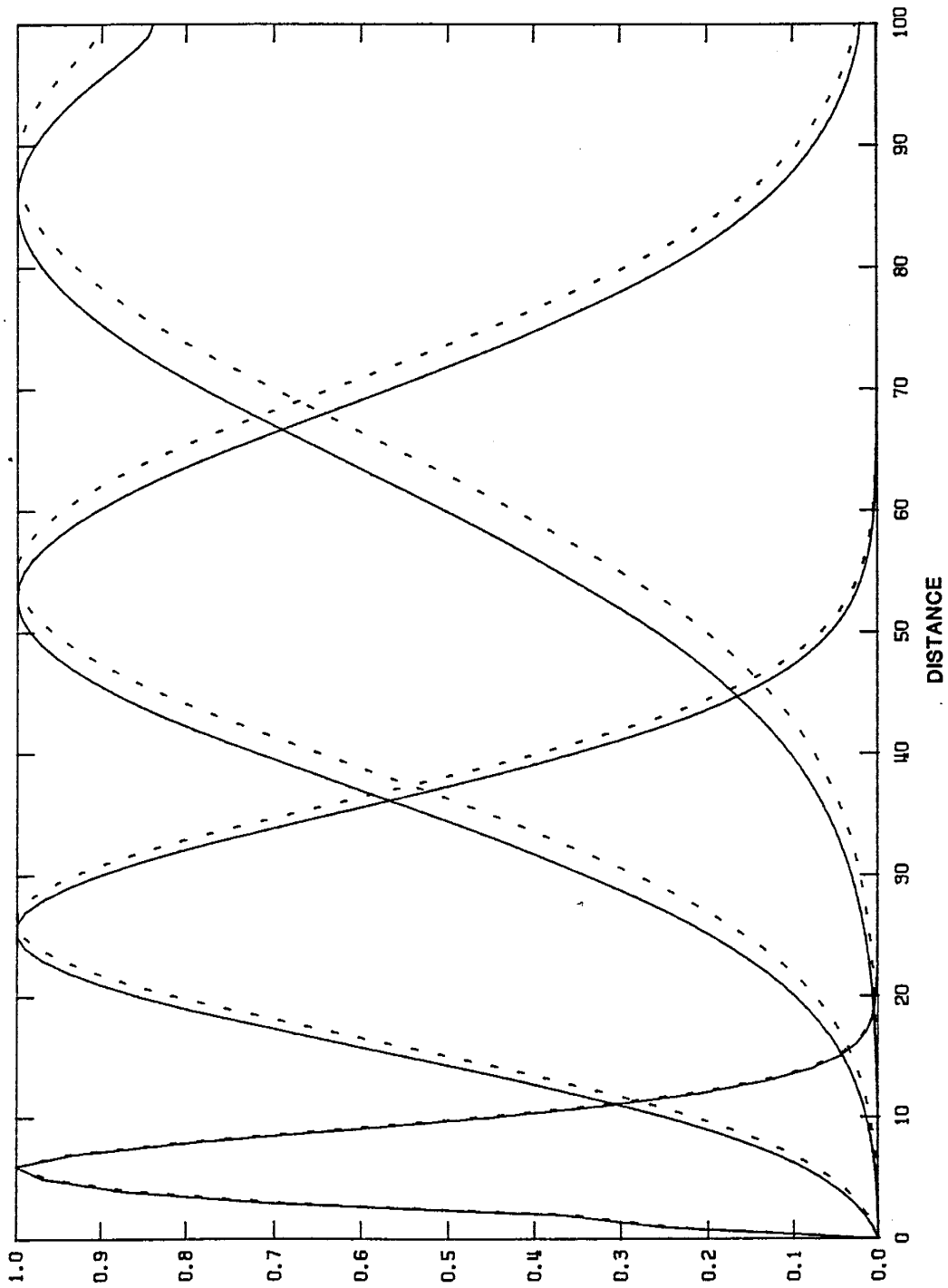
Legend x

— NCG Case

- - - BCG Case

Comparison of numerical solutions from Figure 18 and Figure 21

Figure 22



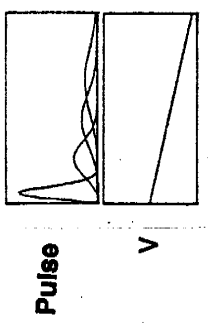
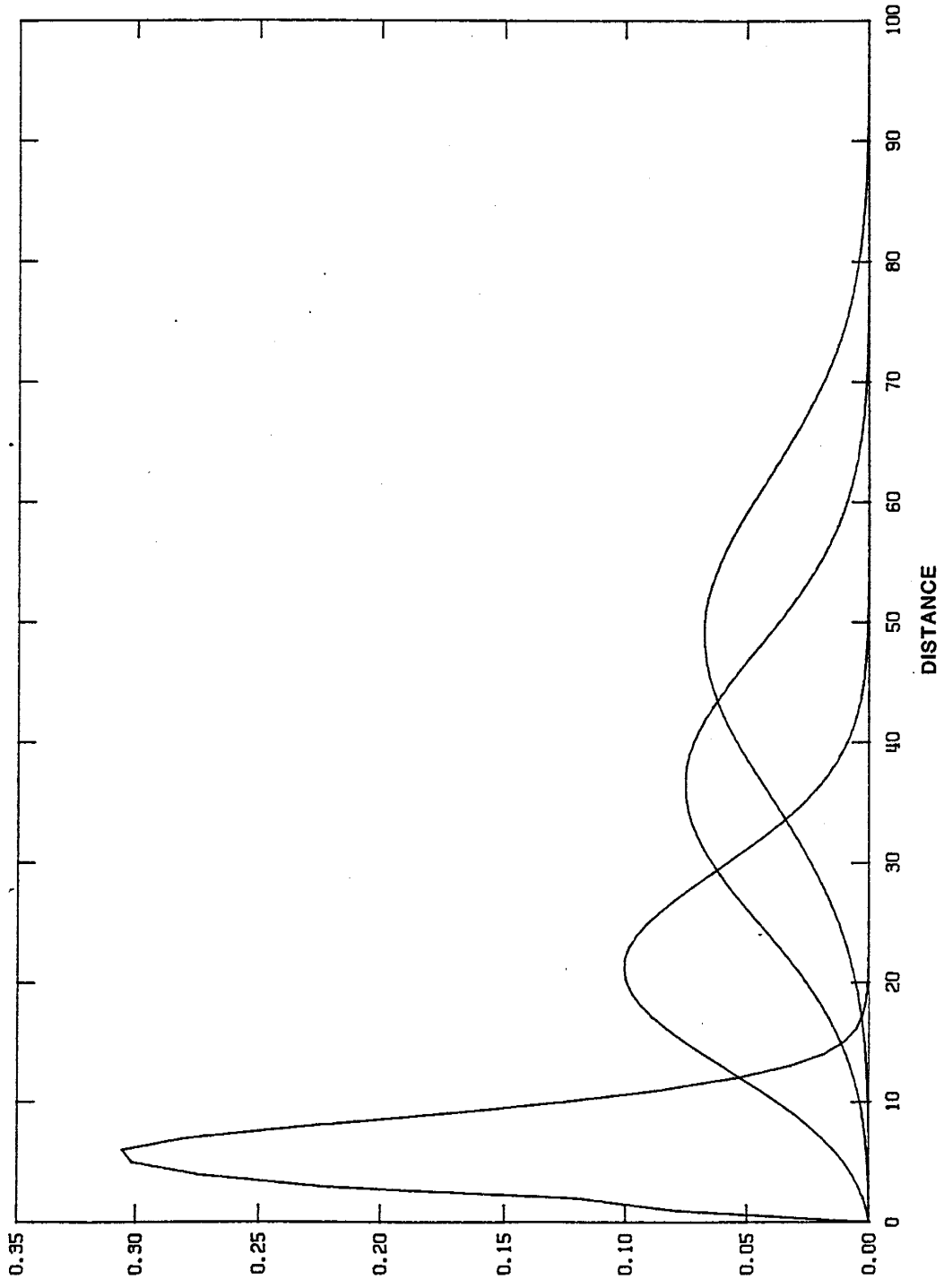
Legend

— NCG Case

- - - BCG Case

Comparison of normalized numerical solutions from Figure 18 and Figure 21

Figure 23



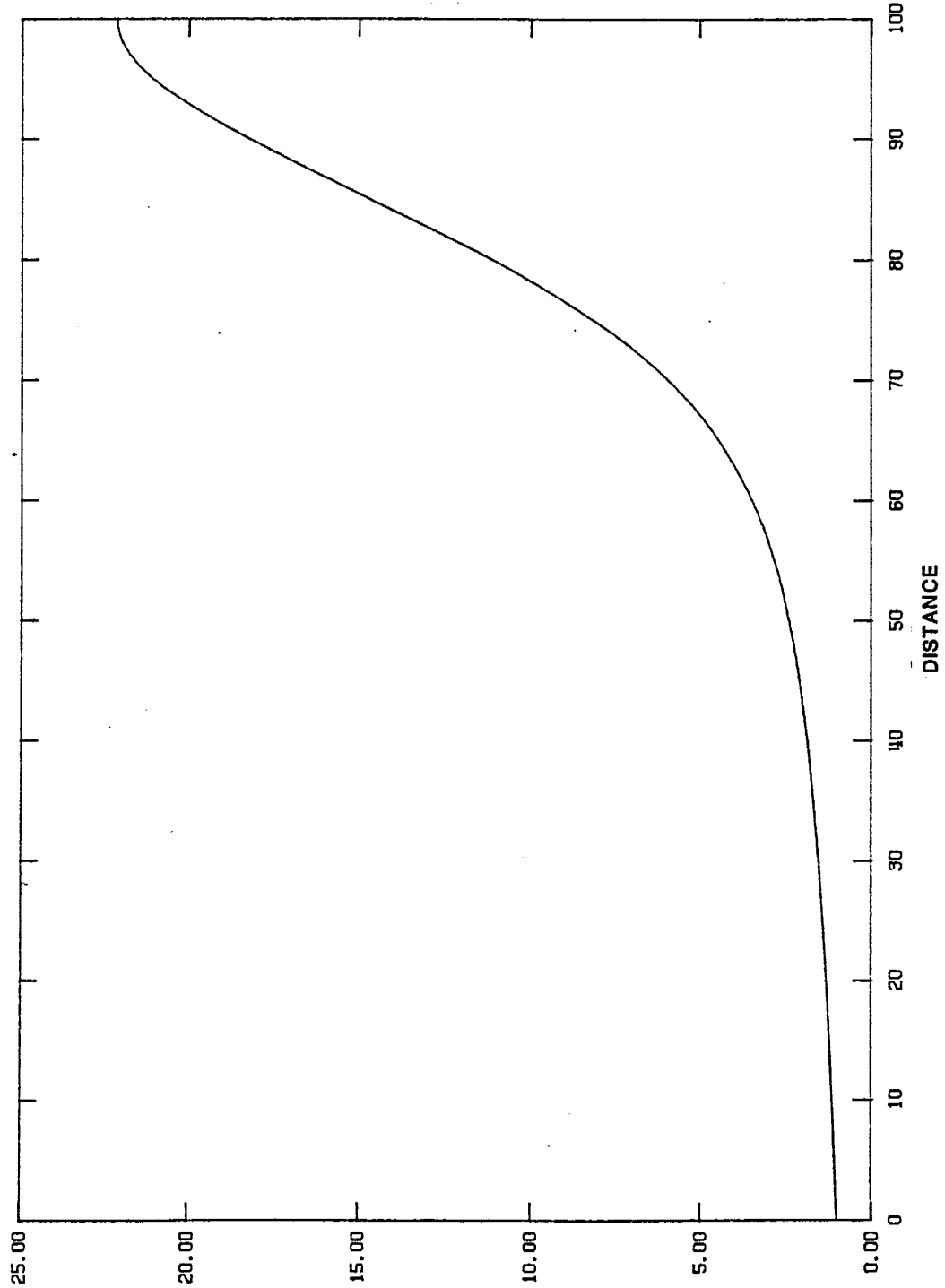
C/S

Legend

— Trace Isotope

Analytical solution for advective-dispersive transport of a tracer pulse in the presence of a sink

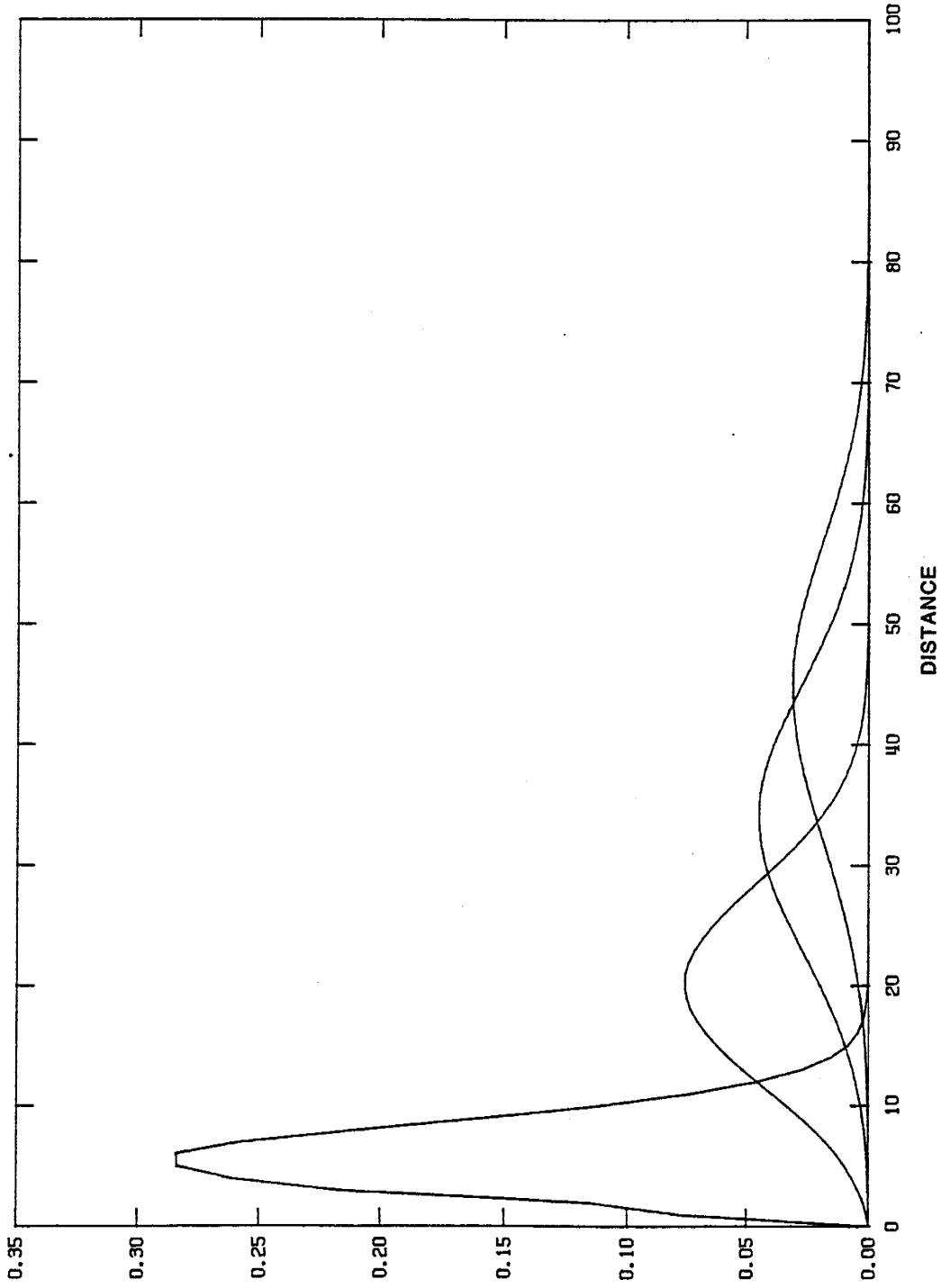
Figure 24



Legend
 — Common Isotope

Analytical solution to the dilution effect of a sink on a constant reference species concentration

Figure 25

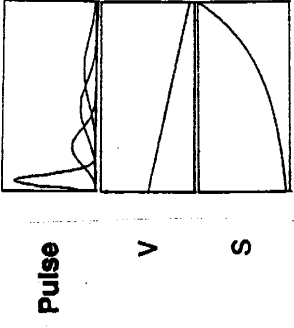


C/S

Legend

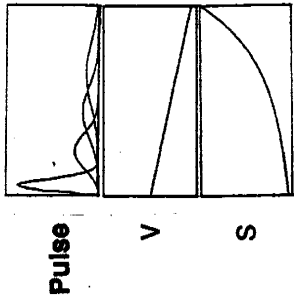
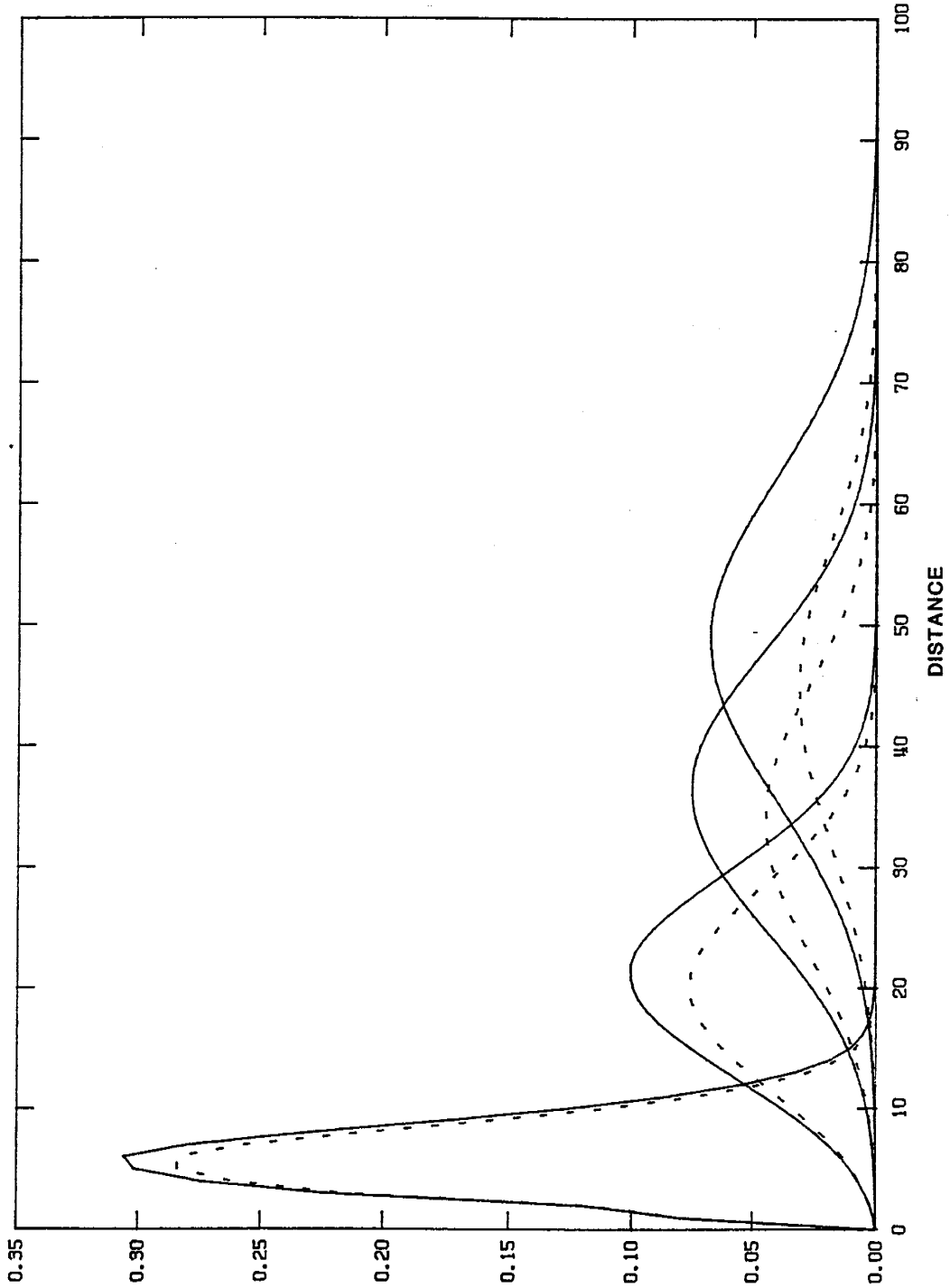
— NCG Case

- - - BCG Case



Analytical solution for advective-dispersive transport of a pulse input, in terms of an isotopic ratio, with the effect of a sink on both the tracer and reference species taken into account

Figure 26



C/S

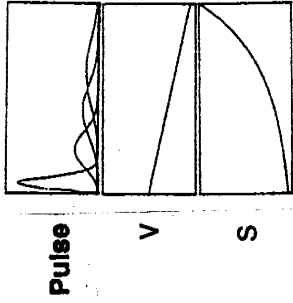
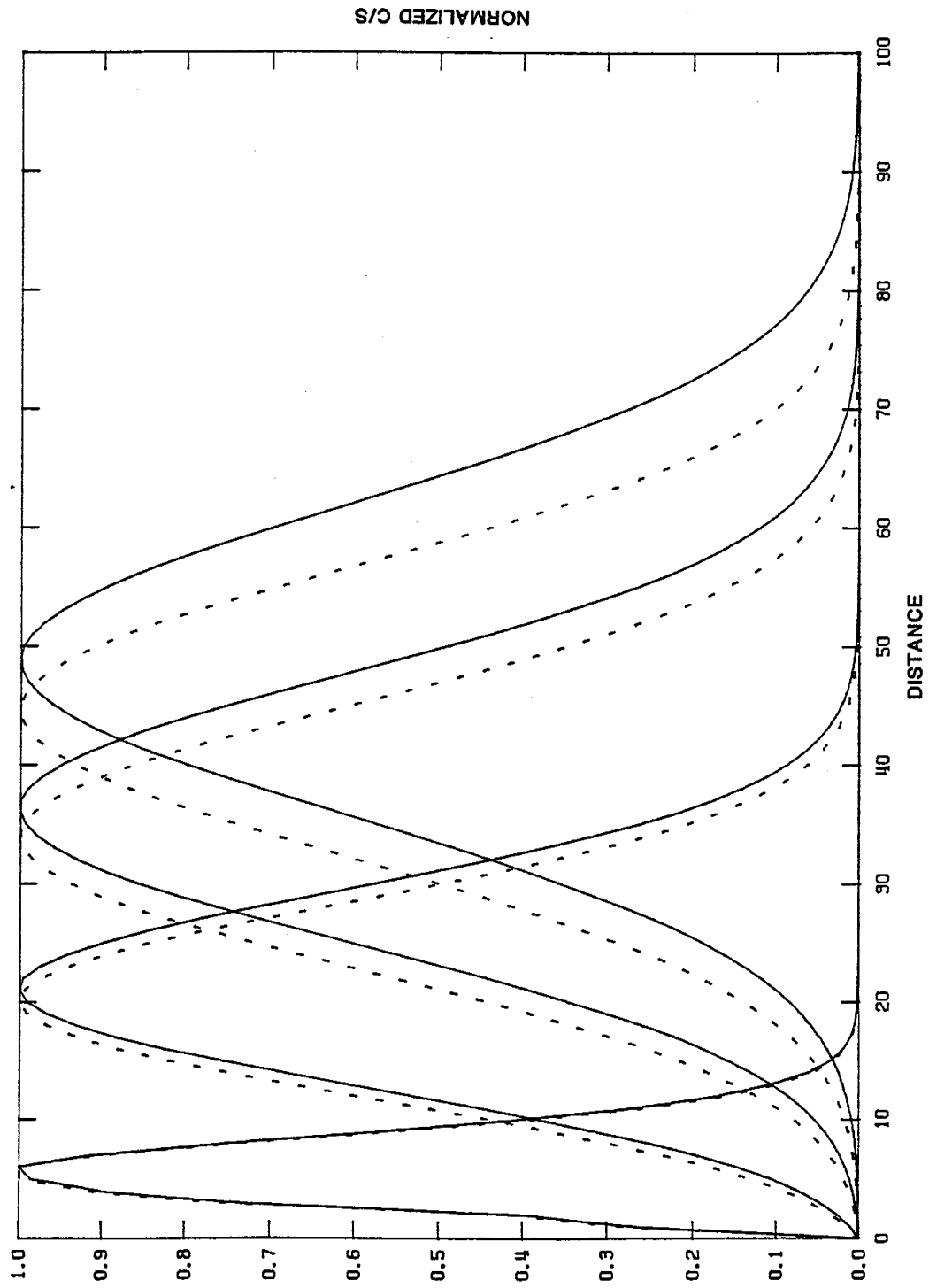
Legend

— NCG Case

- - - BCG Case

Comparison of numerical solutions from Figure 24 and Figure 26

Figure 27



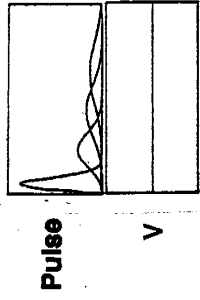
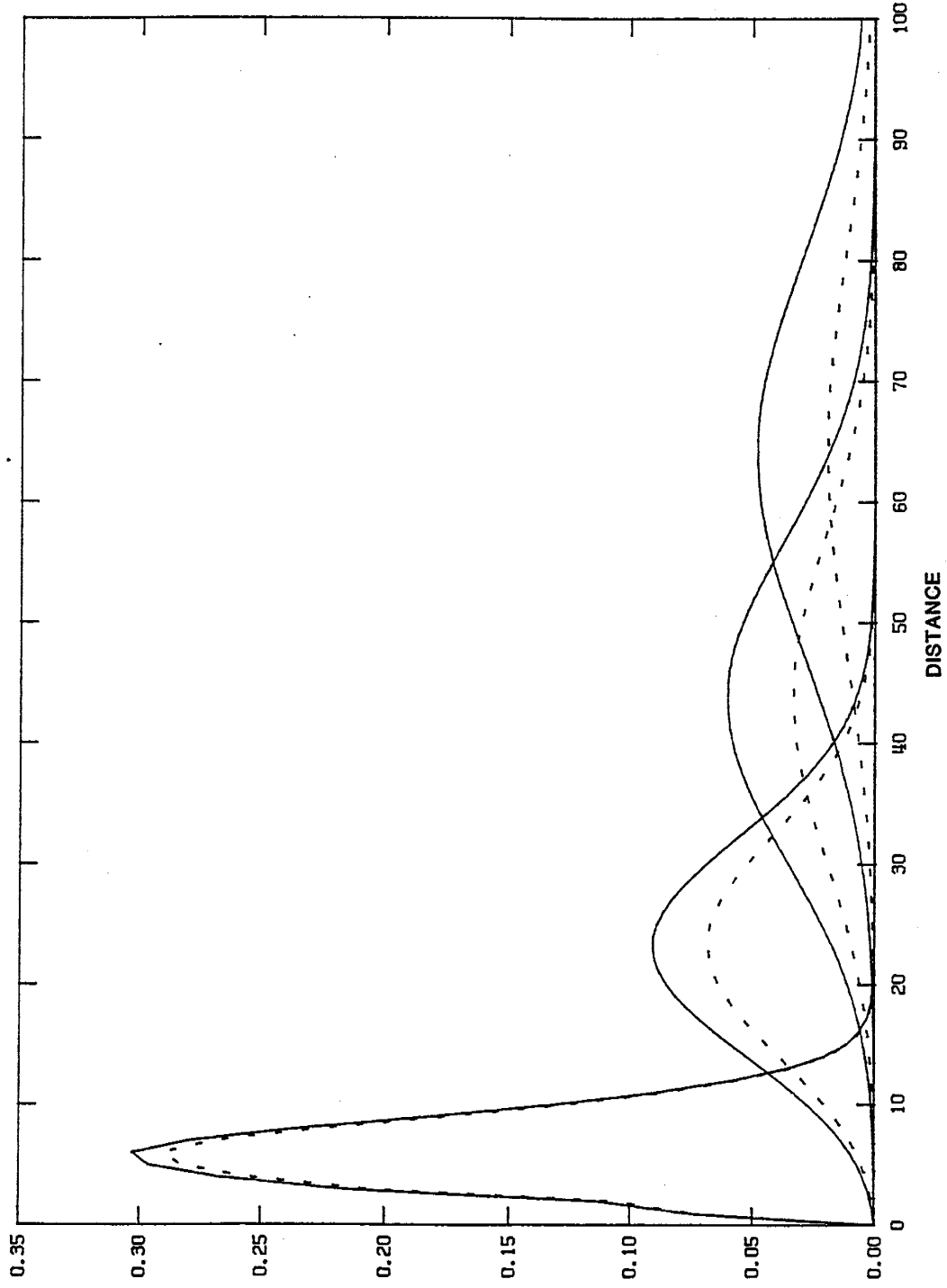
Legend

— NCG Case

- - - BCG Case

Comparison of normalized numerical solutions from Figure 24 and Figure 26

Figure 28



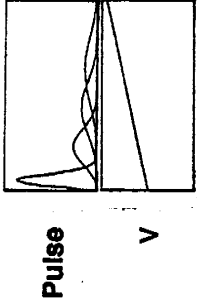
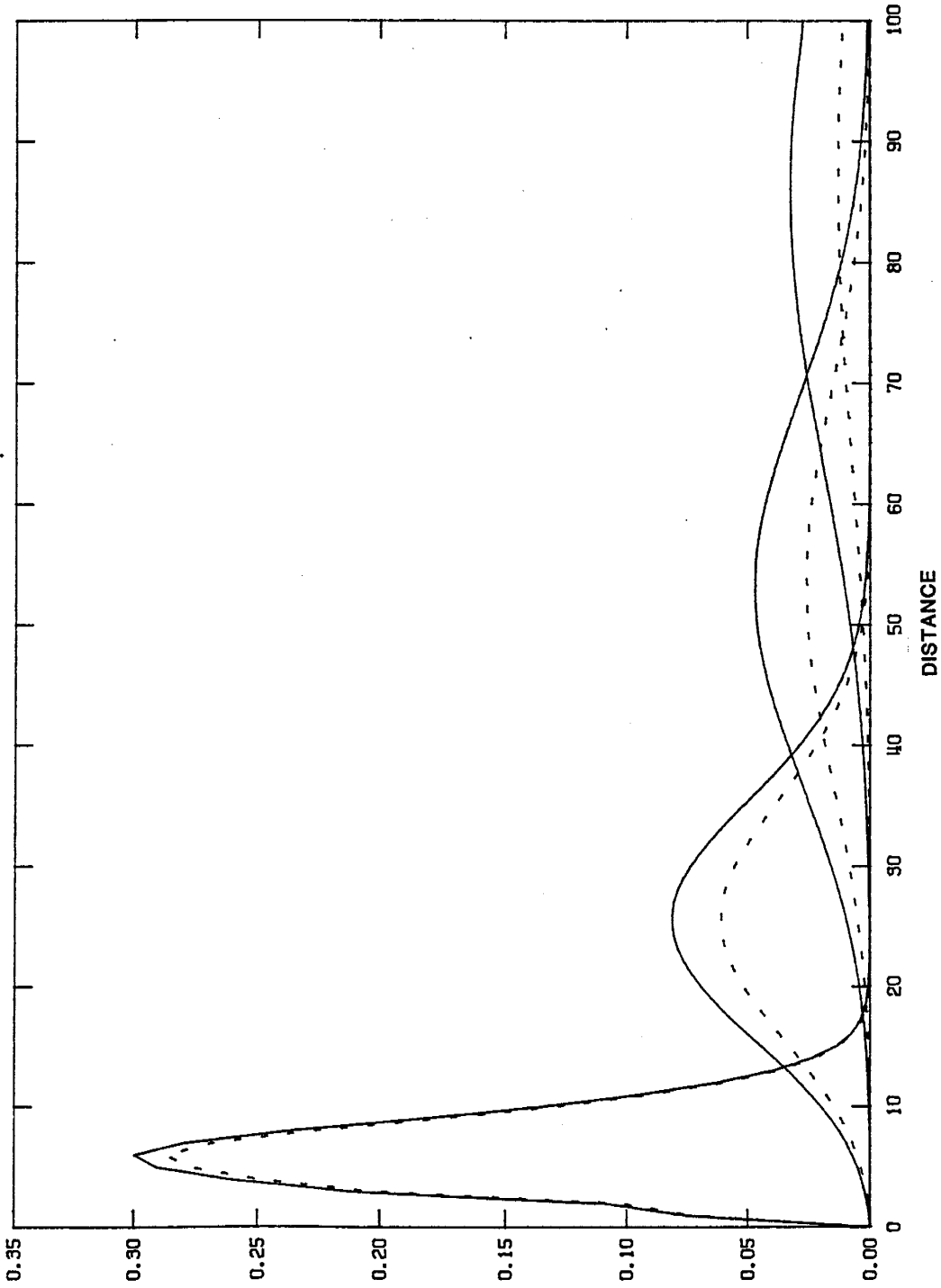
Legend

— Non-radioactive Trace Isotope

- - - Radioactive Trace Isotope

Comparison of the numerical solutions to advective-dispersive transport of a tracer pulse with and without radioactive decay

Figure 29

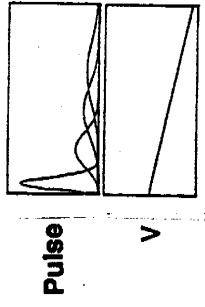
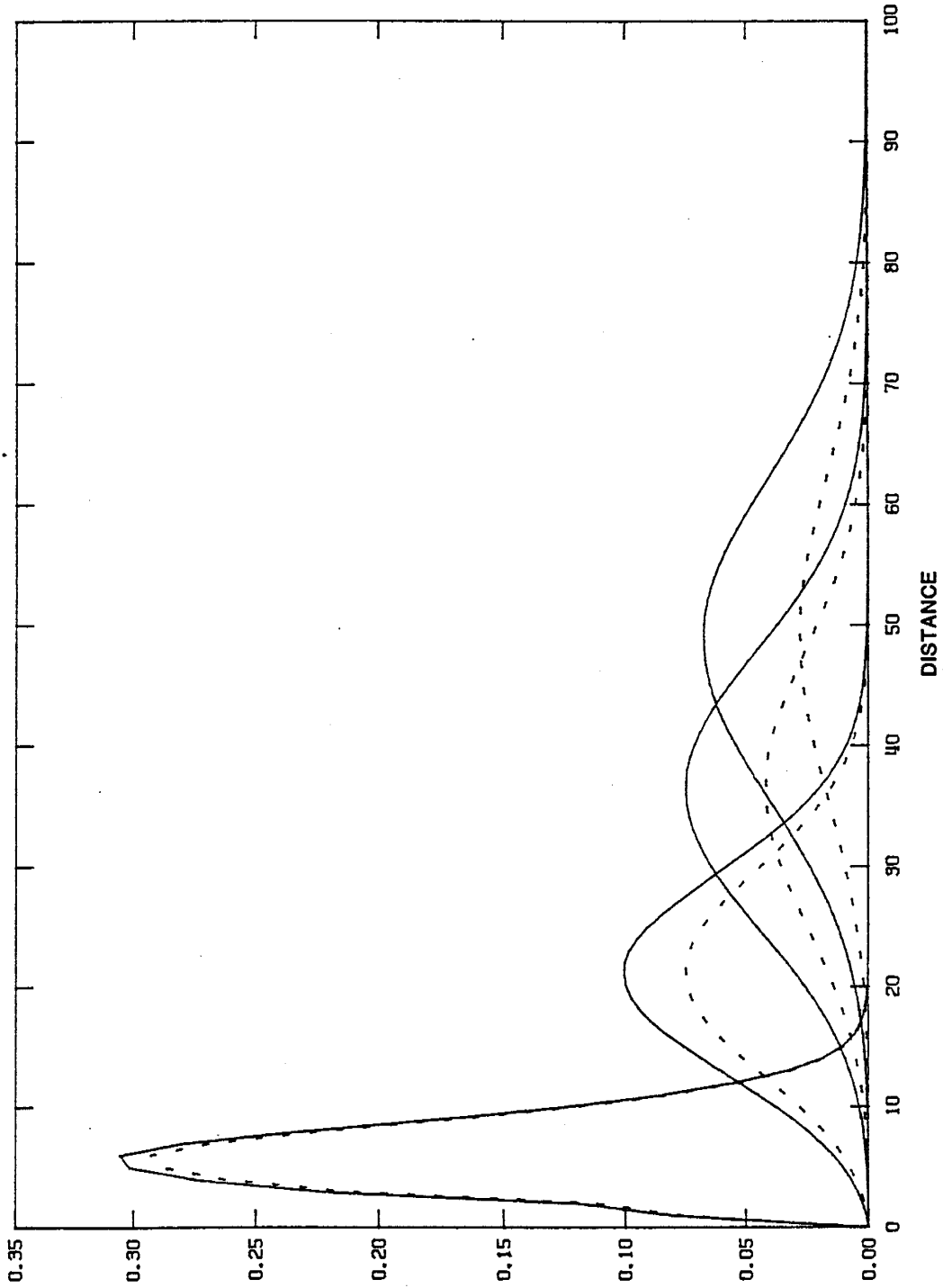


Legend

- Non-radioactive Trace Isotope with a Source
- - Radioactive Trace Isotope with a Source

Comparison of the numerical solutions to advective-dispersive transport of a tracer pulse with and without radioactive decay in the presence of a source

Figure 30

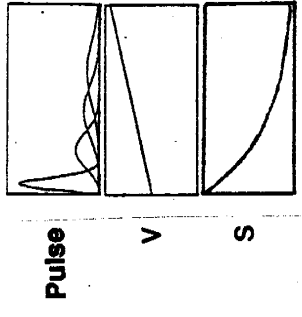
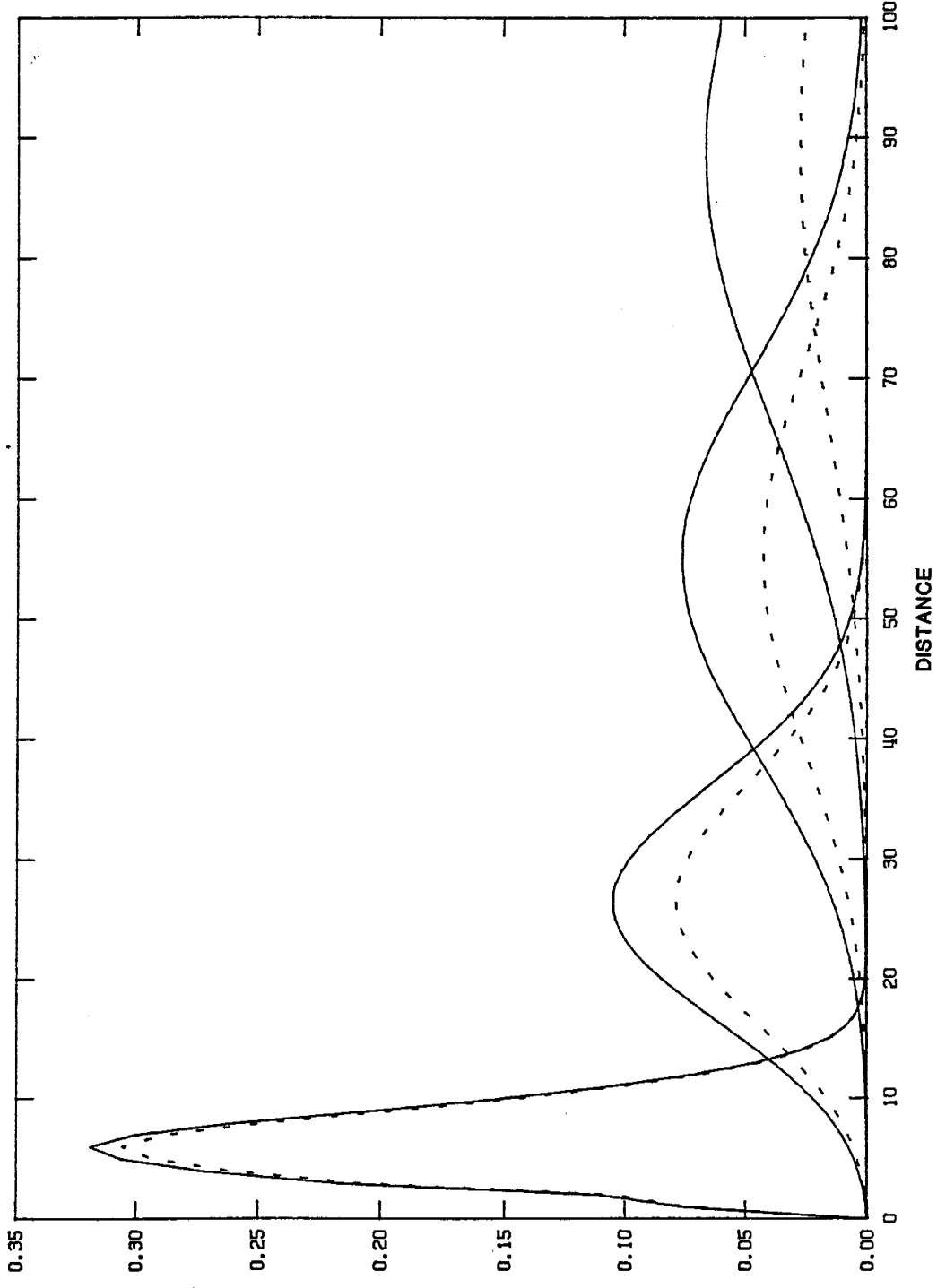


Legend

- Non-radioactive Trace Isotope with a Sink
- - - Radioactive Trace Isotope with a Sink

Comparison of the numerical solutions to advective-dispersive transport of a tracer pulse with and without radioactive decay in the presence of a sink

Figure 31



S/C

Legend

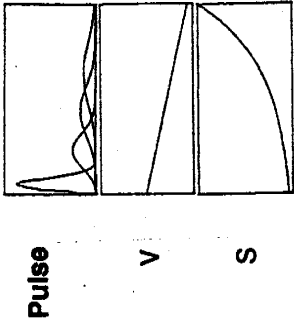
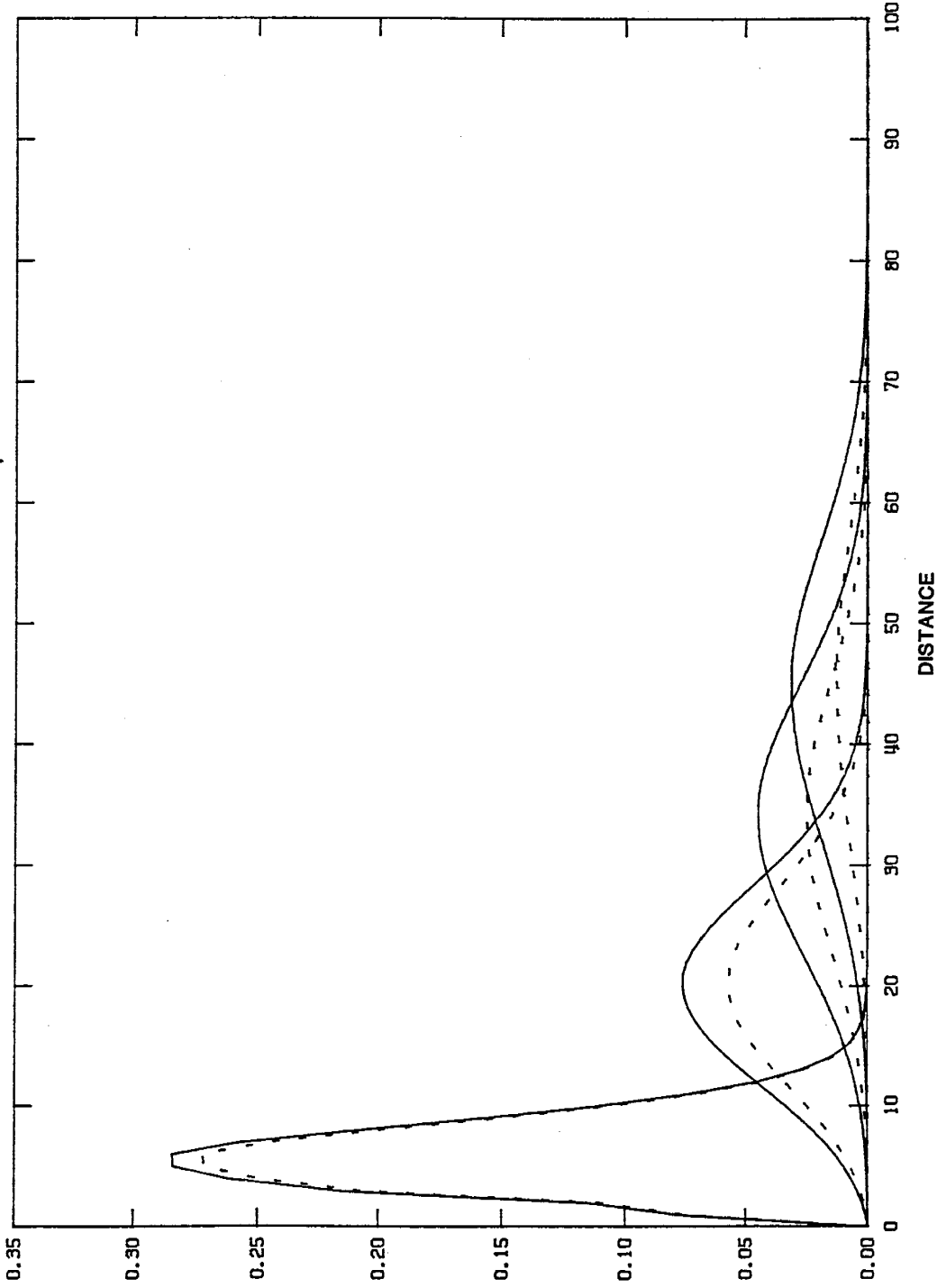
— NCG Case
with a Source

- - - Radioactive BCG
Case with a Source

DISTANCE

Comparison of the numerical solutions to advective-dispersive transport of a tracer pulse, in terms of a isotopic ratio, with and without radioactive decay in the presence of a source

Figure 32



C/S

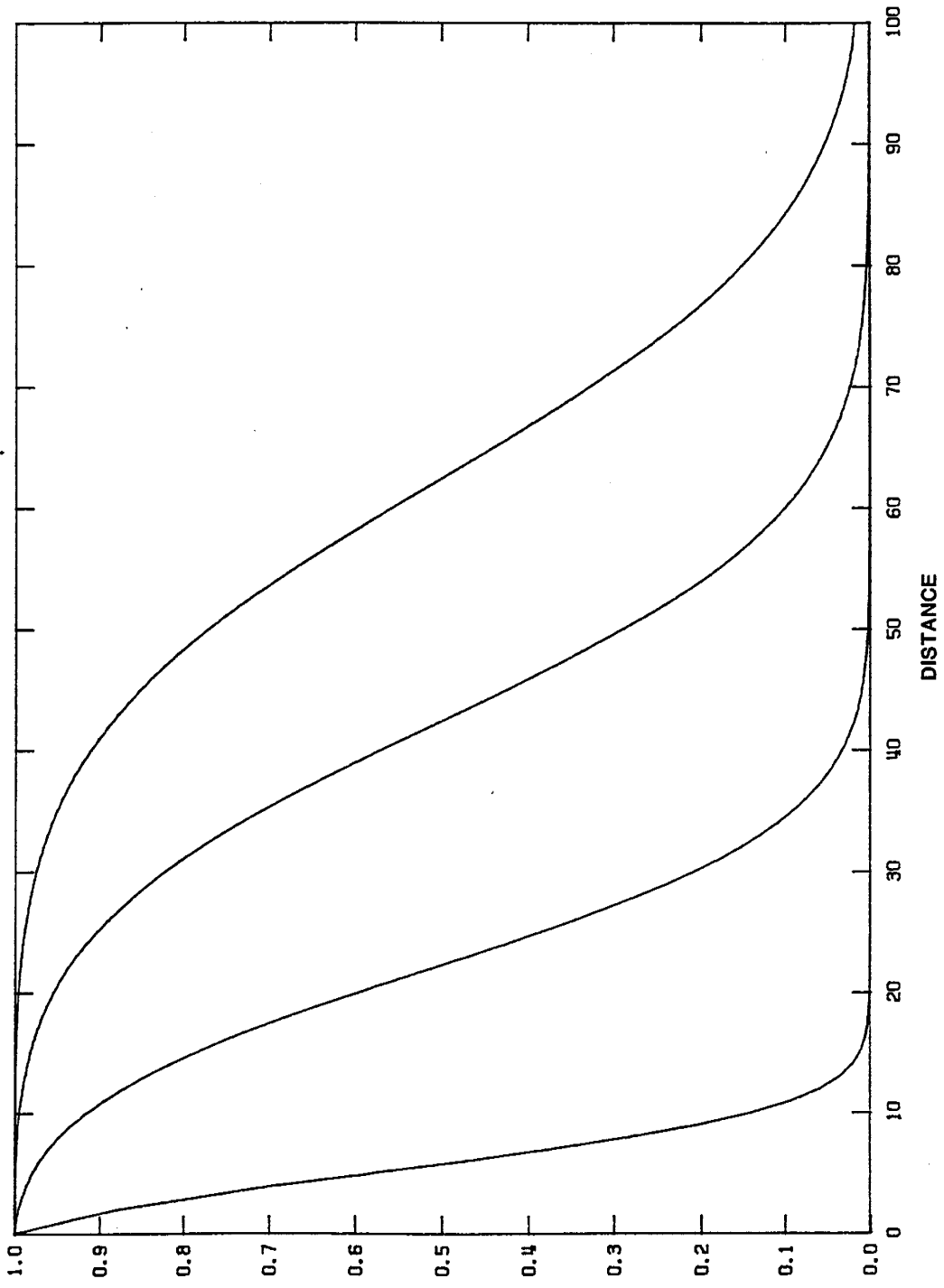
DISTANCE

— NCG Case with a Sink

- - Radioactive BCG Case with a Sink

Comparison of the numerical solutions to advective-dispersive transport of a tracer pulse, in terms of a isotopic ratio, with and without radioactive decay in the presence of a sink

Figure 33

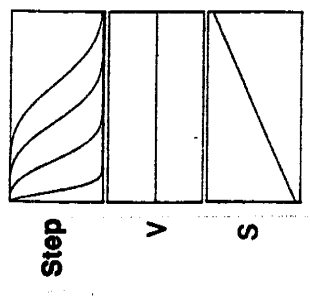
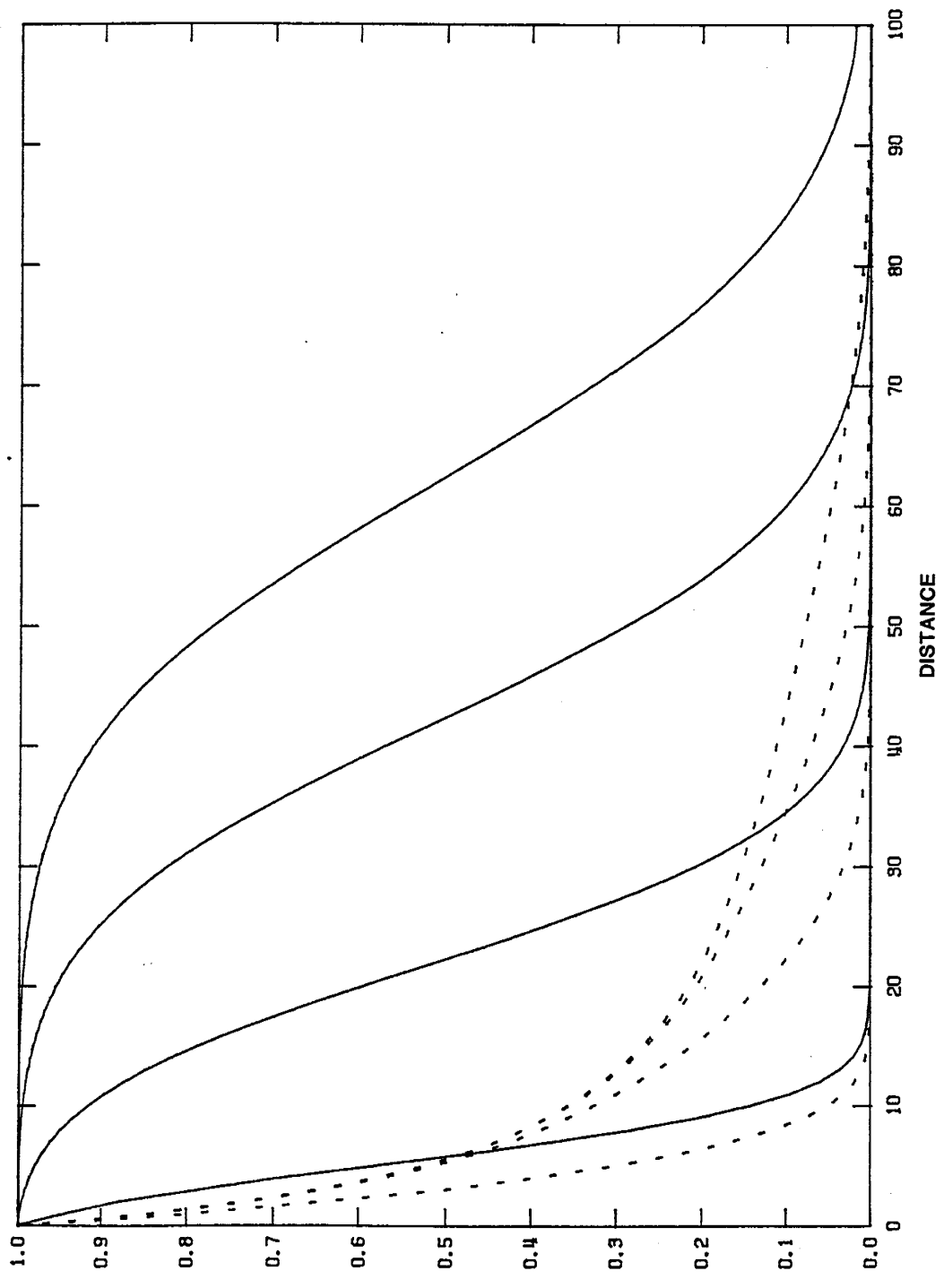


Legend

— Trace Isotope

Numerical solution to advective-dispersive transport of a steady tracer input

Figure 34



C/S

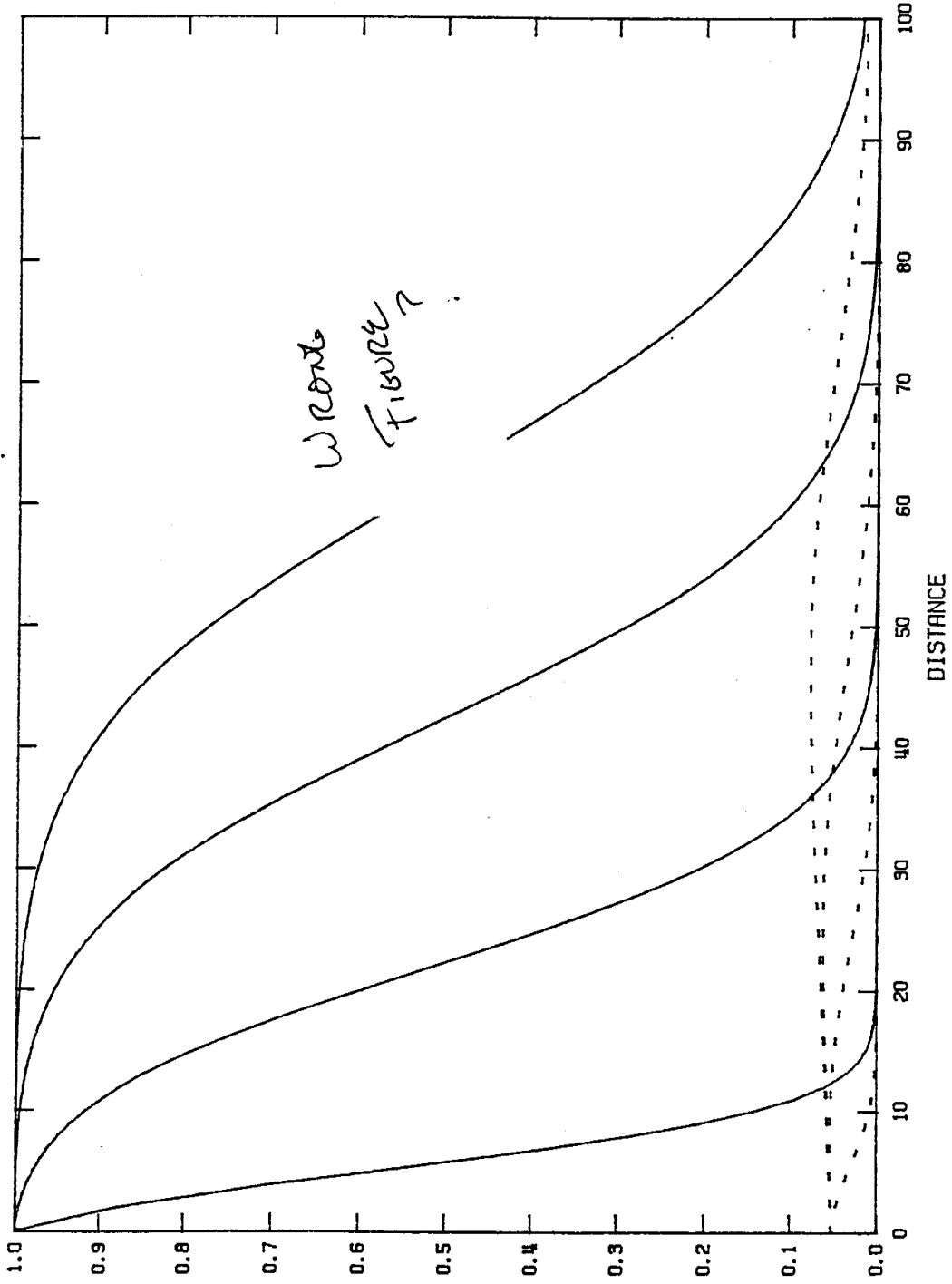
Legend

— NCG Case

- - BCG Case

Comparison of numerical solutions to advective-dispersive transport of a steady tracer input for the assumed and positive linear BCG case

Figure 36



+

+

+

+

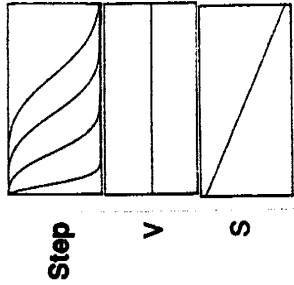
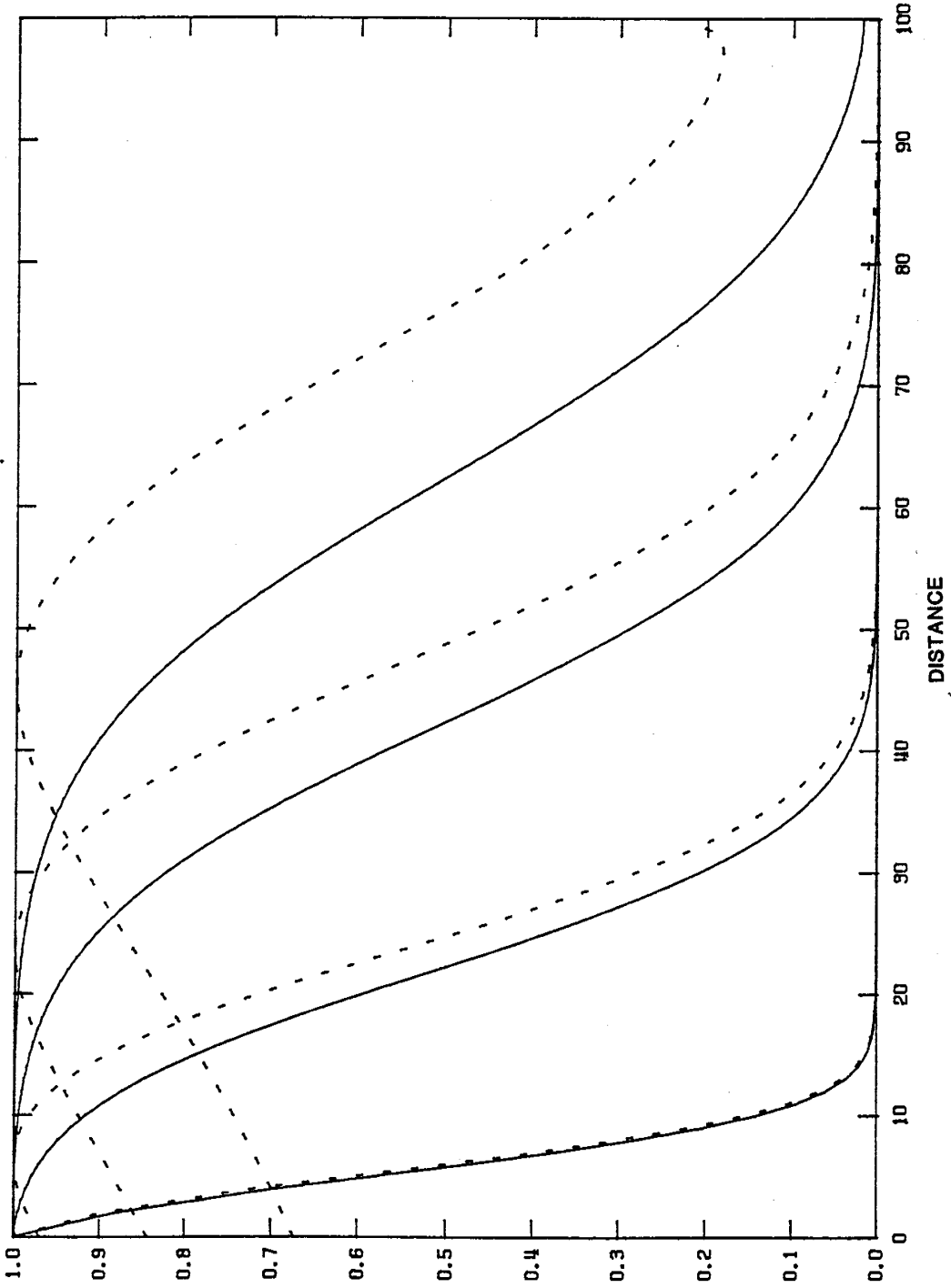
Legend

—

- - -

Wrong
Figure?

Figure 37



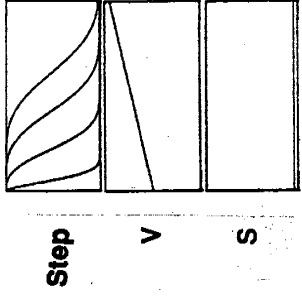
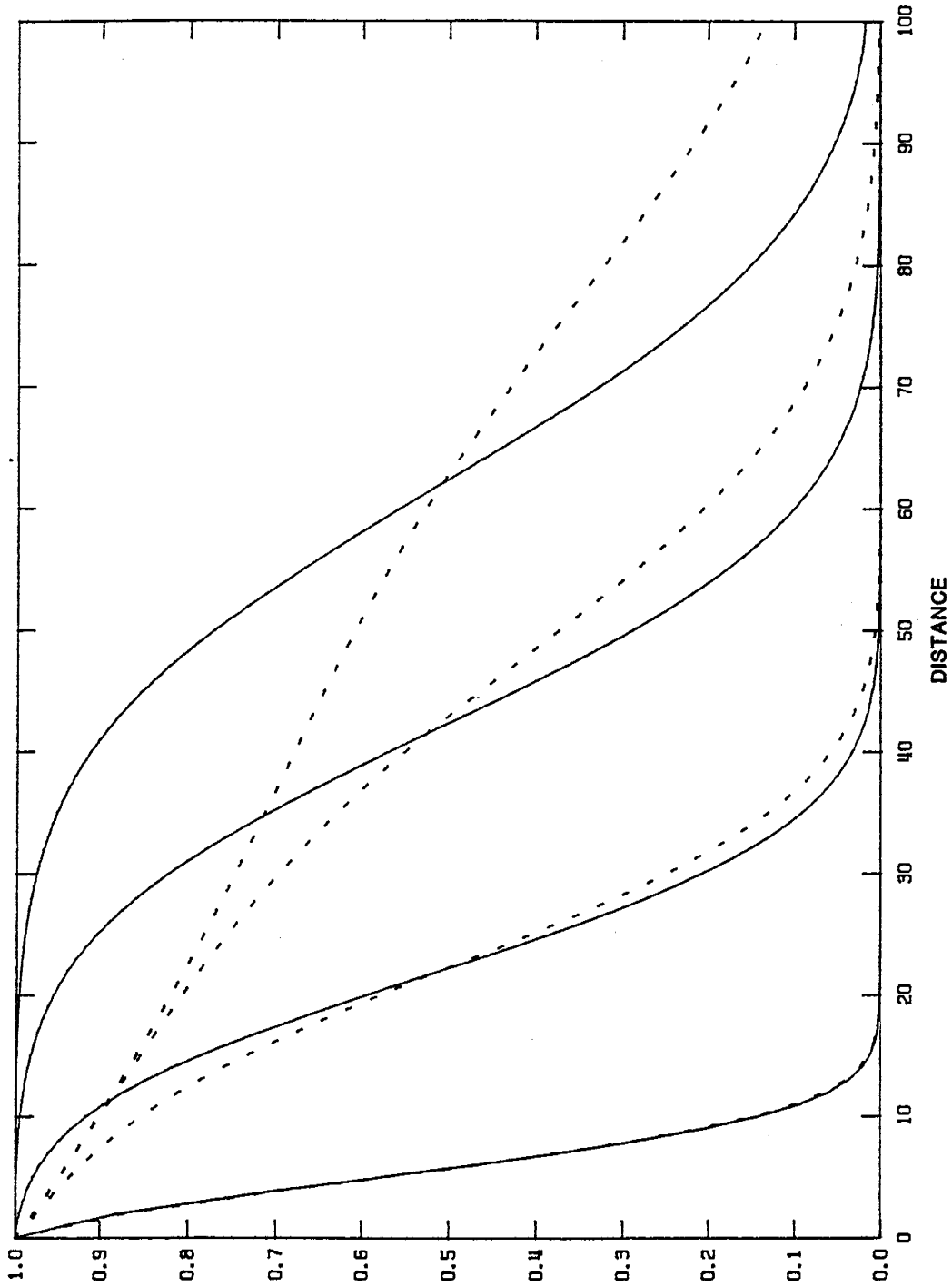
Legend

— NCG Case

- - BCG Case

Comparison of numerical solutions to advective-dispersive transport of a steady tracer input for the assumed and negative linear BCG case

Figure 38

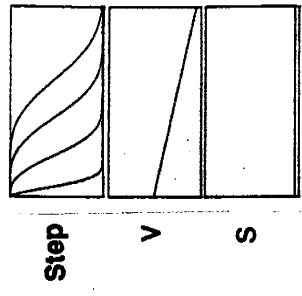
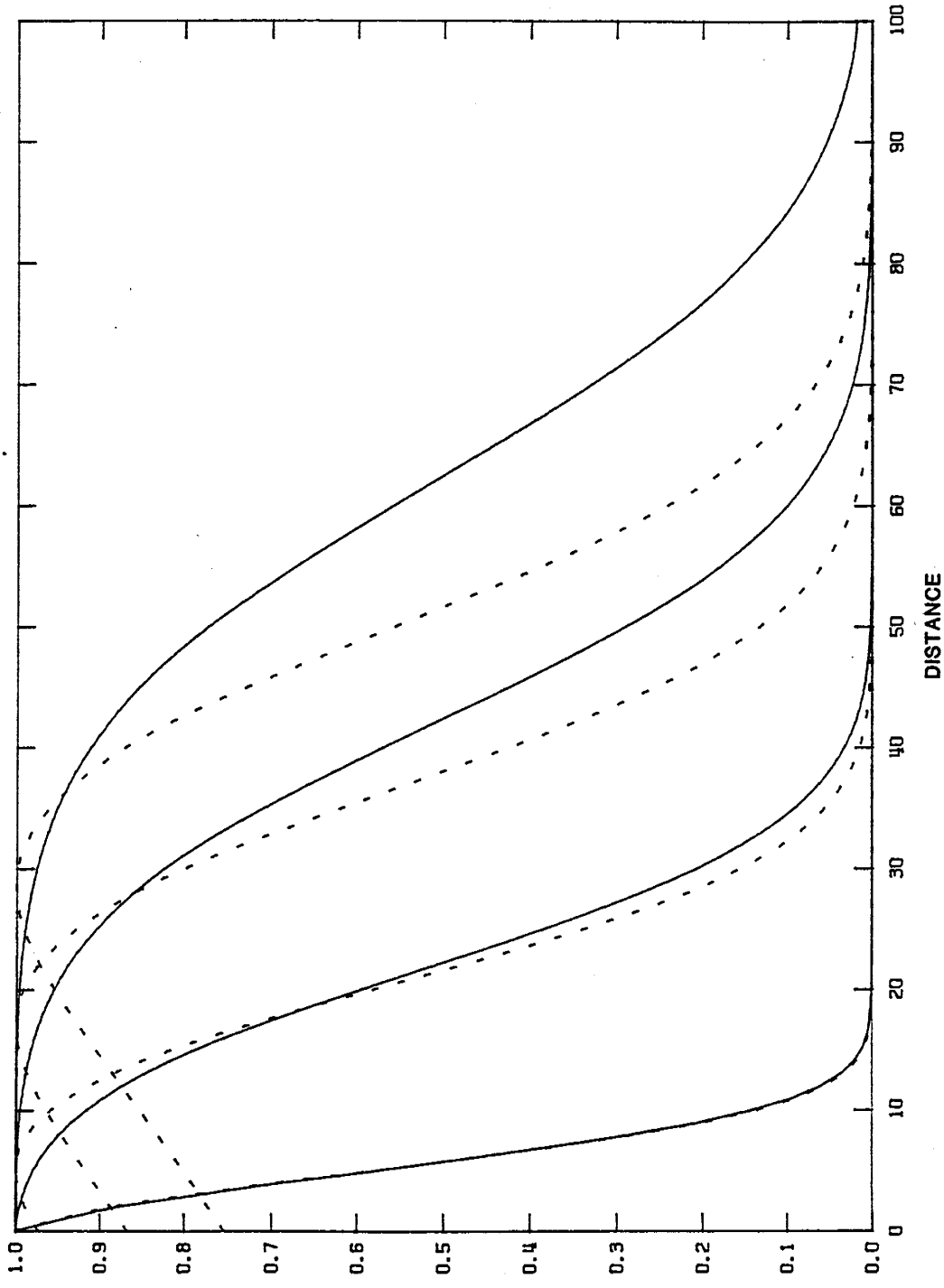


Legend

- Trace Isotope
- - Trace Isotope with a Source

Comparison of numerical solutions to advective-dispersive transport of a steady tracer Input with and without a source

Figure 39



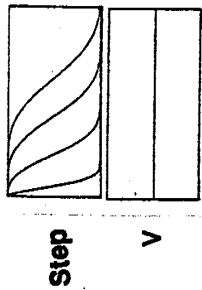
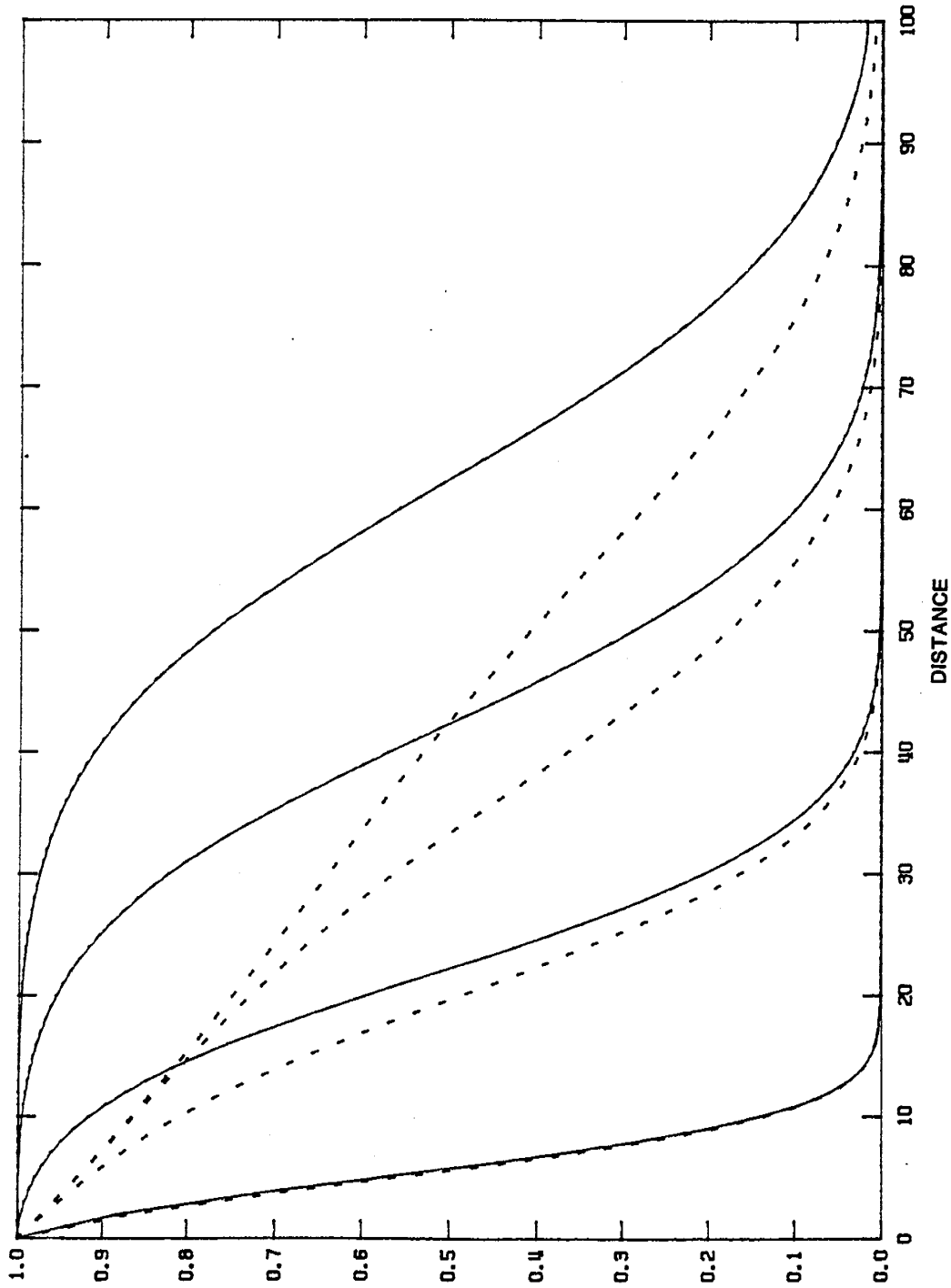
Legend

— Trace Isotope

- - Trace Isotope with a Sink

Comparison of numerical solutions to advective-dispersive transport of a steady tracer input with and without a sink

Figure 40



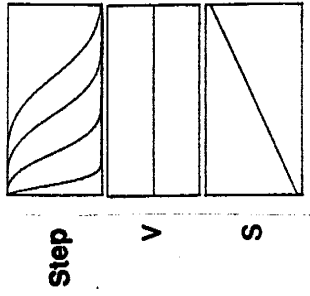
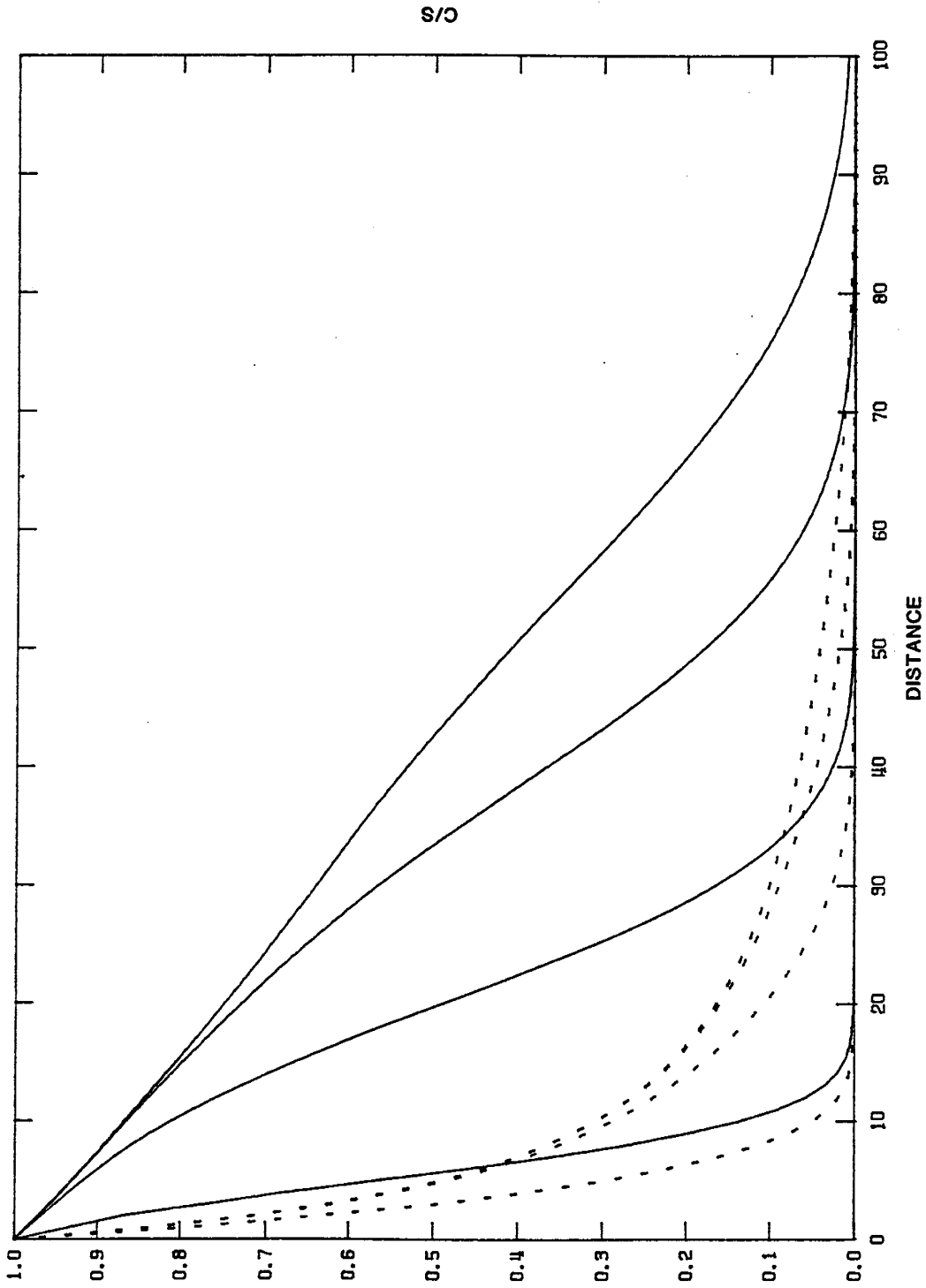
Legend

— Non-radioactive Trace Isotope

- - Radioactive Trace Isotope

Comparison of numerical solutions to advective-dispersive transport of a steady tracer input with and without radioactive decay

Figure 41

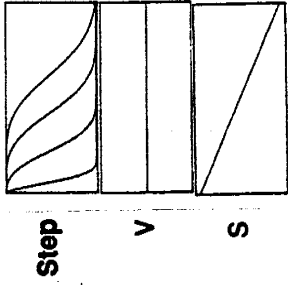
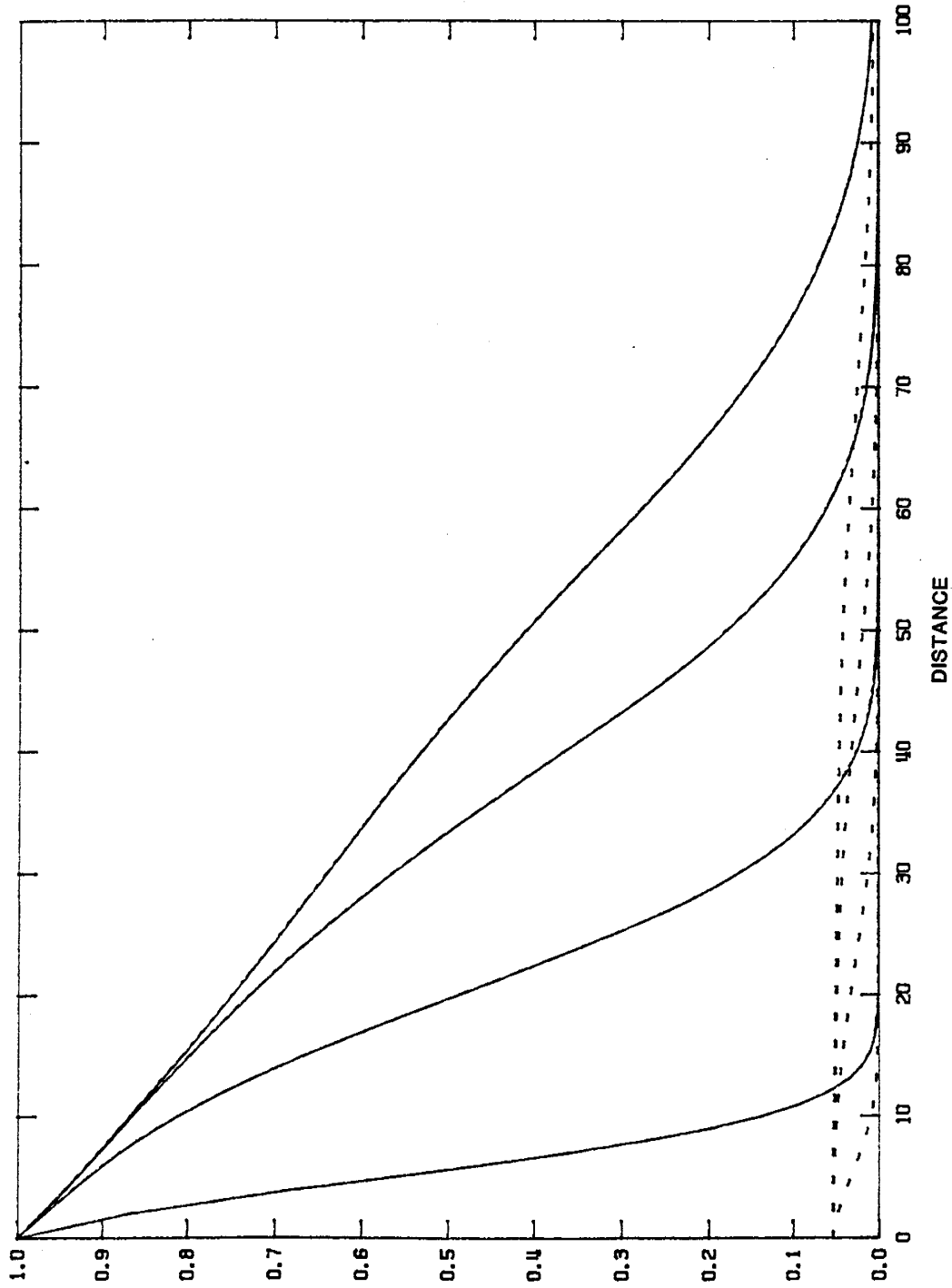


C/S

Legend

- Non-radioactive BCG Case
- - Radioactive BCG Case

Comparison of numerical solutions to advective-dispersive transport of a steady tracer input for the positive linear BCG case with and without radioactive decay



C/S

Legend

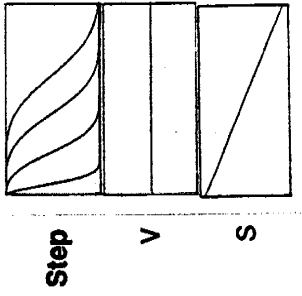
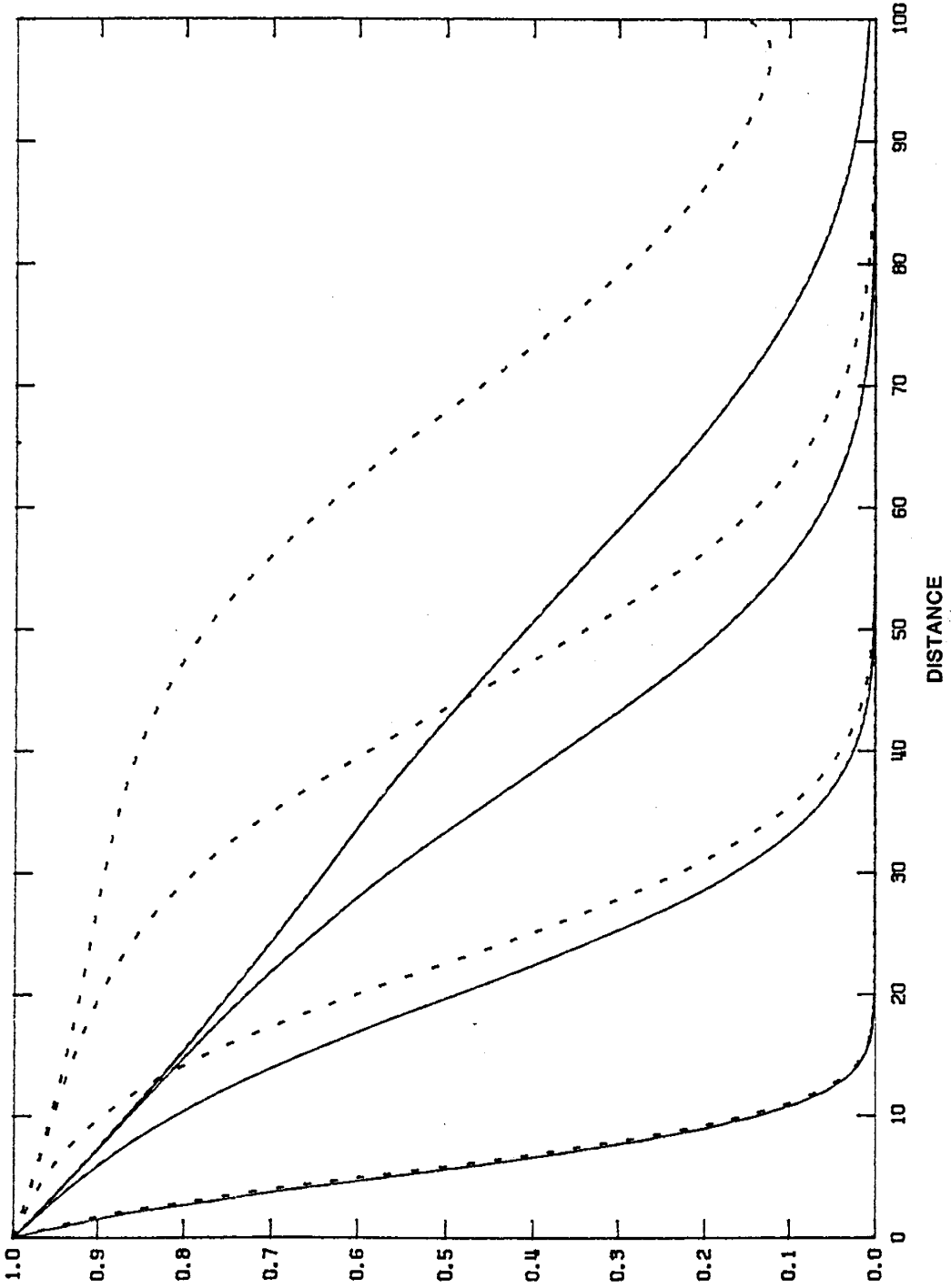
— Non-radioactive
BCG Case

- - - Radioactive
BCG Case

DISTANCE

Comparison of numerical solutions to advective-dispersive transport of a steady tracer input for the negative linear BCG case with and without radioactive decay

Figure 43



NORMALIZED C/S

Legend

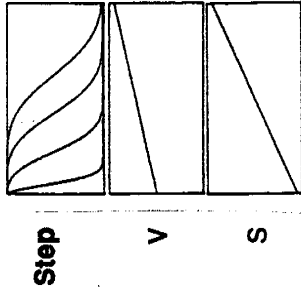
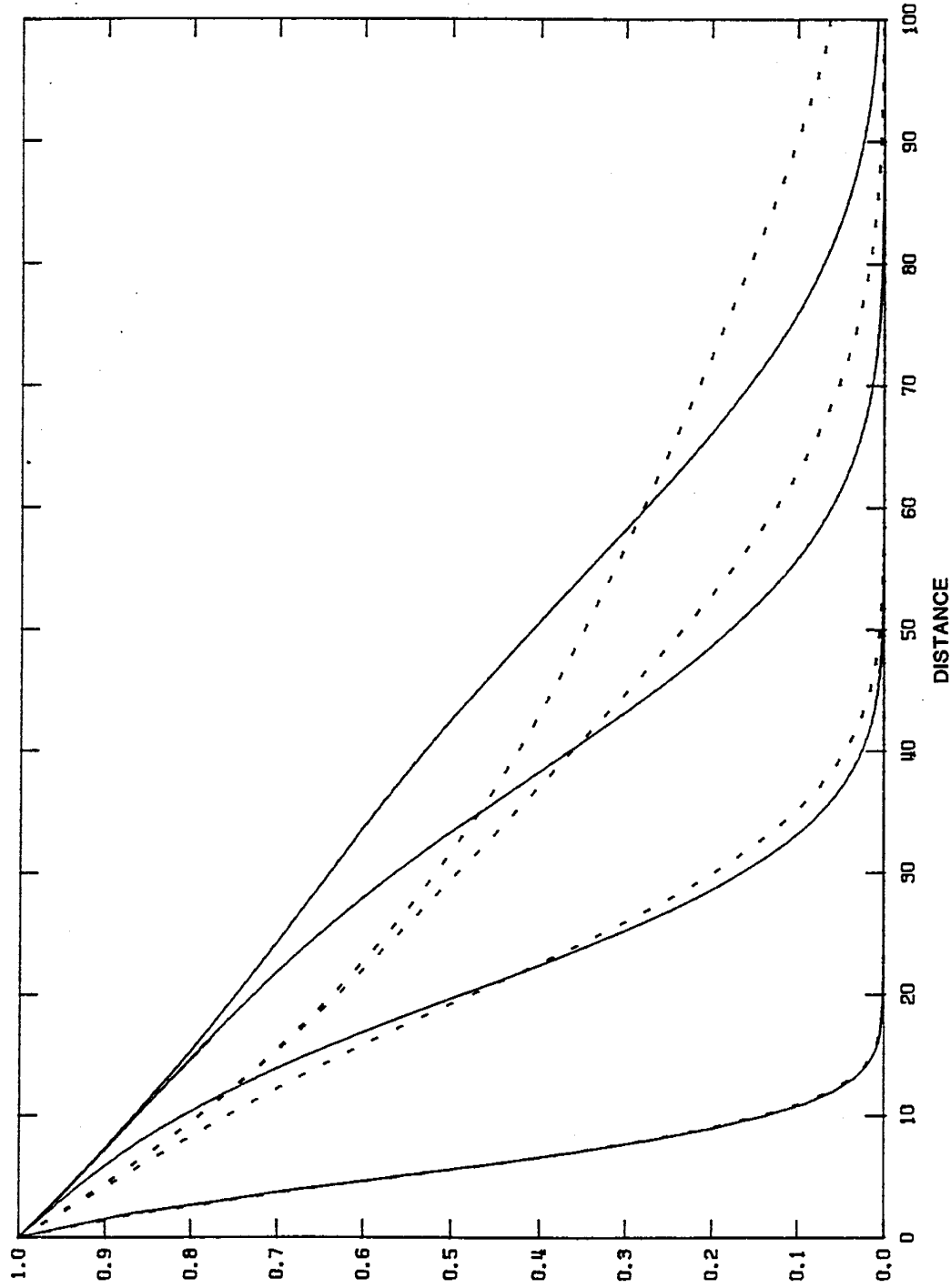
— Non-radioactive BCG Case

- - - Radioactive BCG Case

DISTANCE

Comparison of normalized numerical solutions from Figure 43

Figure 44



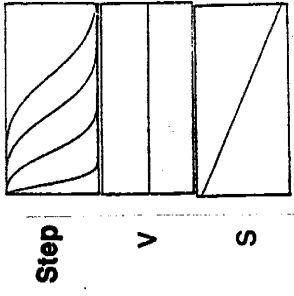
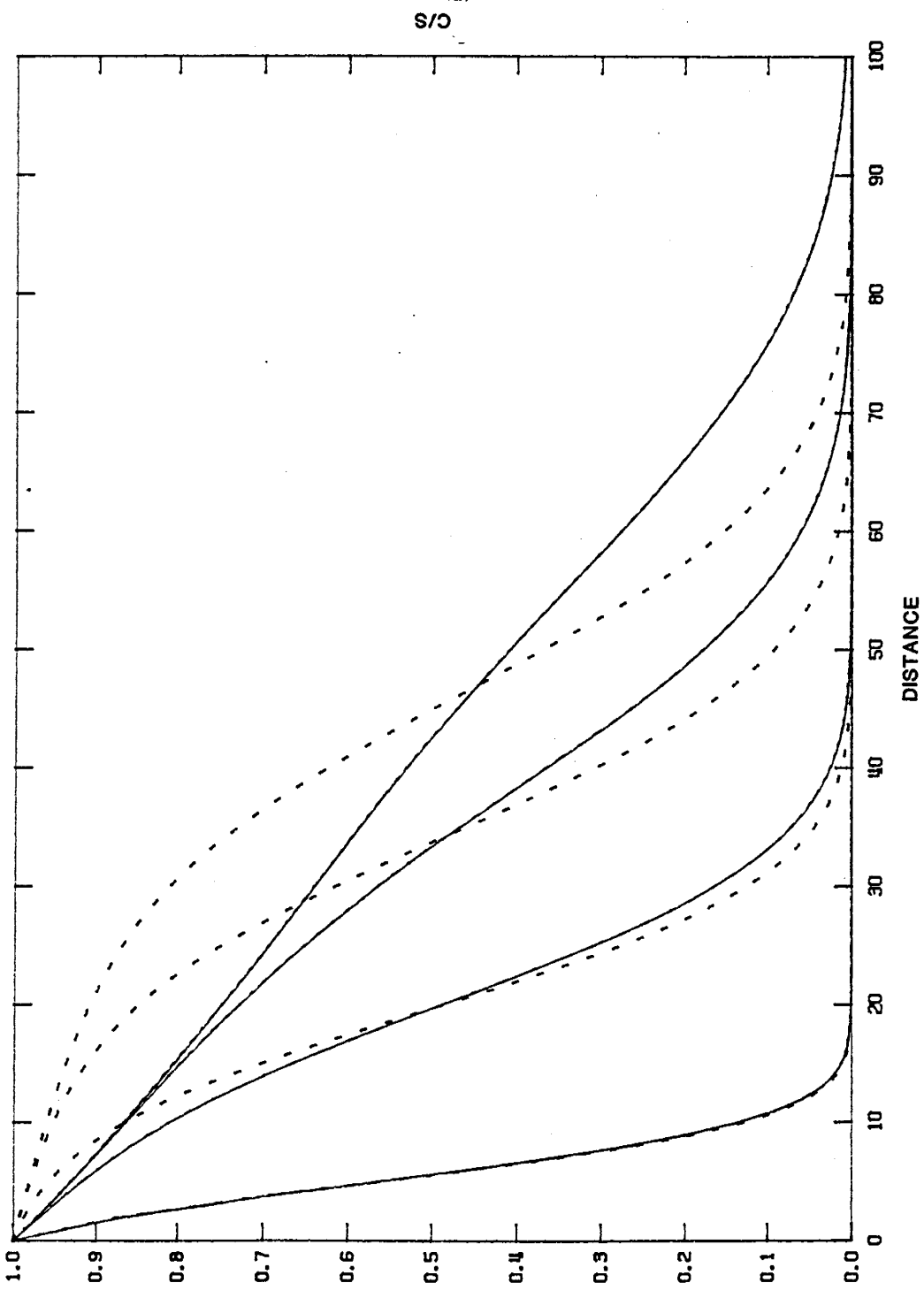
Legend

— BCG Case

- - - BCG Case with a Source

Comparison of numerical solutions to advective-dispersive transport of a steady tracer input for the positive linear BCG case with and without a source

Figure 45



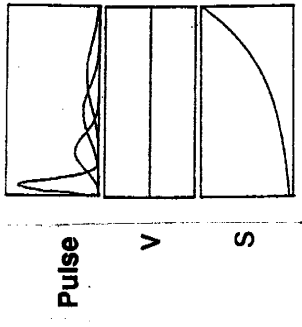
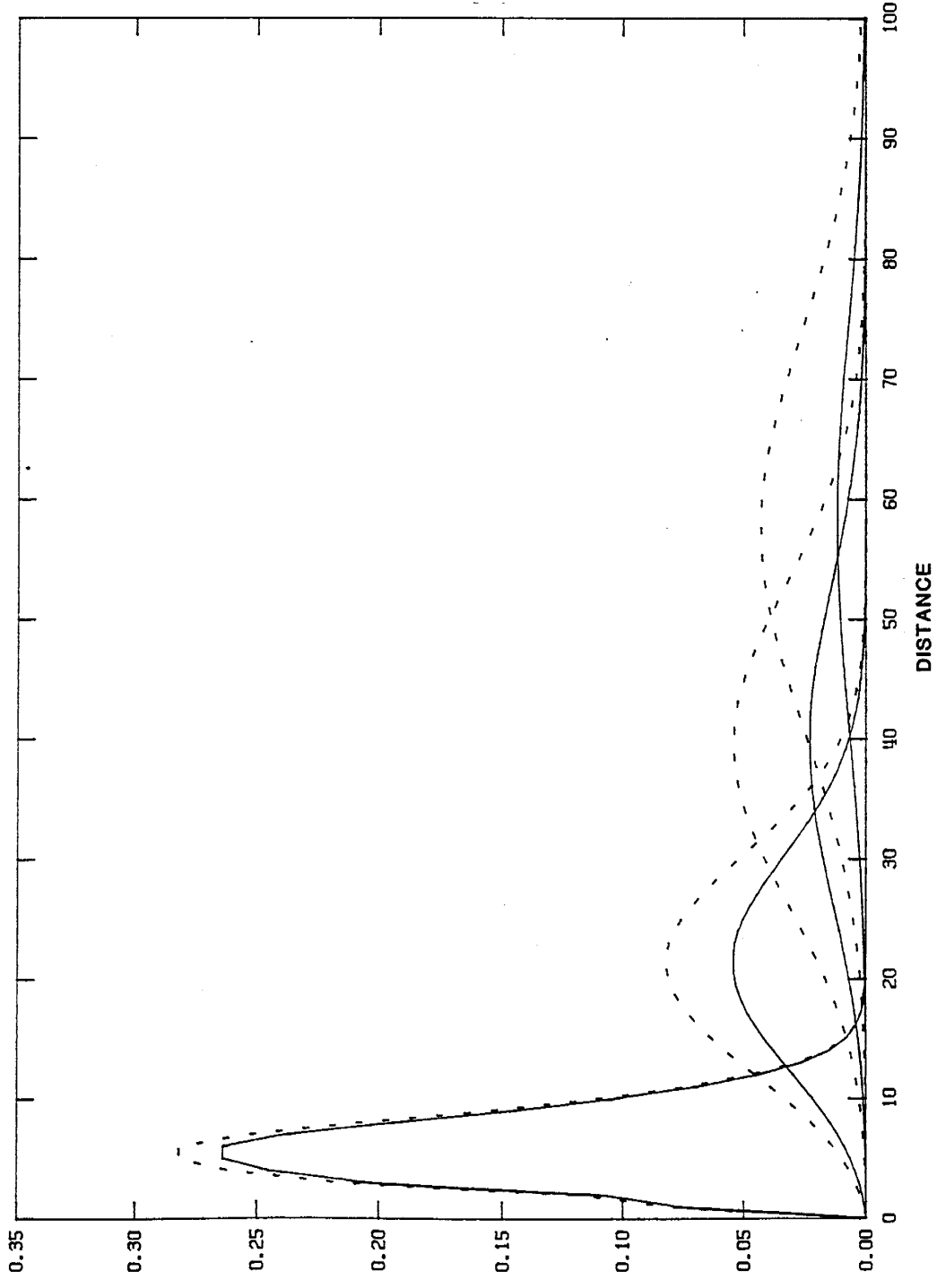
Legend

— BCG Case

- - BCG Case with a Sink

Comparison of numerical solutions to advective-dispersive transport of a steady tracer input for the positive linear BCG case with and without a sink

Figure 46



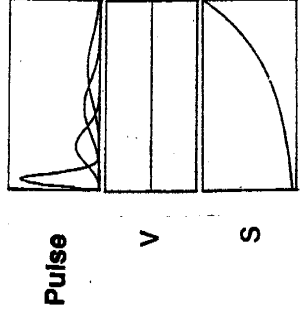
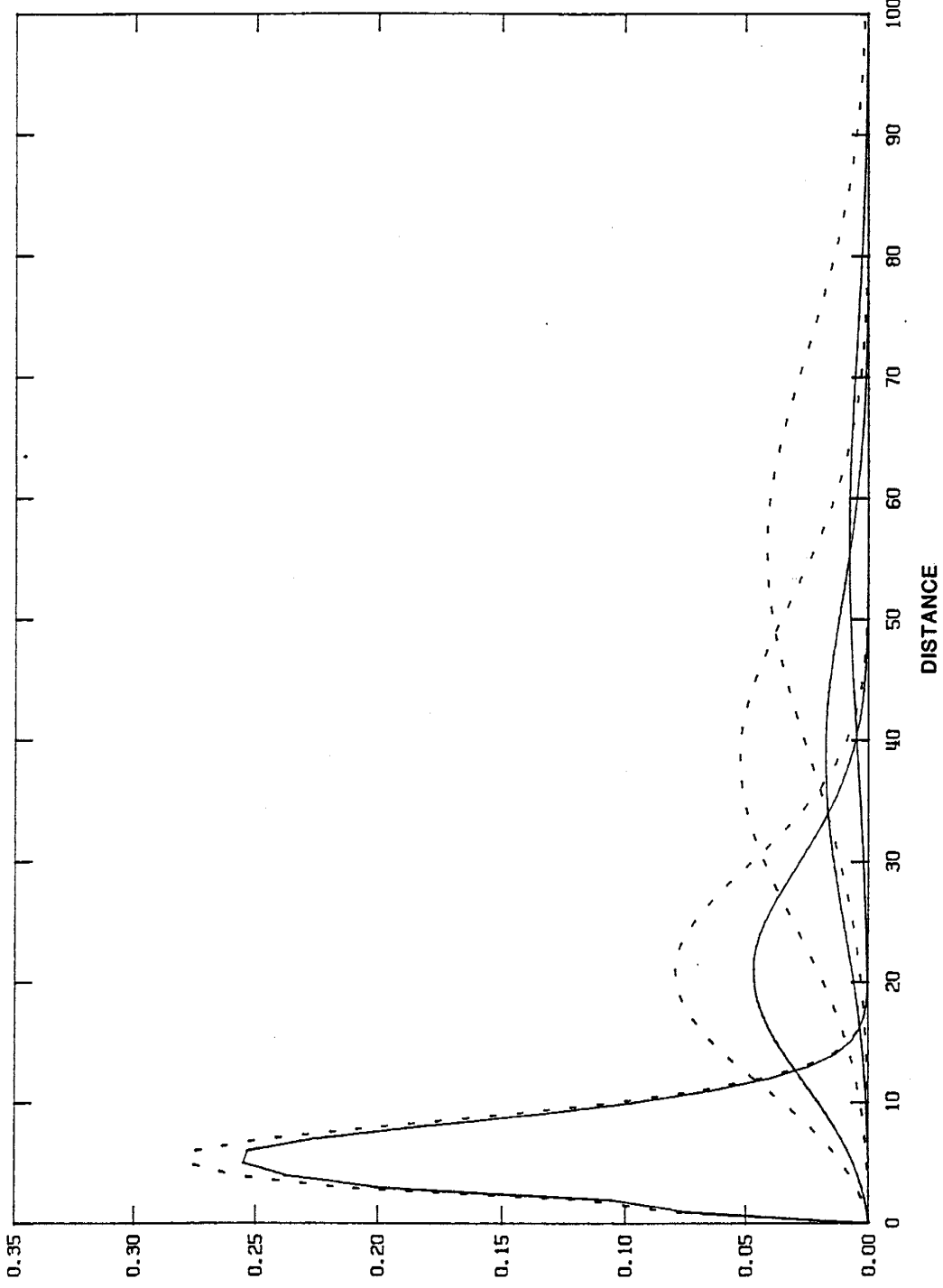
Legend

— NCG Case

- - - BCG Case

Comparison of DIA model with graphical superposition for constant DIA correction

Figure 8X47



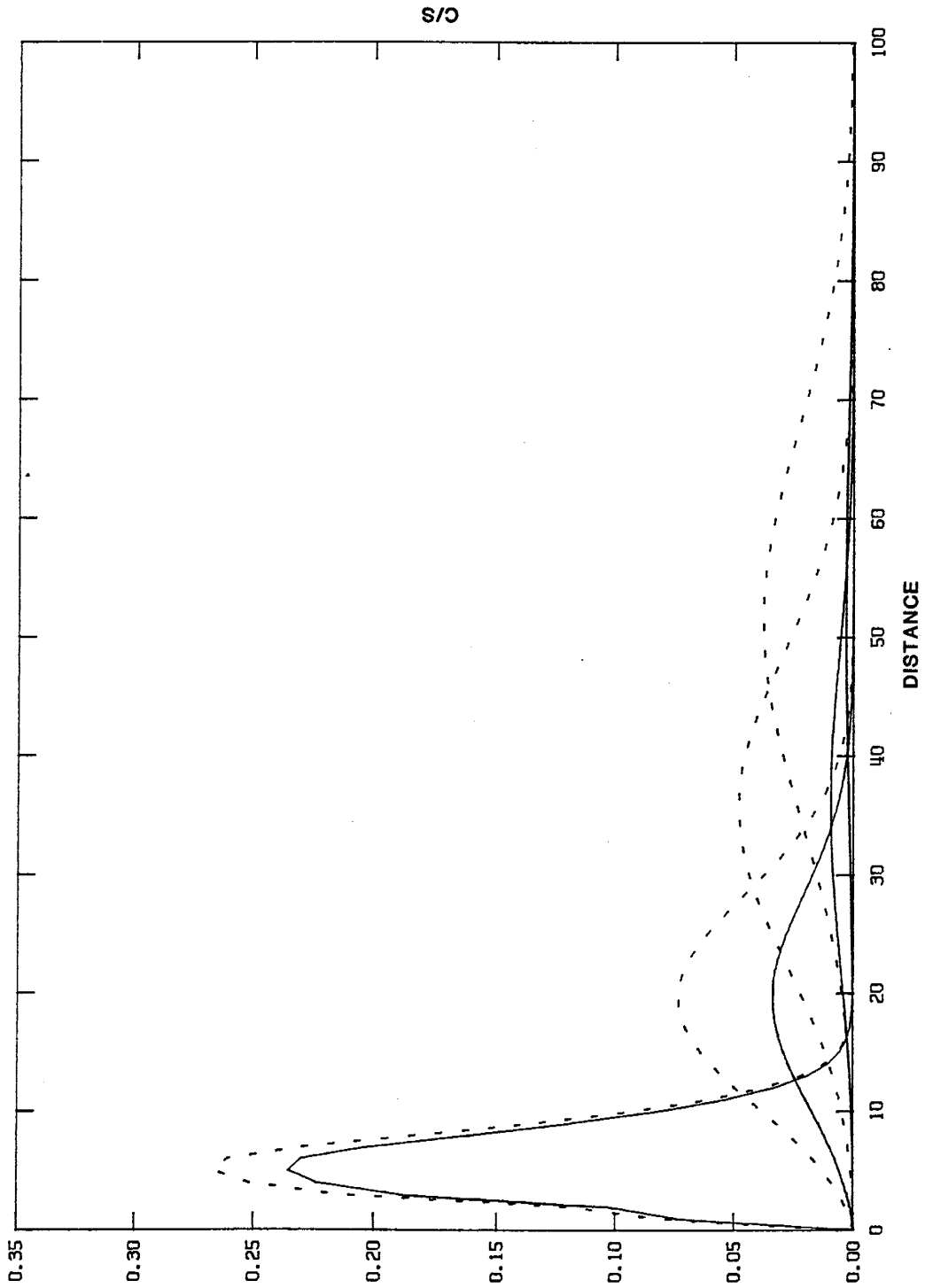
C/S

Legend

— NCG Case

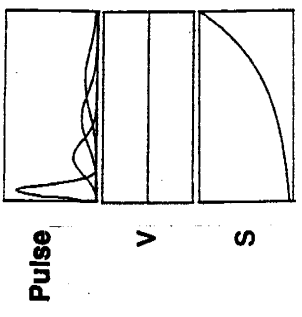
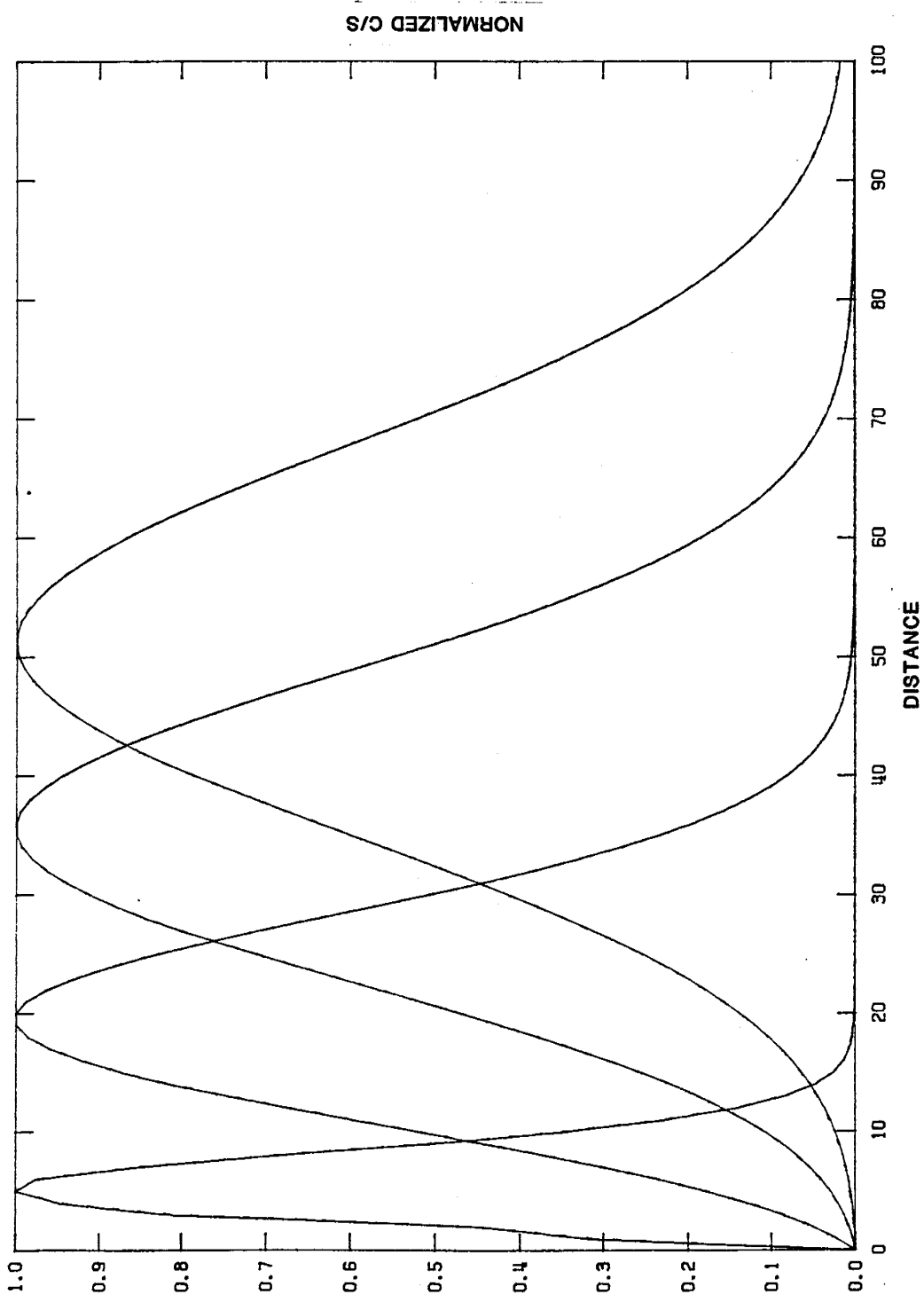
- - BCG Case

Comparison of DIA model with graphical superposition for constant DIA correction



Comparison of DIA model with graphical superposition for constant DIA correction

Figure 5949



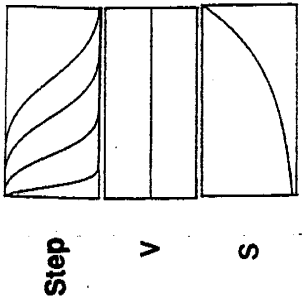
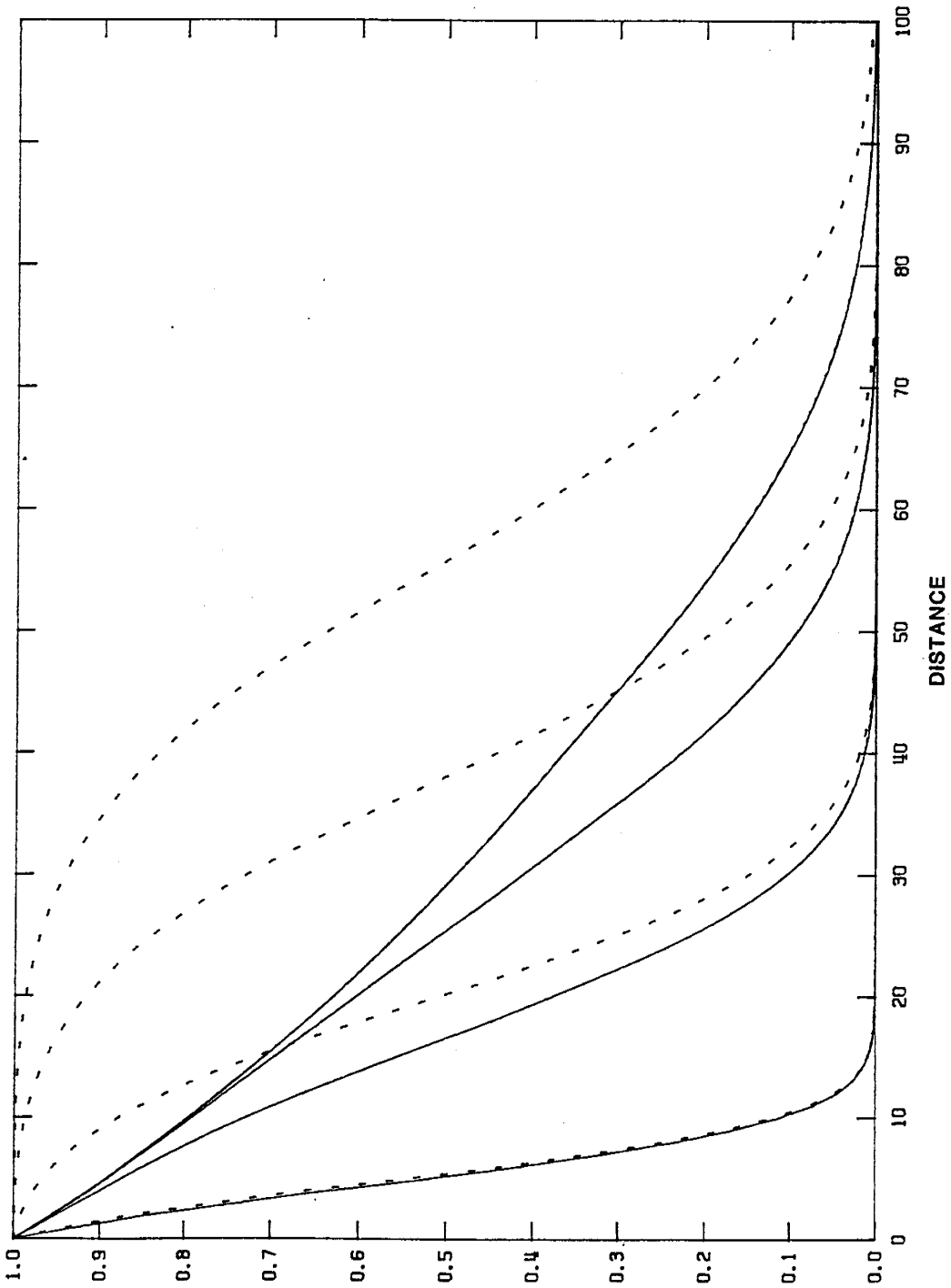
Legend

— NCG Case

-- BCG Case

Comparison of DIA model with graphical superposition for constant DIA correction

Figure 885



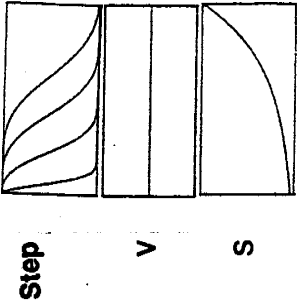
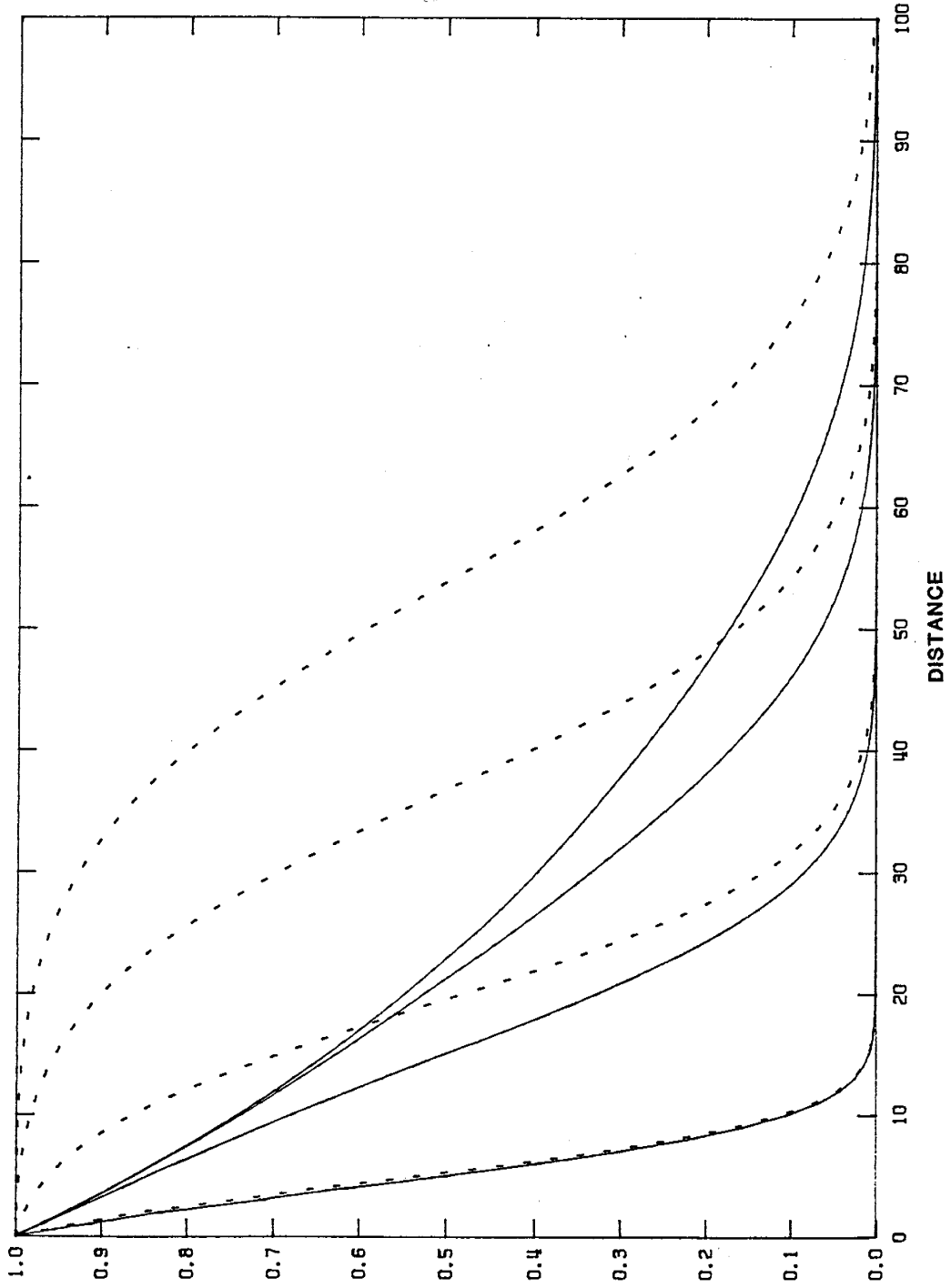
Legend

— NCG Case

- - BCG Case

Comparison of DIA model with graphical superposition for constant DIA correction

Figure 6 x 1

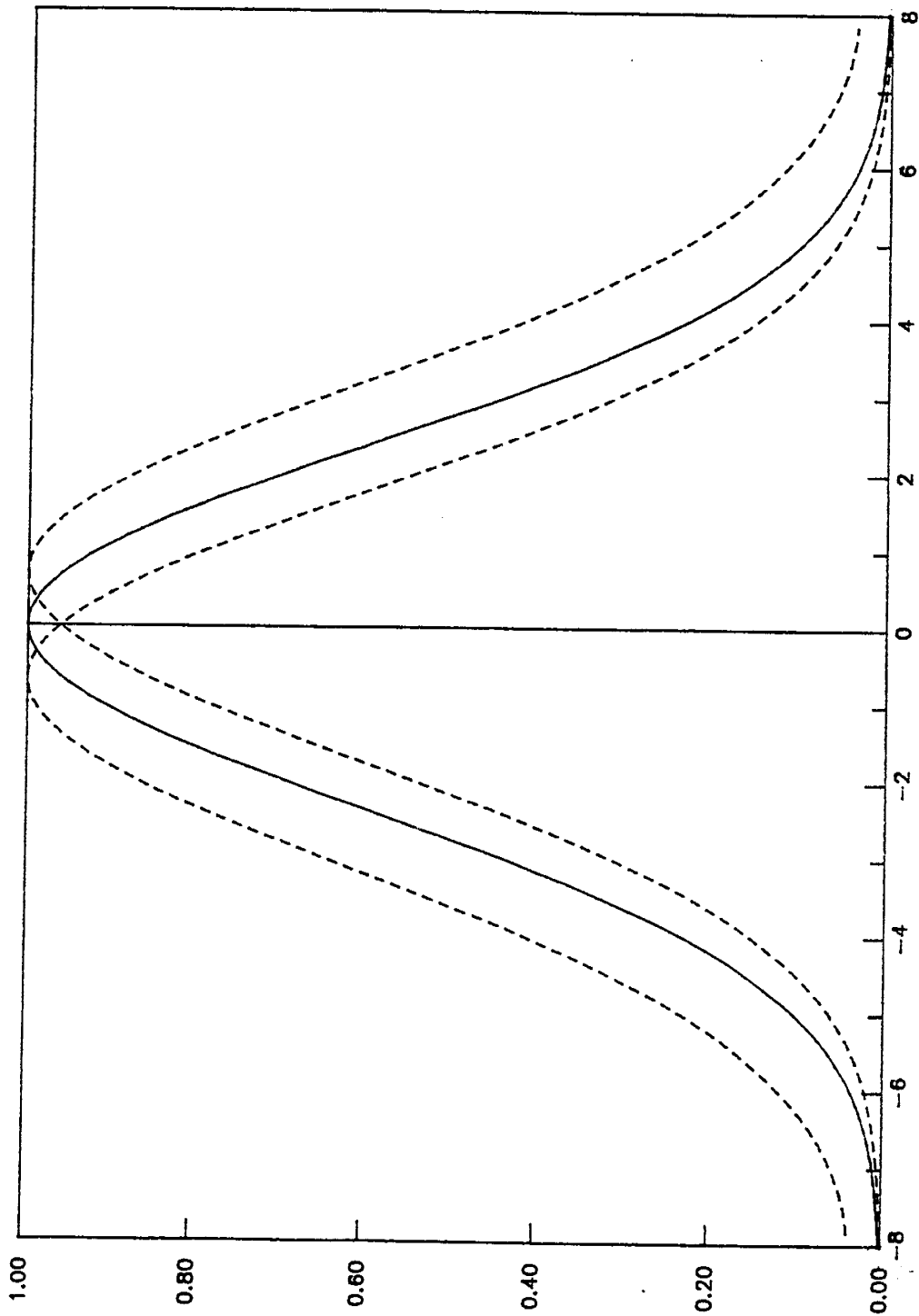


Legend

— NCG Case

- - - BCG Case

Comparison of DIA model with graphical superposition for constant DIA correction

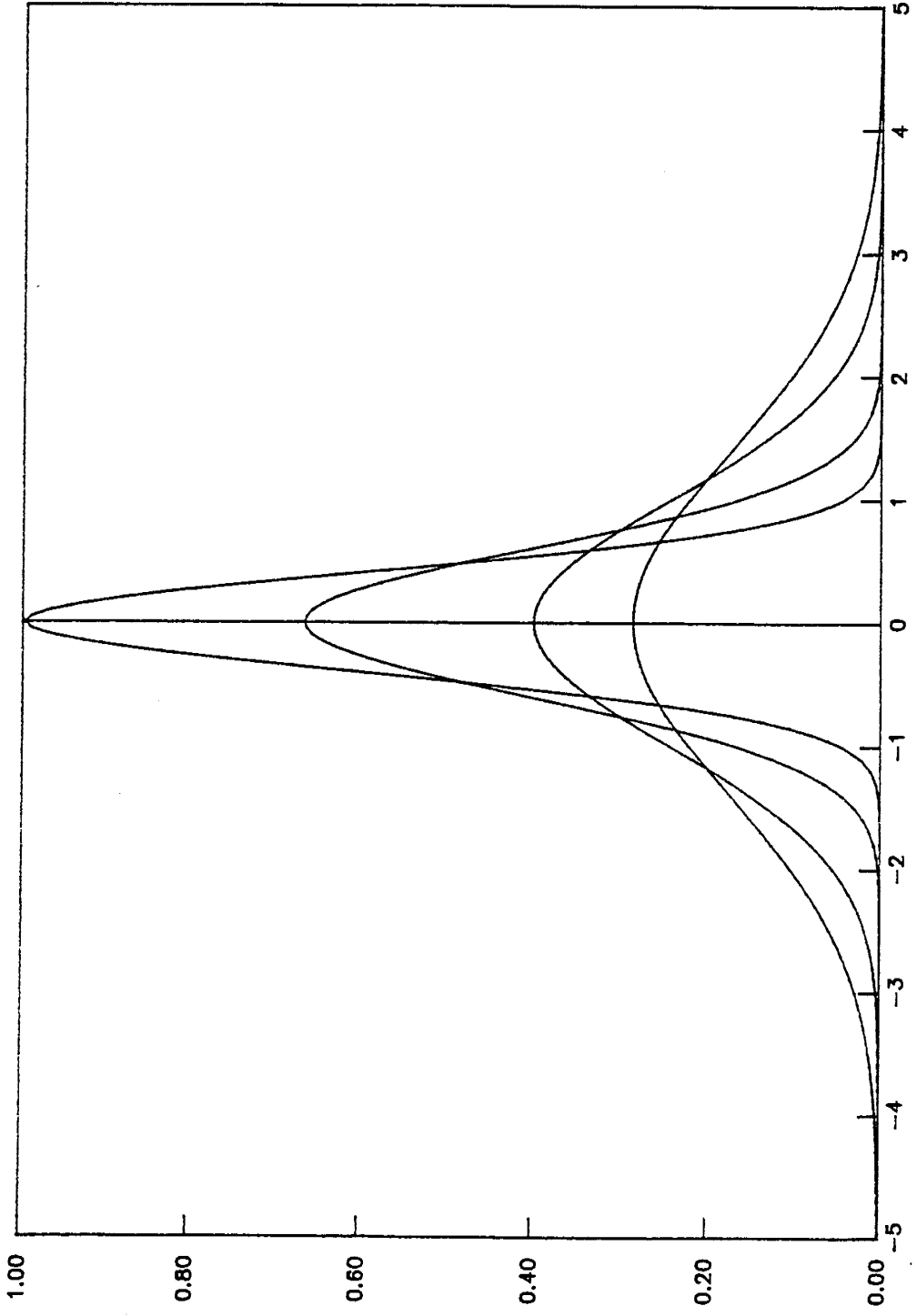


Legend

—

- - -

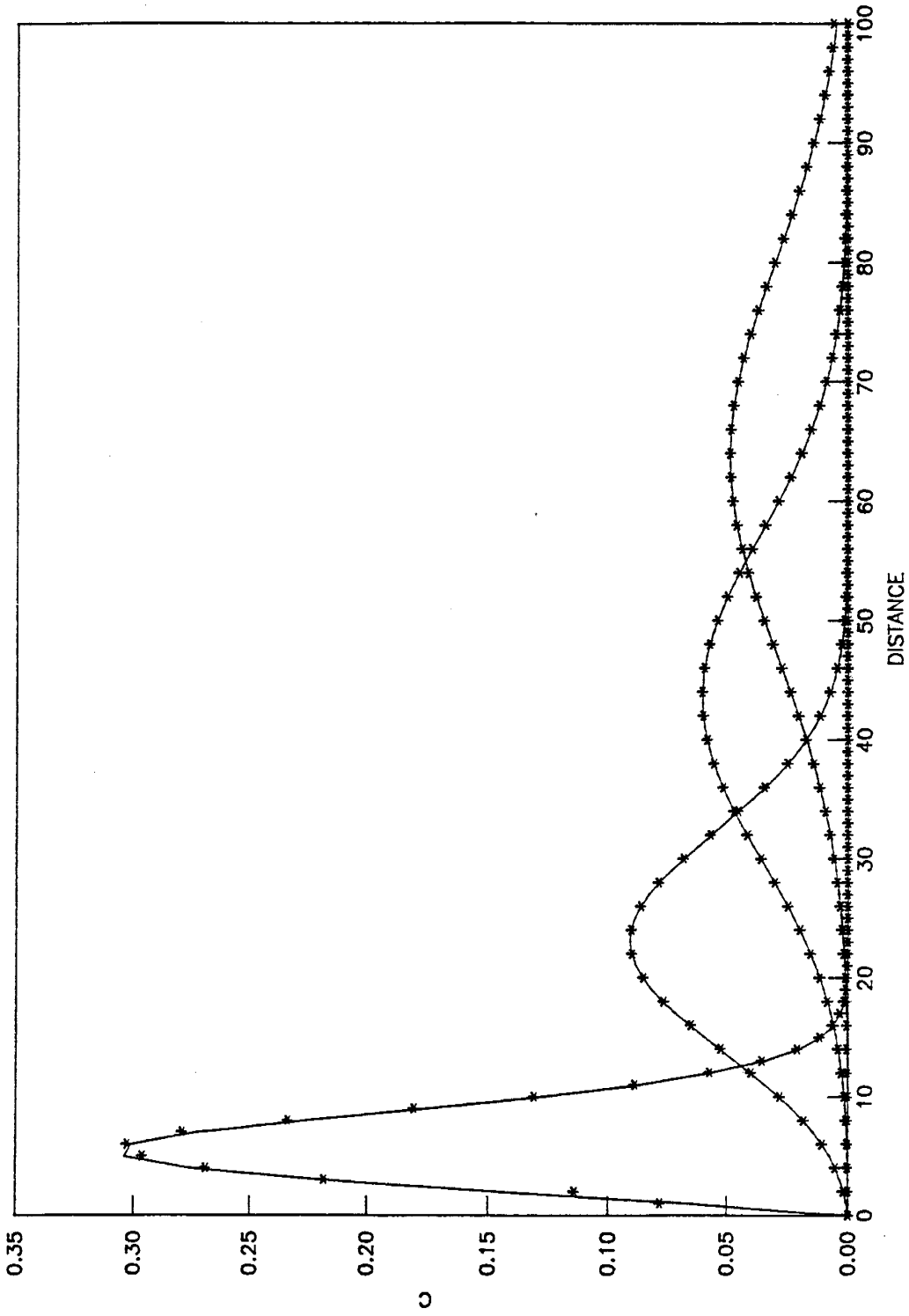
Figure 12



Legend

—

Figure 11



Legend



Figure 10

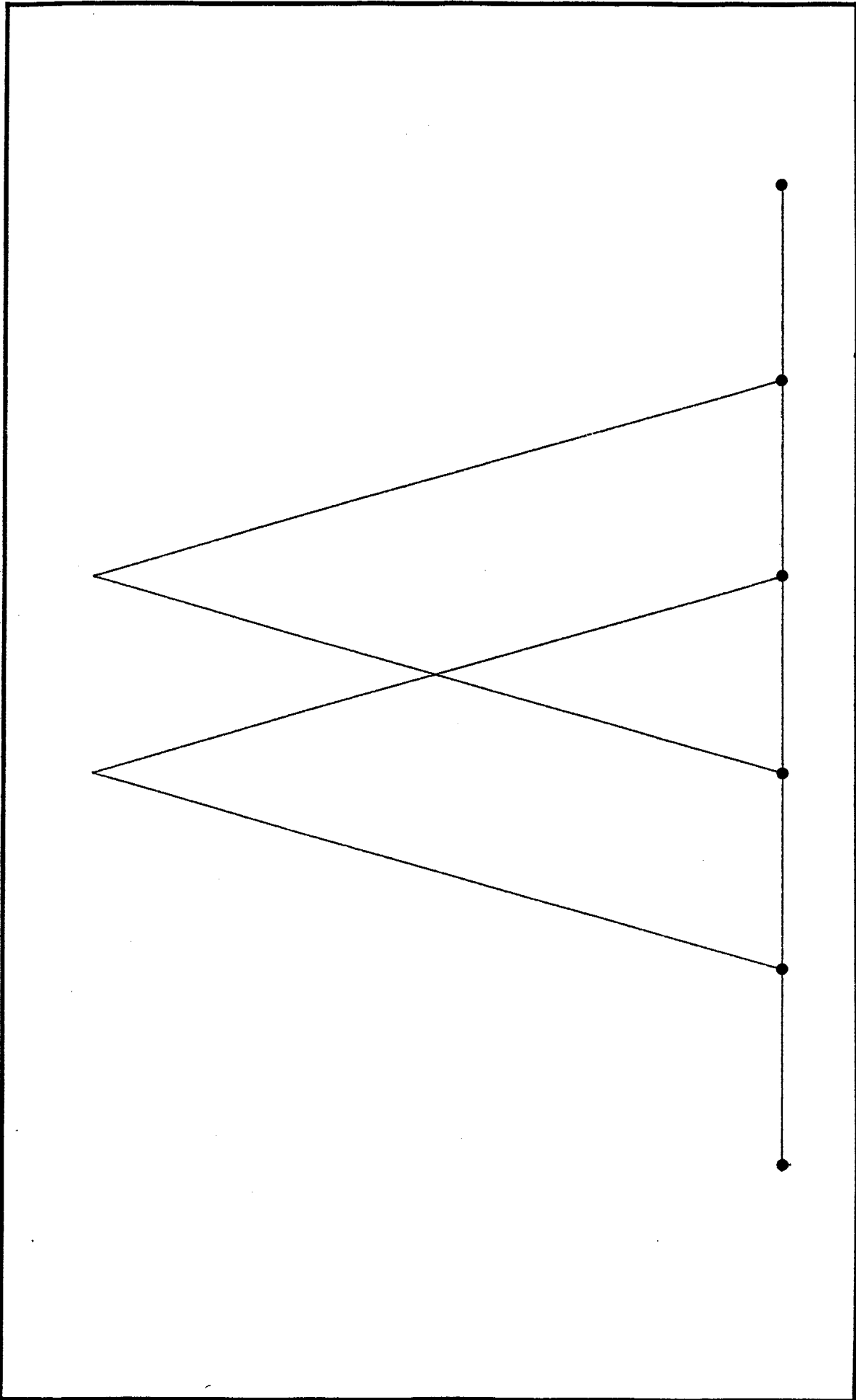
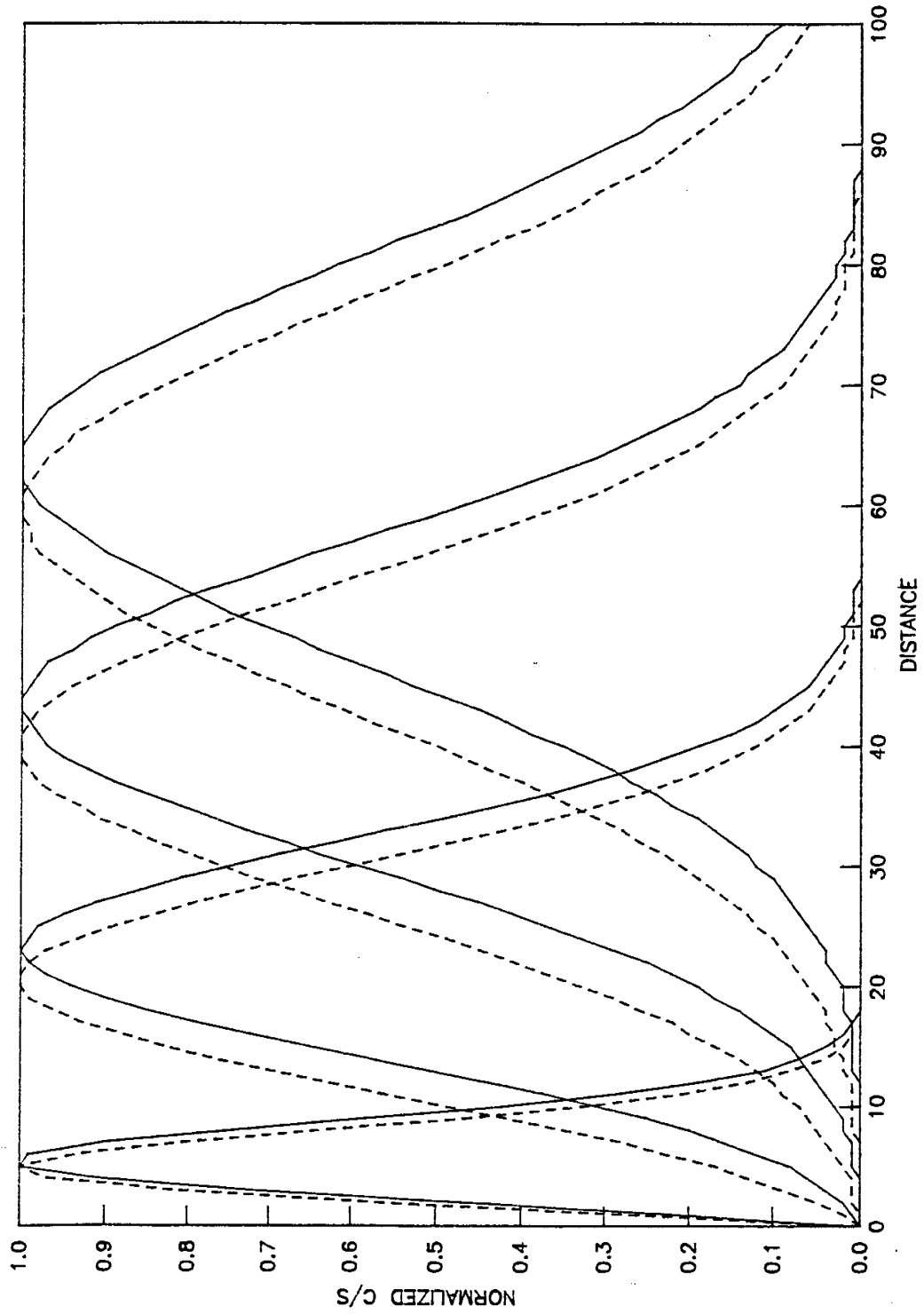


Figure 9

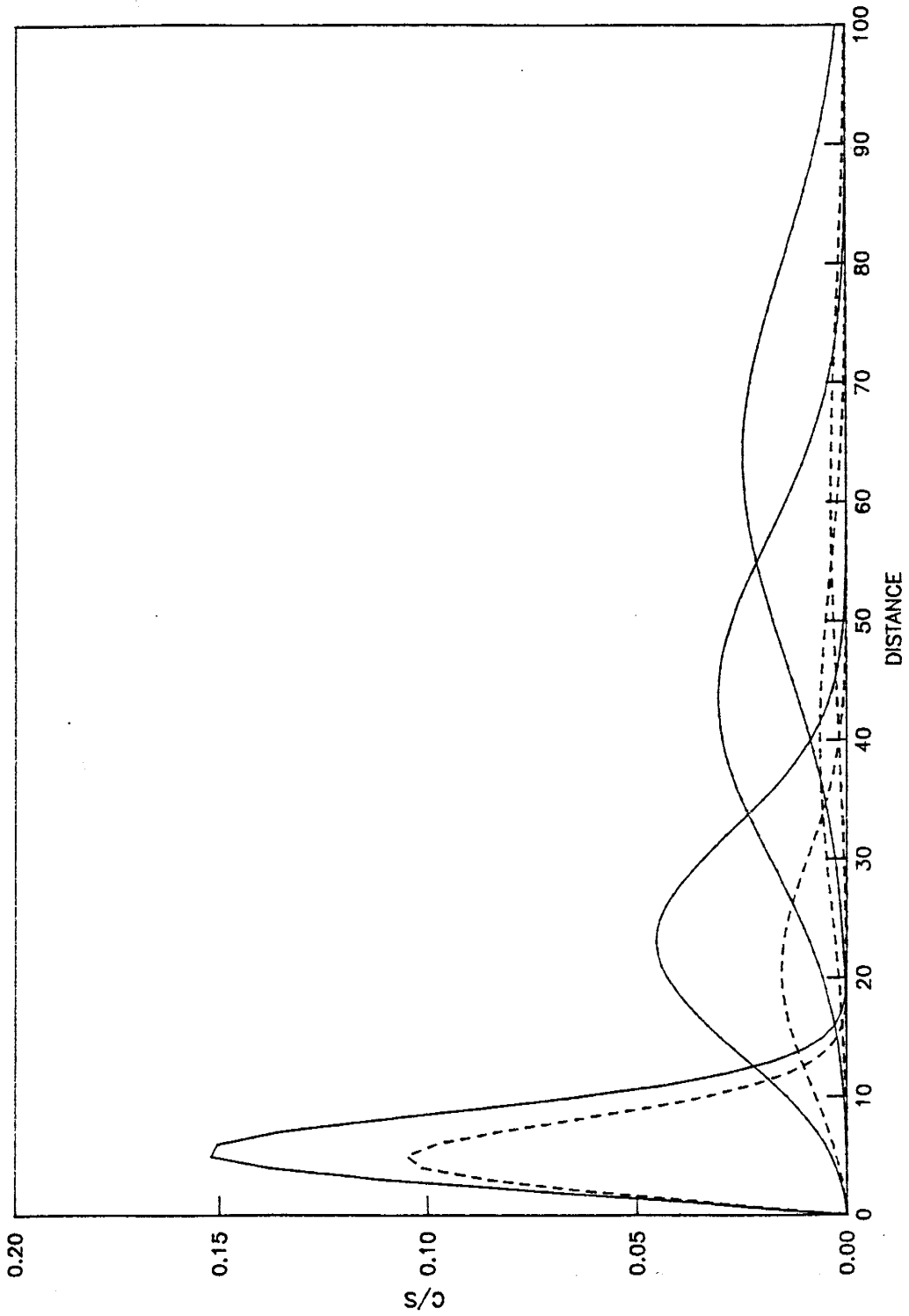


Legend

—

- - -

Figure 8

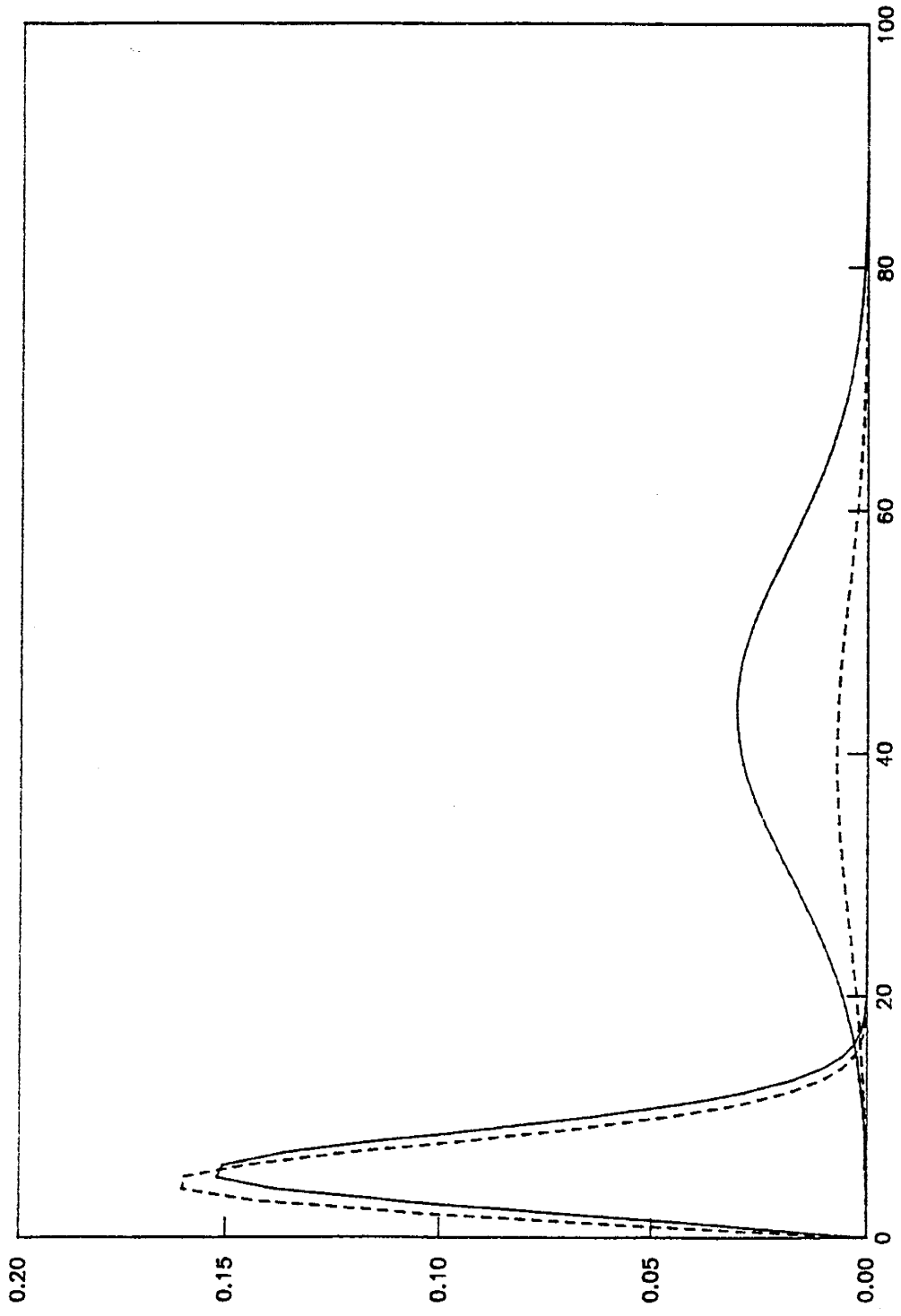


Legend

—

- - -

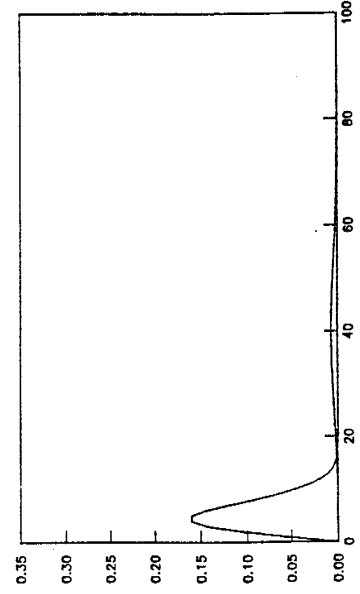
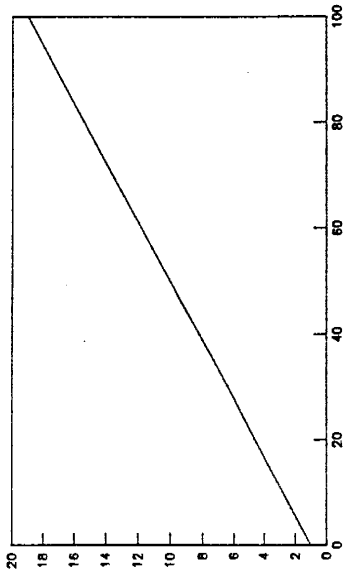
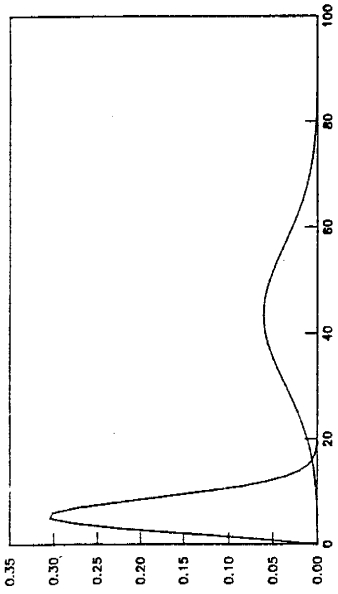
Figure 7



Legend



Figure 6



Legend

Figure 5

4/16/90

JW -

TIME VERSION ON
ITS WAY w/IN

2-3 DAYS. LOOK
FOR IT! *plw*

Legend

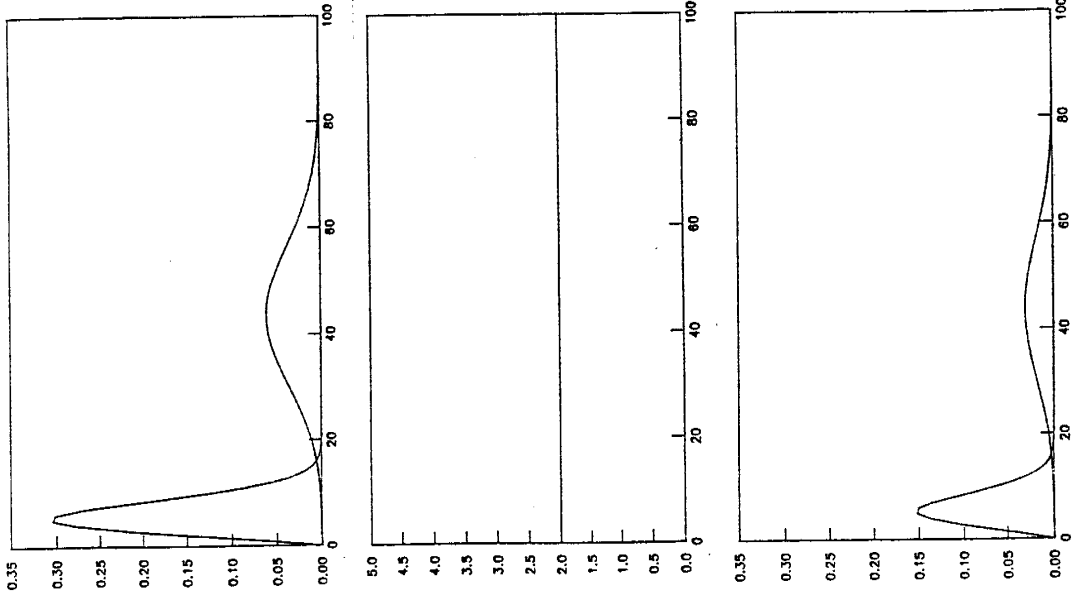


Figure 4